PUBLICATIONS

A. Publications in peer reviewed international journals/manuscript communicated

1. **Gogoi, D.,** Arora, N., Kalita, B., Sarma, R., Islam, T., Ghosh, S. S., Devi, R & Mukherjee, A. K. (2018). Anticoagulant mechanism, pharmacological activity, and assessment of preclinical safety of a novel fibrin(ogen)olytic serine protease from leaves of *Leucas indica*. ***Scientific Reports***, *8*(1), 6210.
2. **Gogoi, D.,** Pal, A., Chattopadhyay, P., Paul, S., Deka, R. C., & Mukherjee, A. K. (2018). First report of plant-derived β-sitosterol with antithrombotic, *in vivo* anticoagulant, and thrombus-preventing activities in a mouse model. ***Journal of Natural Products***, 81(11):2521-2530.
3. **Gogoi, D.,** Pal, A. Chattopadhyay, Ghosh, S.S & Mukherjee, A.K. Characterization, assessment of pre-clinical safety, *in vivo* anticoagulant and antithrombotic activities of an active anticoagulant formulation prepared from the leaves of *Leucas indica* (Communicated).
4. **Gogoi. D.,** Jha, S. & Mukherjee A.K. A novel and simple method for the preparation of anticoagulant active fraction (AAF) from the fruits extract of *Momordica charantia:* Analysis of bioactive components, mechanism of anticoagulant action and prevention of *in vivo* thrombus formation by AAF. (Communicated).

B. Other publications in peer reviewed international journals/manuscript communicated

1. Bora, B., **Gogoi, D.,** Tripathy, D., Kurkalang, S., Ramani, S., Chatterjee, A., & Mukherjee, A. K. (2017). The N-terminal-truncated recombinant fibrin (ogen) olytic serine protease improves its functional property, demonstrates *in vivo* anticoagulant and plasma defibrinogenation activity as well as pre-clinical safety in rodent model. ***International Journal of Biological Macromolecules***, 111:462-474 **.**
2. **Gogoi, D.,** Bhagowati, P., Gogoi, P., Bordoloi, N. K., Rafay, A., Dolui, S. K., & Mukherjee, A. K. (2016). Structural and physico-chemical characterization of a dirhamnolipid biosurfactant purified from *Pseudomonas aeruginosa*: application of crude biosurfactant in enhanced oil recovery. ***RSC Advances***, *6*(74), 70669-70681.

3. Dutta, S., **Gogoi, D.,** & Mukherjee, A. K. (2015). Anticoagulant mechanism and platelet deaggregation property of a non-cytotoxic, acidic phospholipase A_2 purified from Indian cobra (*Naja naja*) venom: inhibition of anticoagulant activity by low molecular weight heparin. ***Biochimie***, *110*, 93-106.
4. Majumdar, S., Sarmah, B., **Gogoi, D.,** Banerjee, S., Ghosh, S. S., Banerjee, S., Chattopadhyay, P., & Mukherjee, A. K. (2014). Characterization, mechanism of anticoagulant action, and assessment of therapeutic potential of a fibrinolytic serine protease (Brevithrombolase) purified from *Brevibacillus brevis* strain FF02B. ***Biochimie,*** *103*, 50-60
5. **Gogoi, D.,** Ramani, R., Bharati, S., Chattopadhyay, P, & Mukherjee, A.K. Characterization of active anticoagulant fraction and a fibrin(ogen)olytic serine protease from leaves of *Clerodendrum colebrookianum*, a traditional ethno-medicinal plant used to reduce hypertension (Communicated)

C. Patents

1. Mukherjee, A.K. & **Gogoi, D**. "Anticoagulant actives and synergistic anticoagulant composition and method for producing the same" International patent published under Patent Corporation Treaty (PCT) (Publication Number- WO 2017/03449 A1; Dated 22/06/2017)
2. Mukherjee, A.K. & **Gogoi, D.** "Anticoagulant actives and synergistic anticoagulant composition and method for producing the same" Indian patent applied (1313/KOL/2015 dated 18.12.2015) (Under examination)

D. Presentations in National and International conferences

1. Gogoi, D. and Mukherjee, AK. Development of cost-effective, novel antithrombotic anticoagulant herbal drug from the leaves of *Leucas indica.* National symposium on role of innovation and technology for sustainable development, RITES, 2018, held on 26 April 2018, IPR cell, Tezpur University, Assam
2. Gogoi, D. and Mukherjee, AK. Pharmacological characterization for therapeutic application of an active fraction isolated from leaves of *Leucas indica.* Translational Research on Natural Products for Therapeutic Uses, 2017, IASST, Guwahati , held on 21 Nov, 2017

3. **Gogoi, D.** and Mukherjee, AK. Structural and physico-chemical characterization of a dirhamnolipid biosurfactant purified from *Pseudomonas aeruginosa*: application of crude biosurfactant in enhanced oil recovery. National Seminar on Petroleum Biotechnology and Bioenergy. Organized by ONGC- Centre for petroleum biotechnology and Department of MBBT on 3-4 March, 2017
4. **Gogoi, D.** and Mukherjee, AK. Cardiovascular drugs development from natural resources. Recent Advances in Snake Venom Research and Snake-bite Therapy: National and International Perspectives (SnakSymp-2016), held on 22-24, Nov, 2016

www.nature.com/scientificreports

SCIENTIFIC REPORTS

OPEN

Anticoagulant mechanism, pharmacological activity, and assessment of preclinical safety of a novel fibrin(ogen)olytic serine protease from leaves of *Leucas indica*

Received: 18 September 2017
Accepted: 26 March 2018
Published online: 18 April 2018

Debananda Gogoi[1], Neha Arora[2], Bhargab Kalita[1], Rahul Sarma[3], Taufikul Islam[1], Sidhhartha S. Ghosh[2], Rajlakshmi Devi[3] & Ashis K. Mukherjee[1]

The harnessing of medicinal plants containing a plethora of bioactive molecules may lead to the discovery of novel, potent and safe therapeutic agents to treat thrombosis-associated cardiovascular diseases. A 35 kDa (m/z 34747.5230) serine protease (lunathrombase) showing fibrin(ogen)olytic activity and devoid of N- and O- linked oligosaccharides was purified from an extract of aqueous leaves from *L. indica*. The LC-MS/MS analysis, *de novo* sequencing, secondary structure, and amino acid composition determination suggested the enzyme's novel characteristic. Lunathrombase is an αβ-fibrinogenase, demonstrating anticoagulant activity with its dual inhibition of thrombin and FXa by a non-enzymatic mechanism. Spectrofluorometric and isothermal calorimetric analyses revealed the binding of lunathrombase to fibrinogen, thrombin, and/or FXa with the generation of endothermic heat. It inhibited collagen/ADP/arachidonic acid-induced mammalian platelet aggregation, and demonstrated antiplatelet activity via COX-1 inhibition and the upregulation of the cAMP level. Lunathrombase showed *in vitro* thrombolytic activity and was not inhibited by endogenous protease inhibitors α_2 macroglobulin and antiplasmin. Lunathrombase was non-cytotoxic to mammalian cells, non-hemolytic, and demonstrated dose-dependent (0.125–0.5 mg/kg) *in vivo* anticoagulant and plasma defibrinogenation activities in a rodent model. Lunathrombase (10 mg/kg) did not show toxicity or adverse pharmacological effects in treated animals.

Cardiovascular diseases (CVDs) such as myocardial infarction, stroke, deep-vein thrombosis, and pulmonary embolism are major causes of mortality worldwide[1,2]. The haemostatic system requires a balance between fibrin formation (coagulation) and fibrin dissolution (fibrinolysis) to prevent the free flow of blood at sites of injury and to ensure the perfusion of blood through tissues[3]. Factor Xa and thrombin are recognized as indispensable components of the coagulation cascade[4]. FXa is the major component of the prothrombinase complex, comprised of factor Va, negatively charged phospholipids, and calcium ions[5]. The prothrombinase complex eventually converts inactive prothrombin to active thrombin for the conversion of soluble fibrinogen into insoluble fibrin polymer (clot), which is ultimately degraded by plasmin[4,6]. Any disruption in this delicate balance leads to thrombosis and/or hemorrhage that results in disseminated intravascular coagulopathy (DIC), which poses a clinical challenge for treatment.

[1]Microbial Biotechnology and Protein Research Laboratory, Department of Molecular Biology and Biotechnology, School of Sciences, Tezpur University, Tezpur, 784028, Assam, India. [2]Department of Biosciences and Bioengineering, Indian Institute of Technology, Guwahati, 781039, Assam, India. [3]Biochemistry Laboratory, Life Sciences Division, Institute of Advanced Study in Science and Technology, Guwahati, 781035, Assam, India. Correspondence and requests for materials should be addressed to A.K.M. (email: akm@tezu.ernet.in)

Higher levels of fibrinogen (hyperfibrinogenemia) have been reported to alter the hemodynamic properties of blood that subsequently enhance the intravascular fibrin deposition and pose as an independent risk factor for both arterial and venous thrombosis[7,8]. Higher levels of fibrinogen have also been reported to induce lipid proliferation that initiates the development of atherosclerosis, resulting in ischemic pathology[9]. Therefore, anticoagulant fibrinogenolytic enzymes capable of inhibiting thrombin have proven to be effective in preventing thrombosis[10–14] and treating hyperfibrinogenemia-associated disorders[15,16]. Such anticoagulant molecules need to be cost-effective and preferably devoid of the risk of hemorrhage, allergic reactions, and other adverse pharmacological complications seen in most of the commercial anticoagulant cardiovascular drugs[17,18].

Herbs containing antithrombotic activities have been suggested to act as medicinal plants that could lead to the discovery of novel therapeutic agents for treating thrombosis-associated diseases[19–23]. The plant *Leucas indica*, belonging to the Lamiaceae family is mostly used in folk medicine for treating asthma and as decoctions in traditional medicine to reduce nasal congestion. Interestingly, studies from our laboratory have discovered the presence of anticoagulant fibrinogenolytic enzyme(s) in the aqueous leaf extracts of this plant. To the best of our knowledge, this is the first report on the biochemical and pharmacological characterization, and elucidation of the anticoagulant mechanism of a fibrin(ogen)olytic serine protease purified from the aqueous leaf extract of *L. indica*. This plant-derived fibrinogenolytic serine protease demonstrated dual inhibition of thrombin and FXa, and did not show *in vivo* toxicity in experimental animals which has never before been demonstrated for any protease, and the finding suggests its therapeutic application as an anticoagulant, antithrombotic drug.

Results

Lunathrombase is a major fibrinogenolytic protease purified from the leaves of *L. indica*. Fractionation of crude aqueous leaf extracts of *L. indica* through an anion exchange matrix resulted in separation of proteins into nine peaks (Fig. 1a). Peak1 (AEX_1) eluted with the equilibration buffer (unbound fractions) and showed significant fibrinogenolytic and anticoagulant activities. Cation-exchange chromatography was used for the AEX_1 fraction, which was separated into eight fractions (CEX_1 to CEX_8) (Fig. 1b). The unbound peak CEX_1 eluted with the equilibration buffer demonstrated significant fibrinogenolytic and anticoagulant activities. HPLC gel filtration of CEX_1 fraction resolved it in three protein peaks (AF_GF1 to AF_GF3); the AF_GF3 fractions eluted in tube no. 45 to 48 with retention time 23 to 24 min showed highest fibrinogenolytic activity (Fig. 1c). The SDS-PAGE (reduced) analysis of 20 µg of protein from the AF_GF3 peak proteins revealed a single, distinct band for a 35 kDa protein (Fig. 1d), which was named lunathrombase. By MALDI-ToF-MS analysis lunathrombase showed a single sharp peak at m/z 34767.52 Da indicating purity of preparation (Fig. 1e). The summary of purification of lunathrombase is shown in Supplementary Table S1. The anticoagulant and fibrinogenolytic activity of all the gel filtration fractions were found to be lower as compared to CEX_1 fraction which was due to other low molecular mass phytochemicals present in this fraction (CEX_1) that contributed to anticoagulant activity. Further, the combined fibrinogenolytic activity of all the three gel filtration fractions results in higher specific activity of cation exchange fraction CEX_1.

Peptide mass fingerprinting, *de novo* sequencing, amino acid composition, and secondary structure analyses of the unique lunathrombase. Tandem mass spectroscopic analysis and *de novo* sequencing of lunathrombase did not reveal its similarity with any plant protein, suggesting that it may be a new plant protein. Nevertheless, one of the MS-MS-derived tryptic fragments of lunathrombase (IITHPNFNGNTLDNDIMLIK) demonstrated a conserved domain belonging to the trypsin-like superfamily suggesting that lunathrombase may be a previously uncharacterized plant protease. The alignment of IITHPNFNGNTLDNDIMLIK with other trypsin (-like) enzymes is shown in Supplementary Fig. S1.

Analysis of the amino acid composition of lunathrombase using Swiss-prot and TrEMBL databases did not reveal any similarity with other proteins from plants (Supplementary Table S2). The combined results indicate that lunathrombase is a novel protease from *L. indica*. In addition, analysis of the CD spectrum of lunathrombase demonstrated that it consists of 23.4% α-helix, 17% beta sheets, with a turn of 28.2% and 31% random coils (Fig. 1f).

Lunathrombase demonstrated anticoagulant and fibrin(ogen)olytic activity and did not contain N- or O-linked oligosachharides. Lunathrombase dose-dependently prolonged the Ca^{2+} clotting time of PPP, and at a concentration of 400 nM, saturation in anticoagulant activity was observed (Fig. 2a). Lunathrombase demonstrated optimum anticoagulant activity at 10 min of pre-incubation with PPP (Supplementary Fig. S2). At a concentration of 500 nM, lunathrombase did not affect APTT, though it significantly ($p < 0.05$) enhanced the PT of PPP (Fig. 2b).

Lunathrombase showed dose- and time-dependent fibrin(ogen)olytic activity. The kinetics of fibrinogen/fibrin degradation indicated that lunathrombase preferentially degraded the Aα chain of fibrinogen/fibrin (Fig. 3a,b). With an increase in incubation time to 120 min, the Bβ chain was slowly removed; however, the γ-chain of fibrinogen/fibrin remained intact after 2 h of incubation at 37 °C (Fig. 3a,b). The fibrinogenolytic activity of lunathrombase was found to be superior to Nattokinase, plasmin, and thrombin (Supplementary Fig. S3); whereas, the fibrinolytic activity of lunathrombase surpassed that of Nattokinase, streptokinase, and plasmin under identical experimental conditions (Supplementary Fig. S4). The *Km and Vmax* values of lunathrombase towards fibrinogen were determined to be 52.64 ± 9.8 µM and 52.33 ± 5.7 µM/min (mean ± SD), respectively (Supplementary Fig. S4) whereas the *Km and Vmax* values of Nattokinase towards fibrinogen were determined at 2.88 ± 1.1 µM and 1.97 ± 0.5 µM/min, respectively (Supplementary Fig. S6). The RP-HPLC analysis indicated that lunathrombase and Nattokinase perhaps cleaves different sites of fibrinogen resulting in different elution profiles of the fibrinogen/fibrin degradation products from the RP-HPLC column (Supplementary Fig. S7).

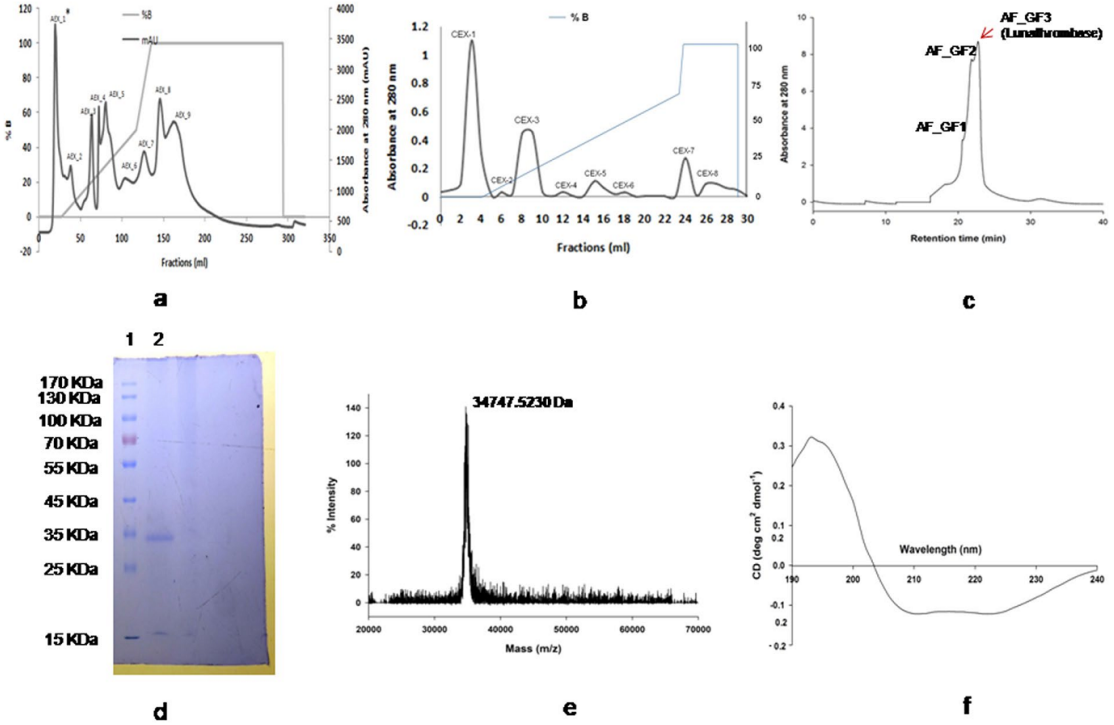

Figure 1. (**a**) Fractionation of crude aqueous shade leave extract of *L. indica* on a PrepTM anion exchange DEAE-cellulose FF 16/10 column. After washing the column with two volume of equilibration buffer (20 mM K.P buffer, pH 7.4),the bound fraction were eluted with a linear gradient of 0.1–1.0 M NaCl in 20 mM K.P buffer at pH 7.4 at a flow rate of 1.0 ml/min. The elution profile was monitored at 280 nm. The first peak (AEX_1) corresponds to the elution of fraction showing highest anticoagulant and fibrin(ogeno) lytic activities. (**b**) Fractionation of the anion-exchange unbound fraction (AEX_1 peak) on cation exchange CM-cellulose (20 mm × 60 mm) column. After washing the column with two volume of equilibration buffer (20 mM K.P buffer, pH 7.4), the bound fraction were eluted with a linear gradient of 0.1–1.0 M NaCl in 20 mM K.P buffer at pH 7.4 at a flow rate of 0.5 ml/min. The elution profile was monitored at 280 nm. The *L. indica* first peak (CEX_1) corresponds to the elution of fraction showing highest anticoagulant and fibrin(ogeno)lytic activities. (**c**) Gel filtration of the CEX_1 on Shodex KW-803 column (5 µm, 8 × 300 mm). After washing the column with two volume of equilibration buffer (20 mM K.P buffer, containing 150 mM NaCl pH 7.4). Elution was carried out with equilibration buffer at a flow rate of 0.5 ml/min. The red arrow indicates elution of lunathrombase (**d**) Determination of purity and molecular mass of AF_GF3 (lunathrombase) by 12.5% SDS-PAGE; Lane 1, protein molecular markers; lane 2, reduced lunathrombase (20.0 µg). (**e**) MALDI-ToF mass spectra of lunathrombase (5.0 µg). (**f**) Circular dichroism (CD) spectra of lunathrombase. Native lunathrombase (0.3 mg/ml) was dissolved in 20 mM potassium phosphate buffer pH 7.0 and the far UV-CD spectra was recorded at room temperature (~25 °C) between 190 and 240 nm against the appropriate buffer (blank). The original unedited gel of Fig. 1d is shown in Supplementary Figure 22.

The lunathrombase-mediated degradation of fibrinogen in the presence of FPA or FPB, or with both FPA and FPB, did not result in the inhibition of fibrin(ogeno)lytic activity, when compared to controls (without fibrinopeptides) (data not shown). This result suggests that free FPA or FPB do not influence the fibrin(ogeno)lytic activity of lunathrombase. Lunathrombase did not hydrolyze albumin or globulin (data not shown). It showed optimum fibrin(ogen)olytic activity at 35–37 °C and at pH 7.0–7.4 (Supplementary Figs S8 and S9). Lunathrombase demonstrated BAEE and TAME hydrolyzing activity with specific activities of 436 ± 9.5 and 321 ± 11.2 U/mg (mean ± SD, n = 3), respectively. Lunathrombase contained 7.0% of neutral sugar, though it did not contain N- or O-linked oligosaccharides (Supplementary Fig. S10).

Inhibitor study shows lunathrombase is a serine protease and its activity is not influenced by the endogenous protease inhibitors of plasma. The fibrin(ogen)olytic activity of lunathrombase was not affected ($p > 0.05$) by any of the tested metal ions (Supplementary Fig. S11), though it was inhibited by PMSF (a serine protease inhibitor), iodoacetamide (a cysteine protease inhibitor), and pBPB (a histidine inhibitor) (Supplementary Table S3 and Supplementary Fig. S12). Nevertheless, EDTA (a metalloprotease inhibitor) and DTT (a disulfide bond reducing agent) failed to inhibit the fibrin(ogen)olytic activity of lunathrombase (Supplementary Table S3, Supplementary Fig. S12). The SDS-PAGE analysis suggested that lunathrombase at the

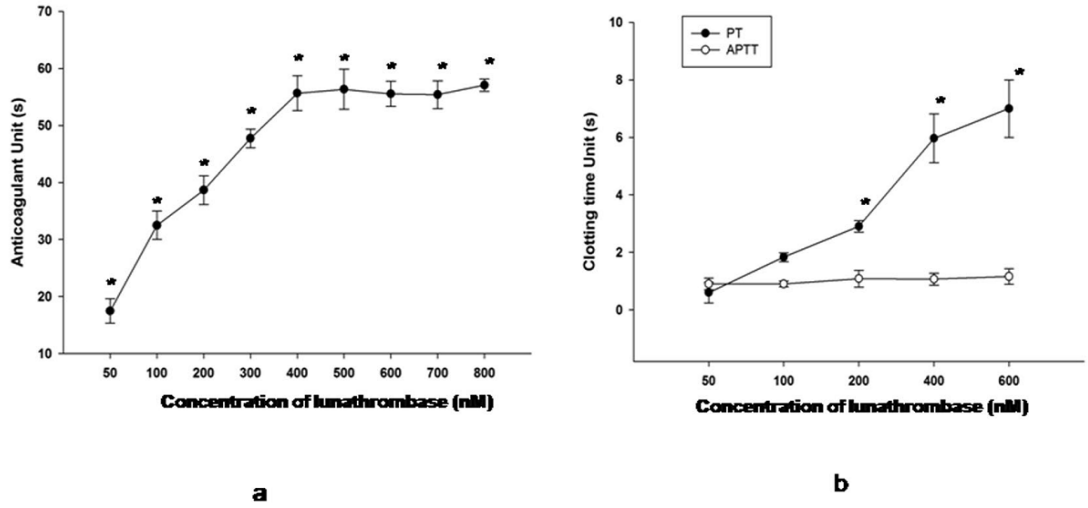

Figure 2. (**a**) Dose- dependent *in vitro* anticoagulant activity of lunathrombase against human platelet-poor plasma. (**b**) Effect of lunathrombase (50–600 nM) on APTT and PT of PPP isolated from human blood. Values are mean ± S.D. of triplicate determinations. Significance of difference with respect to control (without lunathrombase) *$p < 0.05$.

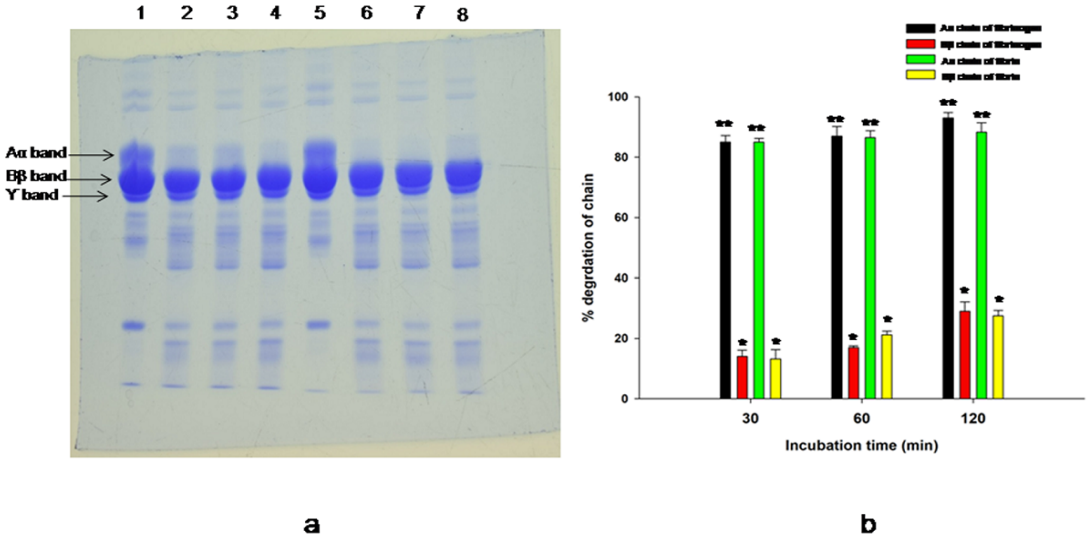

Figure 3. (**a**) Kinetics of fibrinogenolytic activity of lunathrombase. The degradation products were separated by 12.5% SDS-PAGE (reducing conditions). Lane 1, control human fibrinogen (0.25% w/v in 20 mM K-phosphate buffer, 150 mM NaCl, pH 7.4); lanes 2–4, human fibrinogen treated with lunathrombase (0.2 μM) for 30, 60 and 120 min, respectively, at 37 °C, pH 7.4. Kinetics of fibrinolytic activity of lunathrombase. Lane 5, control human fibrin; lanes 6–8, human fibrin treated with 0.2 μM lunathrombase for 30, 60 and 120 min, respectively, at 37 °C, pH 7.4. (**b**) Densitometry analysis to determine the percent degradation of Aα- and Bβ-chains of fibrinogen/fibrin. Significance of difference with respect to control Aα chain of fibrinogen/fibrin (0% degradation), **$p < 0.01$; Significance of difference with respect to control Bβ chain of fibrinogen/fibrin (0% degradation) *$p < 0.05$.

tested dose was unable to degrade extracellular matrix proteins, namely Type-IV collagen, laminin, and fibronectin at physiological conditions (37 °C, pH 7.4) (Supplementary Fig. S13). Further, the endogenous protease inhibitors, α_2 macroglobulin and antiplasmin, did not inhibit the fibrin(ogen)olytic activity of lunathrombase (data not shown).

Lunathrombase inhibits the pharmacological activity of the blood coagulation factors, thrombin and FXa. Lunathrombase significantly inhibited the amidolytic activity of thrombin (Fig. 4a) and FXa (Fig. 4b). The *Ki* value for the inhibition of amidolytic activity of thrombin and FXa by lunathrombase

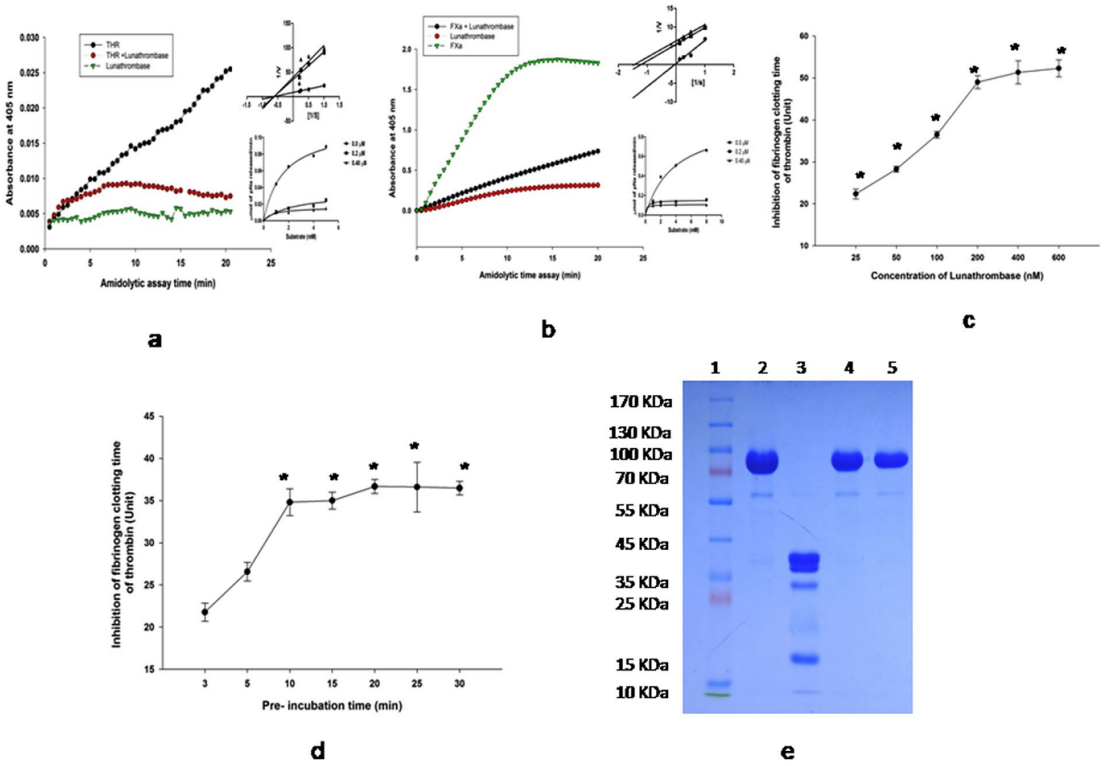

Figure 4. Effect of lunathrombase (0.2 µM) on amidolytic activity of (**a**) thrombin (36.6 nM) against its chromogenic substrate T1637 (0.2 mM). Inset. Michaelis-Menton and Lineweaver-Burk plot showing inhibition of amidolytic activity of thrombin towards T1637 (0.2 mM) by lunathrombase (0–0.4 µM). The plots are the means of 3 independent measurements. (**b**) FXa (0.13 µM) against its chromogenic substrate F3301 (0.2 mM). The values are mean of triplicate determinations. Inset. Michaelis-Menton and Lineweaver-Burk plot showing inhibition of amidolytic activity of FXa towards F3301 (0.2 mM) by lunathrombase (0–0.4 µM). The plots are the means of 3 independent measurements. (**c**) Inhibition of fibrinogen clotting activity of thrombin by lunathrombase (25–600 nM) at 37 °C, pH 7.4. (**d**) Time- dependent inhibition of fibrinogen clotting time of thrombin by lunathrombase (100 nM) at 37 °C, pH 7.4. The fibrinogen clotting time of thrombin under identical experimental conditions (control) was found to be 39.17 ± 1.54 s. The values are mean ± S.D. of triplicate determinations. Significance of difference with respect to control (without lunathrombase) *$p < 0.05$. (**e**) Inhibition of prothrombin activation property of FXa by lunathrombase. After reduction with β-mercaptoethanol, degradation products were separated by 12.5% SDS-PAGE. Lane 1, protein molecular markers; lane 2, 1.4 µM PTH; lane 3, PTH (1.4 µM) incubated with FXa (0.13 µM) for 30 min at 37 °C, pH 7.4; lane 4, [FXa (0.13 µM) pre-incubated with lunathrombase (0.2 µM) for 15 min] + PTH (1.4 µM); lane 5, PTH + lunathrombase.

was determined to be 26.90 ± 0.9 nM and 10.35 ± 1.8 nM (mean ± SD, n = 3), respectively. Lunathrombase dose-dependently prolonged the fibrinogen clotting time of thrombin and the saturated thrombin inhibition was observed at a 200 nM concentration of lunathrombase (Fig. 4c). The optimum inhibition was observed at 10 min of pre-incubation with thrombin and 200 nM lunathrombase (Fig. 4d). Further, lunathrombase (0.2 µM) completely (100%) inhibited the prothrombin activation by FXa (Fig. 4e). Nevertheless, SDS-PAGE analysis did not show thrombin degradation by lunathrombase (data not shown) suggesting that its anticoagulant mechanism does not depend on the catalytic degradation of thrombin.

Spectrofluorometric analysis shows the interaction of lunathrombase with thrombin/fibrinogen/FXa. A steady decrease in the fluorescence intensity of thrombin was observed in the presence of lunathrombase (Fig. 5a). The interaction between lunathrombase and FXa (Fig. 5b) or fibrinogen (Fig. 5c) resulted in an increase in the fluorescence intensity, compared to the fluorescence intensity of individual proteins. The dissociation constant (*Kd*) for the binding of lunathrombase to thrombin, FXa, and fibrinogen was calculated to be 0.2492 µM, 1.908 µM, and 0.5516 µM, respectively (Fig. 5a–c).

Isothermal calorimetry analysis of the interaction between lunathrombase and thrombin or fibrinogen. The titration of thrombin or fibrinogen with lunathrombase resulted in a strong endothermic generation of heat with a clear sigmoidal saturation curve indicating the direct binding interactions (Fig. 5d,e).

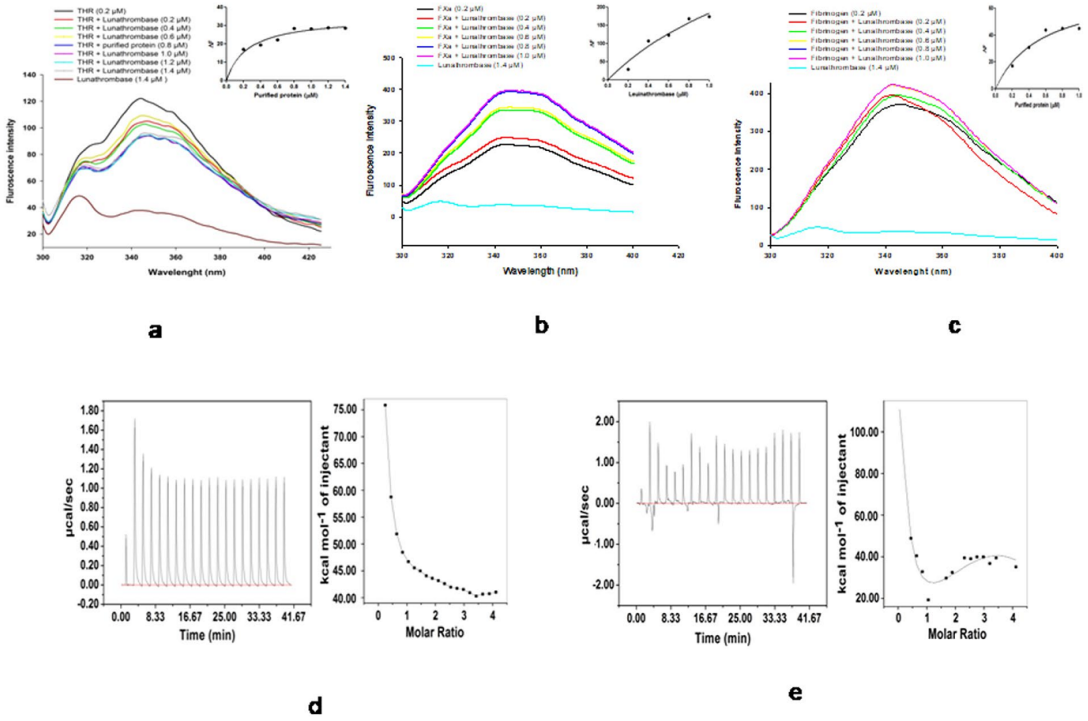

Figure 5. (**a**) Fluorescence spectra showing interaction of thrombin (0.2 µM) with different concentrations of lunathrombase (0.2–1.4 µM). Inset. One site saturation binding curve of lunathrombase for thrombin. (**b**) Fluorescence spectra showing interaction of FXa (0.2 µM) with different concentrations of lunathrombase (0.2–1.4 µM). Inset. One site saturation binding curve of lunathrombase for FXa. (**c**) Fluorescence spectra showing interaction of fibrinogen (0.2 µM) with different concentrations of lunathrombase (0.2–1.4 µM). Inset. One site saturation binding curve of lunathrombase for fibrinogen. (**d**) ITC profile for lunathrombase (10 µM) binding to thrombin (200 µM). Left panel shows heat change upon ligand addition; right panel shows an integrated ITC isotherm and is best fit to a sequential binding site model. (**e**) ITC profile for lunathrombase (10 µM) binding to fibrinogen (200 µM). Left panel shows heat change upon ligand addition; right panel shows an integrated ITC isotherm and is best fit to a sequential binding site model.

The best fit for the titration curve was obtained with a sequential binding site model with a binding constant (*Ka*) of 9.7×10^{-4} M^{-1}, $\Delta H = 2.07 \times 10^{-5}$, $\Delta S = 717$ cal/mol/deg for the interaction between lunathrombase and thrombin, and 1.02×10^{-5} M^{-1}, $\Delta H = 2.3 \times 10^{-5}$, $\Delta S = 816$ cal/mol/deg for the interaction between lunathrombase and fibrinogen.

Lunathrombase has *in vitro* thrombolytic potency but is devoid of hemolytic activity or cytotoxicity against mammalian cells. The *in vitro* thrombolytic potential of lunathrombase and commercial thrombolytic agents (streptokinase, plasmin, Nattokinase and tissue plasminogen activator) is shown in Supplementary Fig S14. The *in vitro* thrombolytic activity of equimolar concentrations of streptokinase, plasmin, Nattokinase, t-PA and lunathrombase was found to be identical. Nevertheless, the thrombolytic potency of lunathrombase, Nattokinase, and plasmin towards a heat-treated blood clot was reduced to 80%, 75%, and 60%, respectively of their original activity to dissolve an unheated blood clot (Supplementary Fig. S14). Streptokinase and tissue plasminogen activator showed negligible activity (<1%) in dissolving a heated blood clot (Supplementary Fig. S14).

Lunathrombase did not show *in vitro* rupturing of mammalian erythrocytes or cytotoxicity against HEK 293 cells (Supplementary Fig. S15). The fluorescence microscopic study indicated that at 24 h of treatment, lunathrombase did not change the cell morphology or membrane integrity of treated-HEK 293 cells in comparison to control cells (Supplementary Fig. S16). Further, no significance difference ($p > 0.05$) was found in G1, S, and G2 phases of lunathrombase-treated cell as compared to control HEK 293 cells (Supplementary Fig. S17).

Lunathrombase showed antiplatelet activity by inhibiting collagen/ADP/arachidonic acid-induced platelet aggregation. A comparable dose-dependent platelet de-aggregation (antiplatelet) property was displayed by equimolar concentrations of lunathrombase and aspirin (Fig. 6a). Lunathrombase also exhibited a dose-dependent inhibition of the collagen/ADP/arachidonic acid-induced aggregation of PRP (Fig. 6b). The concentration at which lunathrombase demonstrated 50% inhibition (IC_{50}) of collagen/ADP/

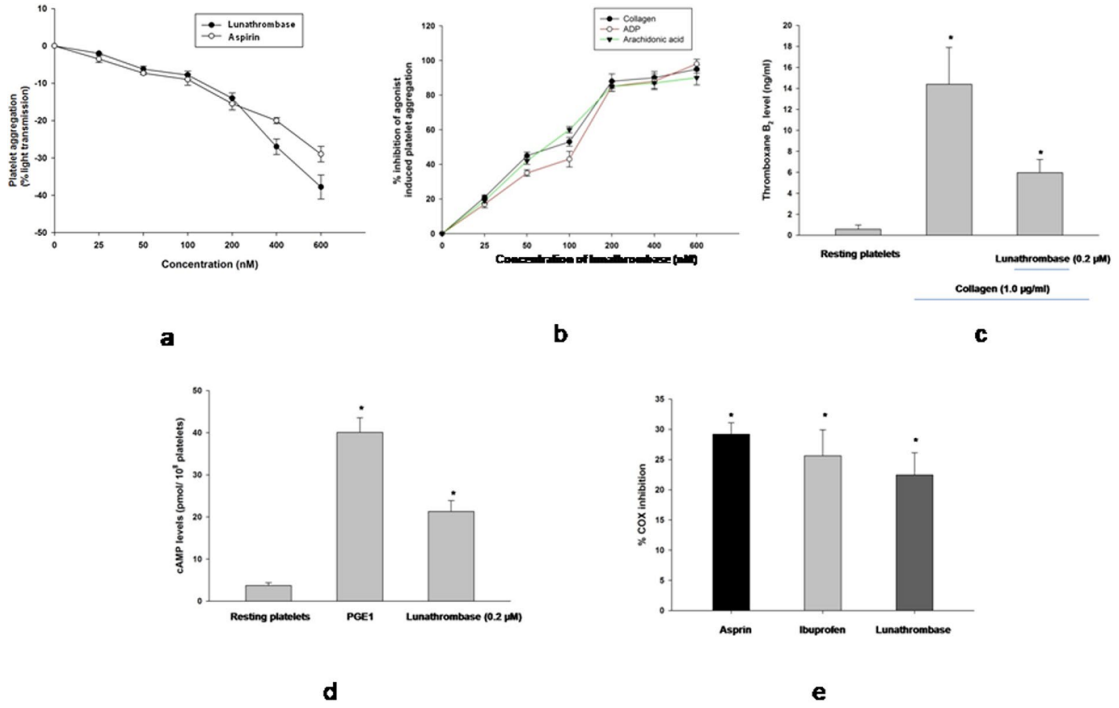

Figure 6. (**a**) Dose-dependent platelet deaggregation by lunathrombase / aspirin. Different concentrations of (0–600 nM) of lunathrombase or aspirin were incubated with platelet rich plasma at 37 °C and absorbance was recorded at 540 nm. Data represent mean ± SD of triplicate experiments. (**b**) Dose-dependent inhibition of collagen / ADP / arachidonic acid -induced platelet aggregation by lunathrombase. Different concentrations of lunathrombase (0–600 nM) was incubated with PRP at 37 °C for 10 min and then collagen (6.2 nM) / ADP (30 µM) / arachidonic acid (15 µM) was added in the reaction mixture. The percent platelet aggregation by collagen/ADP/arachidonic acid in absence of lunathrombase was considered as 100% activity and other values were compared to this. The IC_{50} value of lunathrombase (that showed 50% inhibition of collagen / ADP / arachidonic acid -induced platelet aggregation) was determined from the regression analysis of inhibition curve. Data represent mean ± SD of triplicate experiments. Effect of lunathrombase on (**c**) thromboxane B_2 and (**d**) cAMP formation in activated platelets. Washed platelets were pre-incubated with lunathrombase (0.2 µM) or 0.5% DMSO on intraplatelet levels of cAMP formation in human platelets. Platelets were incubated with PGE1 (0.2 µM, positive control) or lunathrombase (0.2 µM) for measurement of cAMP formations. (**e**) Effect of lunathrombase on COX-1 activity. COX-1 enzyme was pre-incubated with lunathrombase or aspirin or ibuprofen (0.2 µM) for 30 min at 37 °C. The activity of control (without drugs) was considered as 100% and other values were compared with that. All values are means ± S.D. of triplicate determinations. Significance of difference with respect to control (without lunathrombase), *$p < 0.05$.

arachidonic acid-induced platelet aggregation was determined at 152.82 nM, 181.26 nM, and 159.89 nM, respectively (Fig. 6b).

The platelet deaggregation property (antiplatelet activity) of catalytically inactive lunathrombase was reduced to ~30% of its original activity exhibited by the catalytically active lunathrombase (Supplementary Fig. S18). However, there was no difference ($p > 0.05$) between the catalytically active and inactive lunathrombase in inhibiting the collagen/ADP/arachidonic acid-induced platelet aggregation (Supplementary Fig. S18). Fibrinogen induced aggregation of chymotrypsin-treated platelets but did not show aggregation of control (untreated) platelets (Supplementary Fig. S19). On the contrary, native and PMSF-treated lunathrombase caused deaggregation of α-chymotrypsin-treated as well as control platelets. Further, catalytically inactive lunathrombase did not interfere the binding of fibrinogen to platelet receptor GPIIb/IIIa (Supplementary Fig. S20).

Lunathrombase increased cAMP level and inhibited COX-1 enzyme to exert its antiplatelet effect. Lunathrombase (0.2 µM) significantly inhibited the collagen (1 µg/ml)-stimulated TxB_2 formation in washed platelets (Fig. 6c). Exogenous addition of lunathrombase (0.2 µM) to washed platelets increased its endogenous cAMP level (Fig. 6d). Furthermore, lunathrombase inhibited the COX-1 activity of collagen-treated platelets (Fig. 6e). In *in vitro* condition lunathrombase non-competitively inhibited the COX-1 enzyme with a *Ki* value of 5.947 ± 0.97 µM. The *Km and Vmax* values of lunathrombase towards COX-1 enzyme were determined at 1.5 ± 0.16 µM and 138.5 ± 5.7 µM/min (mean ± SD), respectively (Supplementary Fig. S21).

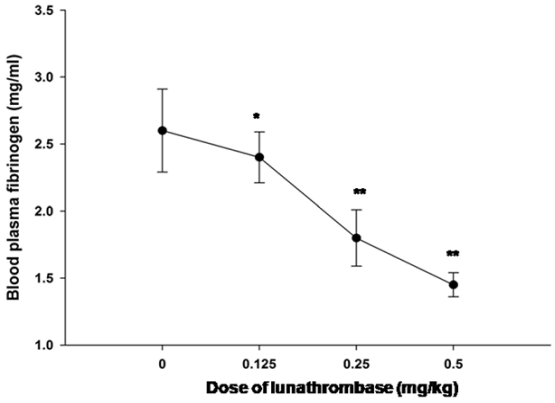

Figure 7. Dose- dependent *in vivo* defibrinogenating activity of lunathrombase 5 h after *i.p.* injection in rats. Values are means ± S.D. of triplicate determinations. Significance of difference with respect to control, *$p < 0.05$, **$p < 0.01$.

	PT (s)	PT (INR)	APTT (s)	APTT (INR)	Tail bleeding time (s)	Plasma clotting time (s)
Control rats	14.84 ± 0.77	1.0	28.37 ± 1.4	1.0	45.33 ± 2.51	175.5 ± 9.14
Lunathrombase- treated rats (0.5 mg/kg)	28.1 ± 2.9*	1.89	30.23 ± 2.11	1.06	110 ± 1.41*	216.3 ± 8.8*
Heparin-treated rats (0.5 mg/kg)	21.48 ± 2.6*	1.44	32.77 ± 2.06	1.16	137.5 ± 4.9*	202.5 ± 10.3*
Nattokinase- treated rats (0.5 mg/kg)	20.1 ± 0.2*	1.35	30.33 ± 4.1	1.06	116.0 ± 8.0	201.3 ± 13.1*

Table 1. A comparison of *in vivo* anticoagulant activity of lunathrombase, heparin and Nattokinase treated Wister rats. The blood was withdrawn 5 h after *i.p.* injection of lunathrombase (0.5 mg/kg) or heparin (0.5 mg/kg) or Nattokinase (0.5 mg/kg).Values represent mean ± SD of six determinations. Significance of difference with respect to control. *$p < 0.01$. INR = ($prothrombin_{test}$/$prothrombin_{control}$).

Lunathrombase was non-toxic to rats but demonstrated *in vivo* anticoagulant and defibrinogenating activity. Lunathrombase at a dose of 10.0 mg/kg was found to be non-toxic to rats and showed no adverse effects or behavioral changes in treated-rats. The hematological parameters of blood from lunathrombase-treated rats (72 h post-treatment) did not show any significant deviation compared to the control group of rats; however, a minor increase in neutrophil content was found in the blood of the treated group of rats compared to control rats, which was within the normal range (Supplementary Table S4). In addition, none of the serum parameter of the treated rats was found to change ($p > 0.05$) in comparison to the serum profile of control group of rats (Supplementary Table S5). Plasma IgG, IgA, and IgE contents of lunathrombase-treated rats did not differ significantly from those of the control group of rats (data not shown). Light microscopic examination of the liver, kidney, and cardiac tissues of the lunathrombase-treated rats did not show any morphological alterations or pathophysiological symptoms (data not shown).

Lunathrombase demonstrated dose-dependent *in vivo* defibrinogenation of rat plasma (Fig. 7) with a corresponding dose-dependent increase in the *in vitro* tail bleeding time, Ca-clotting time and PT of PPP in the treated group of rats compared to the control group (Table 1).

Discussion

The present study is the first to report on the purification and characterization of a fibrin(ogen)olytic serine protease showing strong anticoagulant, antithrombotic, and thrombolytic activities from the leaves of *L. indica*. The proteomics and amino acid composition analyses suggest that lunathrombase is a previously uncharacterized novel plant protease. Lunathrombase is an αβ-fibrinogenase, because it can degrade both α- and β-chains of fibrinogen[24–28], demonstrating a fibrinogen degradation pattern that differs from other plant proteases[1,21,29–31]. The significant inhibition of the enzymatic activity of lunathrombase by serine protease inhibitors unambiguously demonstrates that lunathrombase is a serine protease and lack intramolecular and intermolecular disulfide linkage(s)[32–34]. Failure to inhibit the protease activity of lunathrombase by α_2MG or antiplasmin suggests that this enzyme may also exert its activity *in vivo*.

Defibrinogenation, inhibition of platelet aggregation, and/or interference with components of the blood coagulation cascade are some of the key mechanisms by which proteolytic enzymes exert their anticoagulant effect[1,32,35]. The anticoagulant action of lunathrombase is due to its fibrinogenolytic property which is substantiated by its potency to inhibit thrombin and FXa as well as its antiplatelet effect. Spectrofluorometric analysis suggested the interactions between lunathrombase and thrombin/FXa/fibrinogen[36,37]. The higher *Kd* value indicated stronger interactions between lunathrombase and thrombin/FXa compared to those between lunathrombase and fibrinogen. Nevertheless, lunathrombase exerts its catalytic activity only on fibrinogen and would therefore

inhibit thrombin/FXa by a non-enzymatic mechanism. The lower *km* value of lunathrombase towards fibrinogen, compared to Nattokinase and fibriongen indicates higher specificity of the former enzyme for the physiological substrate instead of Nattokinase.

The interaction between lunathrombase and thrombin/fibrinogen was also ascertained by ITC titration, which indicated a direct interaction between lunathrombase and thrombin/fibrinogen. The higher ΔH values suggest that the interactions are enthalpy-driven with the primary contributions to the complex stabilization likely resulting from electrostatic interactions and/or hydrogen bonds[38,39]. The *Kd* value is inversely proportional to the *Ka* value; the higher the *Ka* value for lunathrombase towards thrombin vs. fibrinogen indicates its higher affinity for thrombin, which is consistent with the spectrofluorometric analysis. The anticoagulant mechanism of lunathrombase appears to differ from that of the currently available anticoagulant drugs such as heparin and warfarin that act via the indirect inhibition of thrombin and by vitamin K antagonism, respectively[40,41]. The dual inhibition of thrombin and FXa by lunathrombase may lead to its consideration as an alternative new drug to the traditional cardiovascular drugs[15].

A close association exists between platelet aggregation and the initiation of thrombus formation[42]. ADP or collagen, bind to the purinergic receptors P2Y1 and P2cyc, GPVI receptors, Integrin αIIbβ3, and the fibrinogen receptor on the platelet surface to induce platelet aggregation and adhesion[43,44]. The precise control of platelet function is an obligatory requirement for preventing thrombotic events[44–46]. The inhibition of platelet aggregation by lunathrombase was corroborated by a significant increase in the platelets cytosolic cAMP level. The activation of human platelets is inhibited by intracellular cAMP and cGMP-mediated pathways[47]. An increase in the intraplatelet levels of cAMP has been shown to downregulate the expression of the P2Y1R ADP-receptor, which is necessary for shape change[48], maintaining GPVI (collagen receptor) in a monomeric form, keeping platelets in a resting state[49,50], and inhibiting the release of sCD40L from platelets via the HSP27/p38 MAP kinase pathway[51]. The COX-1 isoenzyme is involved in the synthesis of prostaglandin that participates in platelet aggregation via the prostaglandin derivative, thromboxane B_2[52,53]. The inhibition of COX-1 leads to inhibition of thromboxane B_2 synthesis, which results in the inhibition of platelet aggregation[53]. Although *ex-vivo* study has shown the inhibition of COX-1 by lunathrombase; however, being a large molecule its direct interaction with intracellular COX-1 is unlikely. Therefore, it may inhibit COX-1 as well as up regulate the intracellular cAMP level by an indirect mechanism(s) which remains to be explored. Further, lunathrombase deaggregates platelets by both enzymatic and non-enzymatic mechanisms, though the latter mechanism predominates. However, the equipotent inhibition of collagen / ADP/ arachidonic acid-induced platelet aggregation by native and catalytically inactive lunathrombase indicates that these inhibitions are independent of the enzymatic activity of lunathrombase.

Limited proteolysis with α-chymotrypsin exposes glycoproteins GPIIb and GPIIIa, the two subunits of the platelet fibrinogen receptor GPIIb/IIIa complex at the surface of platelets, without interfering with cell activation or granular secretion[54]. Subsequently, fibrinogen binds to α-chymotrypsin-treated platelets to induce their aggregation[54]. Nevertheless, platelet deaggregation of α-chymotrypsin-treated platelets, caused by both native and PMSF-treated (catalytically inactive) lunathrombase suggests that this protease does not hydrolyze the fibrinogen receptor GPIIb/IIIa complex of platelets to exert the antiplatelet activity. Proteins harboring an RGD motif are shown to bind to GPIIb/IIIa platelet receptor and they may interfere the binding of fibrinogen to the receptor thereby inhibiting platelet aggregation[55,56]. Although presence of RGD motif in lunathrombase is unknown; however, this protease did not show binding to platelet GPIIb/IIIa receptor, and did not interfere the binding of fibrinogen to this receptor to inhibit platelet aggregation. This unequivocally indicates that the platelet deaggregation property (antiplatelet activity) of lunathrombase is not associated with impeding the binding of fibrinogen to platelet GPIIb/IIIa receptor. The exact mechanism of the anti-platelet activity of lunathrombase is our next goal of study. Further, the characterization of the clot bursting activity of lunathrombase provides a fair indication that lunathrombase is a plasmin-like, direct-acting fibrinolytic enzyme reinforcing its possible therapeutic application as a thrombolytic agent.

Administration of lunathrombase at a dose of 10.0 mg/kg, which is approximately 90 times greater than its anticoagulant dose (0.125 mg/kg), did not produce acute toxicity or adverse pharmacological effects in rats, indicating its preclinical safety and high therapeutic index. Hyperfibrinogenemia in blood is associated with increased risk of cardiovascular disorders[57] and may promote the growth of lung and prostate cancer cells through interactions with fibroblast growth factor 2[58]. Lunathrombase also demonstrated *in vivo* defibrinogenation potential which leads us to anticipate the possible therapeutic applications of lunathrombase for treating and/or preventing cardiovascular diseases and the need for clinical trials.

Conclusion

Ethnomedicines are regarded as depositories of potential therapeutic molecules that may affect the process of hemostasis. Lunathrombase is a previously uncharacterized non-toxic fibrinogenolytic from leaves of *L. indica*. It was characterized biochemically and pharmacologically and shown to exert dual inhibition of both thrombin and FXa via different non-enzymatic mechanisms. The potent *in vitro* and anticoagulant effects of lunathrombase suggest its pharmacological significance as an anticoagulant drug. It also showed *in vitro* antiplatelet and thrombolytic activities and *in vivo* defibrinogenating activity. In summary, therapeutic applications of lunathrombase for preventing and/or treating hyperfibrinogenemia- and thrombosis-associated cardiovascular disorders seem promising.

Materials and Methods

Chemicals. Coagulation proteins were purchased from Calbiochem, Germany. Human thrombin, prothrombin, human fibrinogen, and extracellular matrix (ECM) proteins like type-IV collagen, laminin, and fibronectin were purchased from Sigma Aldrich, USA. All commercially available drugs, like tissue plasminogen activator, streptokinase and plasmin were purchased from Sigma Aldrich, USA. Nattokinase was purchased from Healthy

Origins, Pittsburg, USA. PT and APTT kits were purchased from Tulip diagnostics, Mumbai. LDL, HDL, and triglycerides assay kits were purchased from Diatek Healthcare Pvt. Ltd., Kolkata, India. The cholesterol assay kit was purchased from Sirus Biocare Pvt. Ltd., Kolkata, India, the fibrinogen assay kit was purchased from R^2 Diagnostics, USA, and the immunoglobulin EIA kits were obtained from Thermo Fisher Scientific, USA. All other reagents were of analytical grade and purchased from Sigma Aldrich, USA.

Collection of plant leaves and preparation of the aqueous extract. Leaves of *L. indica* were collected from 20 cm tall herbs, from areas surrounding the Sivasagar district, Assam (26.9844°N, 94.6314°E). The identity of the plant was confirmed by the Botanical Survey of India (BSI), Shillong, Meghalaya and a voucher specimen was deposited (accession number 37604). Fresh leaves of *L. indica* (100 g wet weight) were homogenized in a blender for 10 min and the extraction was carried out by stirring the crushed fresh leaves in ultrapure water (arium® advance EDI water purification system, Sartorius) (The pH of the water was adjusted to 7.4 by adding 0.01 N NaOH) for 4 h at 4 °C. The extract was filtered through muslin cloth followed by 0.45 µM pore-sized filter paper (Whatman, USA) and the filtrate was centrifuged (Multifuge X1R, Thermo Scientific) at 10,000 rpm for 10 min at 4 °C. The supernatant was collected, lyophilized, weighed, and stored at 4 °C until further use.

Purification of the fibrinogenolytic protease (lunathrombase). The dried extract (25.0 mg dry weight) was dissolved in 500 µl of 20 mM potassium phosphate buffer, pH 7.4, filtered through a 0.2 µm nylon syringe filter (Genetix Biotech Asia Pvt. Ltd.), and then loaded on a Hi Prep™ anion- exchange column (pre-equilibrated with the above buffer) attached to a Fast Protein Liquid Chromatography (FPLC) system (AKTA purifier 10, Wipro-GE Healthcare Biosciences, Upsala, Sweden). After washing the unbound and the non-specifically bound proteins with two volumes of equilibration buffer, the bound proteins were eluted using a 0.1–1.0 M NaCl gradient at a flow rate of 1 ml/min at 4°C. Fractions of 2 ml were collected and the elution of protein was measured at 280 nm. The protein content, anticoagulant activity, and fibrino(geno)lytic activity of each peak were screened (see below).

The fractions showing the significant anticoagulant and fibrinogenolytic activity were pooled, concentrated using a lyophilizer and then fractionated through a CM-Cellulose cation-exchange column (20 mm × 60 mm) that had been pre-equilibrated with 20 mM potassium phosphate buffer, pH 7.4 Fractions were eluted using a 0.1M-1.0 M NaCl gradient at a flow rate of 0.5 ml/min. Fraction elutions were monitored at 280 nm and 2.0 ml of each fraction was collected. Each fraction was screened for protein content[59], anticoagulant activity, and fibrino(geno)lytic activity (see below).

The fractions showing the highest anticoagulant and fibrinogenolytic activity were pooled, lyophilized, and dissolved in 100 µl of 20 mM sodium phosphate buffer, pH 7.4. The solution was filtered through a 0.2 µm syringe filter and fractionated on a Shodex KW-803 column (5 µm, 8 × 300 mm) pre-equilibrated with the same buffer containing 150 mM NaCl. Fractionation was carried out with an equilibration buffer at a flow rate of 0.5 ml/min at 4°C in a UHPLC system (Dionex Ultimate Mate 3000 RSLC, Dreieich, Germany). Fraction elutions were monitored at 280 nm and 1.0 ml fractions were collected. The protein content of the peak showing the highest anticoagulant and fibrinogenolytic activity was determined and selected for further study.

Determination of purity and molecular mass of lunathrombase. The purity and molecular mass of the lunathrombase (20.0 µg) was determined by SDS-PAGE (12.5%) under reducing conditions[60]. Protein was visualized by staining with 0.1% Coomassie Brilliant Blue R-250 and destaining with methanol/acetic acid/water (40:10:50). The approximate molecular mass of lunathrombase was determined from a plot of log MW of standards vs. migration distance[32,33]. The purity of lunathrombase (5.0 µg) was also determined by MALDI-TOF mass spectrometric analysis (4800 plus, MDS SCIEX, Applied Biosystem) as previously described[61].

Determination of amino acid composition, secondary structure, and LC-MS/MS analysis of lunathrombase. For amino acid composition analysis, our previously elucidated procedure was followed[14]. The amino acid composition of lunathrombase was searched for in Swiss-prot and TrEMBL databases using the AAcompldent of Expert Protein Analysis System (ExPASy) software (http://www.expasy.org/tool/aacompident)[14,59]. The secondary structure of lunathrombase was determined by measuring the circular dichroism (CD) spectrum (JASC0 J-815 CD Spectrometer) as described previously[60]. Yang's reference was set for the CD analysis. CDPRO CLUSTER software was used to determine the secondary structure of lunathrombase[14].

For the LC-MS/MS analysis, lunathrombase was in-gel trypsin digested following our previously described procedure[62]. The LC-MS/MS analysis of extracted tryptic peptides was done as we described previously[62,63]. The data was used to search for the identification of protein on the MASCOT 2.4 search engine against Swiss-Prot, TrEMBL, and non-redundant protein sequence databases from NCBI and the data were analyzed in Proteome Discoverer 1.3 software (ThermoFisher Scientific, Germany). A minimum of two high confidence peptides were used as a prerequisite to identify the protein. The *de novo* (independent database) sequencing with an average local confidence (ALC) score of ≥50% was derived directly from the MS/MS spectrum using PEAKS 7.0 software. The identified peptides were subjected to a BLAST search in NCBInr for Swissprot protein sequences (swissprot) and Protein Databank Proteins (PDB) against Lamiaceae family proteins, green plant proteins and all NCBI databases using the blastp algorithm (http://blast.ncbi.nlm.nih.gov/Blast.cgi).

Protease assay. Human fibrinogen (2.6 µM)/human fibrin (Sigma–Aldrich, USA) (dissolved in 1x PBS, pH 7.4) was incubated with lunathrombase/Nattokinase/streptokinase/plasmin/thrombin (0.2 µM) from 15 to 120 min at 37 °C. The reaction was terminated by adding 20 µl of 6x SDS-PAGE Loading dye containing 3 mM β-mercaptoethanol and the tubes were heated at 100 °C (Digital block heater, Select Bioproducts) for 5 min. A

control was run in parallel where 1x PBS, pH 7.4 was added. The digested fibrinogen/fibrin was separated by 12.5% SDS-PAGE at 120 V, and the protein bands were visualized by staining with Coomassie Brilliant Blue R-250 and destaining with methanol/acetic acid/water (40:10:50)[33]. The gel was scanned and analyzed by ImageJ software (version 1.47) (Wayne Rasband, NIH, USA) to calculate the percent degradation of α- and β-chains of fibrinogen/fibrin by lunathrombase/ Nattokinase/streptokinase/plasmin/thrombin considering the band intensity of these chains in the untreated (control) fibrinogen as 100%.

In another set of experiments, the human fibrinogen solution (2.5 mg/ml in 20 mM potassium phosphate buffer containing 100 mM NaCl, pH 7.4) was incubated with 0.2 µM of either lunathrombase or Nattokinase (commercial anticoagulant) for 15 min at 37 °C. The resulting supernatant was filtered through a 0.2 µm membrane filter and the fibrinogen degradation products were separated on a RP-UHPLC (Dionex Ultimate Mate 3000RSLC, Dreieich, Germany) Acclaim® 300 C18 column (2.1 mm × 150 mm, 3 µm, 300 Å) as described previously[33]. From the standard curve of human fibrinopeptides A and B (Sigma-Aldrich, USA) eluted from the RP-HPLC column under identical conditions, the amount of lunathrombase-induced release of fibrinopeptides A and B from human fibrinogen was determined. A control was also run in parallel where fibrinogen solution alone was incubated with 0.1 ml of 1x PBS, pH 7.4[33].

Biochemical characterization. The optimum conditions for fibrin(ogen)olytic activity were determined by incubating 0.2 µM of lunathrombase with human fibrinogen (2.6 µM) (Sigma Aldrich, USA) at different pH (from 2–12) and temperatures (from 10–80 °C) followed by measuring the fibrin(ogen)olytic activity[32].

The activity of lunathrombase against other blood proteins (bovine serum albumin and bovine serum γ-globulin) was determined by incubating 0.2 µM of enzyme with 2.6 µM of substrate dissolved in 20 mM potassium phosphate buffer, pH 7.4 at 37 °C for 30 min. Protease activity was determined by the colorimetric method, as described previously[32]. One unit of protease activity was defined as 1 µg of tyrosine liberated per min per ml of enzyme[32].

Esterolytic activity was assayed by the spectrophometric method using N_α-*p*-Tosyl-L- arginine methyl ester hydrochloride (TAME) and N_α-Benzoyl-L- arginine ethyl ester hydrochloride (BAEE) as substrates. TAME esterase activity (in 50 mM Tris-HCl, 100 mM KCl, pH 8.1) was determined as described by Costa *et al.*[64]. One unit of TAME-esterase activity is defined as an increase in absorbance of 0.01 at 244 nm during the first 10 min of the reaction at 37 °C. For BAEE-esterase activity, the protocol described by Rutkowski[65] was followed. The assay was carried out in 100 mM Tris-HCl, pH 8.0 at 37 °C for 10 min. One unit of BAEE-esterase activity is defined as an increase in absorbance of 0.01 at 254 nm during the first 5 min of the reaction at 37 °C. For every experiment, a control was run in parallel instead of lunathrombase, using an equivalent volume of buffer. Activity was expressed as units of TAME or BAEE/mg of lunathrombase.

The *Km* and *Vmax* values of lunathrombase against fibrinogen were determined by incubating a fixed concentration (0.2 µM) of protease under study or Nattokinase with different concentrations of fibrinogen (1 to 6 µM) at 37 °C for 60 min and the protease activity at each concentration of substrate was determined. The kinetic parameters of lunathrombase and Nattokinase were determined by nonlinear regression analysis using GraphPad Prism 5.0 software[12].

The effect of lunathrombase on extracellular matrix (ECM) proteins such as laminin, type-IV collagen, and fibronectin was determined by incubating lunathrombase with substrate at a 15:1 ratio (w/w), in a total volume of 20.0 µl of 1x PBS buffer, pH 7.4 at 37 °C for 12 h. The reaction was stopped immediately after the stipulated time interval by chilling in ice and adding 5.0 µl denaturing buffer containing SDS and β-mercaptoethanol. The degradation products were analyzed on 10% SDS-PAGE after staining with 0.25% Coomassie Brilliant Blue R-250.

The influence of metal ions (Cu^{2+}, Co^{2+}, Ca^{2+}, Zn^{2+}, Mg^{2+}, Mn^{2+}, and Fe^{2+}) was determined by pre-incubating the lunathrombase (0.2 µM) with the respective metal ions (2.0 mM at final concentration in 1x PBS buffer, pH 7.4) for 30 min at 37 °C and then assaying the fibrin(ogen)olytic activity. Irreversible chemical modification of the histidine, cysteine, and serine residues was performed by pre-incubating the lunathrombase (0.2 µM) with 4-bromophenacyl bromide (pBPB), iodoacetamide (IAA), and phenylmethylsulfonyl fluoride (PMSF) at final inhibitor concentrations of 2 mM and 4 mM at room temperature for 60 min and then assaying the protease activity[14,32]. For disulfide bond reduction and metalloprotease activity, lunathrombase was treated with DTT and EDTA, respectively (2 mM and 4 mM) at 37 °C for 60 min.

In another set of experiments, lunathrombase (0.2 µM) was pre-incubated with α_2-macroglobulin or antiplasmin (3.0 µM) for 60 min at 37 °C and the fibrin(ogen)olytic activity was then determined as described above. For every experiment, a control was run where the protease was incubated with an equivalent volume of assay buffer. The activity of the control was considered as 100% and the other values were compared to that[14,32].

The total neutral sugar in lunathrombase was determined following the phenol-sulfuric colorimetric method[66]. From the standard curve of glucose, the amount of neutral sugar was determined. To determine the extent of N-linked or 0-linked oligosaccharides, lunathrombase was treated with PNGase and neuraminidase, respectively, following the instructions of the manufacturer (New England Biolabs, Inc., Ipswich, MA). Briefly, after denaturing lunathrombase at 100 °C for 10 min, the reaction was incubated with PNGase or neuraminidase for 4 h at 37 °C and the reaction products were separated by 12.5% SDS-PAGE under a reducing condition[33]. Native (untreated) and denatured lunathrombase were used as controls. The gel was stained with Commassie Brilliant Blue R-250 and destained with methanol/ acetic acid/water (40:10:50) to visualize the protein bands.

Assay of anticoagulant activity and hemolytic property of lunathrombase. Goat blood obtained from a slaughterhouse was collected in 3.8% tri-sodium citrate and platelet poor plasma (PPP) and prepared according to our previously described protocol[62,67]. Different concentrations (50–800 nM) of lunathrombase were pre-incubated with 300 µL of PPP for 3 min at 37 °C, and clotting was initiated by adding 40 µL of 250 mM $CaCl_2$[62].

For controls, instead of lunathrombase, the same volume of 1x PBS, pH 7.4 was used. One unit of anticoagulant activity of lunathrombase was defined as 1 s increase in clotting time for the control PPP[62,68].

The activated partial thromboplastin time (APTT) and prothrombin time (PT) of lunathrombase-treated and control (untreated) PPP were measured using commercial kits[62]. The hemolytic activity of lunathrombase was determined against mammalian washed erythrocytes, as described by Doley *et al.*[69].

Thrombin and FXa inhibitory effect of lunathrombase and determination of the inhibitory constant (*Ki*). Different concentrations of lunathrombase (25–600 nM) or 1x PBS, pH 7.4 (control) were pre-incubated with thrombin (3 µl, 10 NIH U/ml in 20 mM potassium phosphate buffer, pH 7.4) for 30 min at 37 °C. The reaction was started by adding 2.6 µM human fibrinogen (dissolved in 20 mM potassium phosphate buffer, pH 7.4) and the time of fibrin clot formation was monitored by visual inspection[12,33].

For the FXa inhibition assay, lunathrombase (0.2 µM)/1x PBS (control) was pre-incubated with FXa (0.13 µM) in 20 mM sodium phosphate buffer, pH 7.4 at 37 °C for 30 min. Thereafter, 1.4 µM prothrombin (the physiological substrate for FXa) was added and the reaction mixture was incubated at 37 °C for 1 h. The prothrombin degradation products were analyzed by 12.5% SDS-PAGE under reducing conditions[12].

The inhibition of the amidolytic activity of thrombin (3.0 µl, 10 NIH/ml) or FXa (0.13 µM) by lunathrombase (0.2 µM) was determined as described previously[12,14]. For the kinetics analysis, the reaction rate (V) was plotted against the substrate concentration (S) at each inhibitor concentration, and the data was fitted to a hyperbolic Michaelis - Menten model using GraphPad Prism 5.0 software[12]. The inhibitory constant (*Ki*) was determined using the competitive and non-competitive model for enzyme inhibition for thrombin and FXa, respectively using the above software[12].

Determination of interaction between lunathrombase and thrombin/fibrinogen/FXa by spectrofluorometric analysis. Thrombin (0.2 µM), fibrinogen (0.2 µM) and FXa (0.2 µM) were each incubated with different concentrations of lunathrombase (0.2 µM-1.0 µM) for 3 min at room temperature. The fluorescence intensity of the reaction mixture was monitored (excitation wavelength = 280 nm) by recording the emission spectrum in the range between 300 and 425 nm using a fluorescence spectrometer (LS55, Perkin Elmer) as we described previously[12,14]. The dissociation constant (*Kd*) for the binding of lunathrombase with thrombin/fibrinogen/FXa was determined as described previously[12,14].

Isothermal titration calorimetry titration to determine the interaction of lunathrombase with thrombin and fibrinogen. ITC experiments were performed at 37 °C on a MicroCal^{TM} iTC-200 system (GE Healthcare) in a high gain mode at a reference power of 10 µcals^{-1}. Human thrombin or fibrinogen (200 µM in 1x PBS buffer, pH 7.4) was titrated against 10 µM of lunathrombase dissolved in the same buffer. A total of 20 injections were made with 300 s time intervals in between[70]. For longer titrations, the syringe was refilled and injections continued into the same cell sample. Control runs were performed in which cell samples and syringe samples were titrated with buffer and the data from these runs was subtracted from the experimental data. Data analysis was performed with Origin software whereas data fitting was done using a "sequential binding" model.

Determination of *in vitro* thrombolytic activity. For the *in vitro* thrombolytic activity assay, lunathrombase or commercial thrombolytic agents such as s tissue plasminogen activator (tPA)/ streptokinase (indirect thrombolytic agent)/ plasmin (direct thrombolytic agent)/ Nattokinase (fibrinolytic agent) at a final concentration of 1.0 µM or 1x PBS buffer, pH 7.4 (control) was incubated with a mammalian (goat) blood clot for 3 h at 37 °C. The thrombolytic activity was determined as described by Majumdar *et al.*[14]. The *in vitro* thrombolytic activity was expressed as mg of blood clot (thrombus) lysed per µM of lunathrombase/commercial thrombolytic agents, compared to the control[14]. In another set of experiments, the blood clot was heated at 80 °C for 30 min to denature the endogenous fibrin(ogen)olytic factors (plasmin, plasminogen etc.) prior to the thrombolytic activity assay[14].

Antiplatelet effect of lunathrombase against collagen/ADP/arachidonic-induced platelet aggregation. The collection of blood from healthy volunteers (who were not under medication) was approved by the Tezpur University Ethical Committee and informed consent was obtained from all participants. Platelet rich plasma (PRP) was prepared from citrated human blood, following the procedure described previously[62,71]. Lunathrombase/aspirin (0–600 nM) was added to 100 µl of the PRP and the absorbance was measured continuously at 540 nm for 5 min, as stated above. The percent platelet aggregation after 300 s of incubation of platelets with agonists was calculated as described previously[62].

In another set of experiments, PRP was pre-incubated with lunathrombase (0–600 nM) for 5 min prior to the addition of collagen (6.2 nM)/ADP (30 µM)/arachidonic acid (15 µM). The aggregation induced by the identical concentration of collagen/ADP/arachidonic acid was considered to be 100% activity and the decrease in lunathrombase-induced platelet aggregation (antiplatelet activity) was compared to that[62].

Effect of catalytically inactive lunathrombase on washed platelet and collagen/ADP/arachidonic acid-induced platelet aggregation. To inhibit the catalytic activity of lunathrombase, it was incubated with PMSF (4 mM) at 37 °C for 60 min. Thereafter, excess PMSF was removed by a Nanosep 3 K Omega membrane filter (Pall Corporation, USA) and the PMSF-inactivated enzyme was assayed for its catalytic inactivation by the protease assay. The effect of catalytically inactive lunathrombase (0.2 µM) on washed platelets and collagen / ADP / arachidonic acid-induced platelet aggregation was assayed as described above[62]. The activity of native lunathrombase was considered as 100% and other values were compared to that.

Effect of lunathrombase on α-chymotrypsin-treated platelets. Washed platelets (1×10^6) were treated with freshly prepared α–chymotrypsin (8 U/ml) for 15 min at room temperature and then centrifuged at 1500 × g for 15 min[72]. The pellet containing the platelets was washed with Ca^{2+}- free Tyrode's buffer (5 mM HEPES, 137 mM NaCl, 2.7 mM KCl, 12 mM $NaHCO_3$, 0.42 mM Na_2HPO_4, 1 mM $MgCl_2$, 0.1% glucose, and 0.25% bovine serum albumin) three times and then suspended in the same buffer. The platelet aggregation was initiated by adding human fibrinogen (0.2 µM)/lunathrombase (0.2 µM)/catalytically inactive lunathrombase (0.2 µM) to the chymotrypsin-treated or control platelet suspension. As a control, BSA (0.2 µM) was also added to the chymotrypsin-treated platelet to determine the platelet aggregation.

Determination of binding of catalytically-inactivated lunathrombase with human GPIIb/IIIa and fibrinogen by ELISA. The binding of PMSF-inactivated Lunathrombase to human GPIIb/IIIa and fibrinogen was assessed by ELISA as described earlier[73,74]. Briefly, human fibrinogen (1000 ng) was coated to the wells of Nunc ELISA plates. After washing the unbound proteins by 1x PBS, pH 7.4 and blocking the wells with 5% fat-free milk in 1x PBS, pH 7.4, the wells were incubated with graded concentrations (0.2–1.0 µM) of PMSF-inactivated lunathrombase or 1x PBS (control) and incubated at room temperature for 2 h. Thereafter, human GPIIb/IIIa (500 ng) was added to the wells and further incubated for 2 h at room temperature. Thereafter, mouse anti-GPIIb/IIIa antibody (1: 1000 dilutions) was added to wells, incubated for 2 h, washed with 1x PBS, pH 7.4 for three times. Rabbit anti-mouse IgG-HRP conjugated secondary antibody (1:2000 dilutions) was incubated for 2 h at room temperature to detect the primary antibody. Color was developed by adding substrate (1x TMB/H_2O_2) to the well for 30 minutes in dark condition and reaction was stopped by adding 50 µl of 2 M H_2SO_4. The absorbance was taken at 492 nm against blanks in Multiskan GO (Thermoscientific, USA) microplate reader. The binding of GPIIb/IIIa to control fibrinogen was considered as 100% binding and other values were compared to that.

In another set of experiments, PMSF-inactivated lunathrombase (0.2–1.0 µM) or 1x PBS, pH 7.4 (control) was added to the human GPIIb/IIIa (500 ng) coated wells, incubated at room temperature for 2 h and washed with 1x PBS. Then, anti-GPIIb/IIIa antibody (1: 1000) was added, incubated at room temperature for 2 h, washed with 1x PBS and then HRP-conjugated anti-mouse IgG (1:2000) was added to wells and incubated for 2 h at room temperature to detect the primary antibody. The absorbance was taken at 492 nm against blanks.

Determination of cAMP, thromboxane level of platelets, and COX-1 inhibitory effect of lunathrombase. Platelet suspensions (1×10^8 platelets/ml) were pre-incubated with lunathrombase (0.2 µM) for 5 min and thereafter 2 mM EDTA and 50 µl indomethacin (1 mM) were added to the suspensions. The thromboxane B_2 level (TxB_2) and cAMP levels of the supernatants were measured by an enzyme immuno assay (EIA) kit (R&D systems, USA) following the instructions of the manufacturer. The cAMP level in the platelet suspensions incubated with 0.2 µM PGE1 (positive control) was also measured under identical conditions. The cyclooxygenase-1 (COX-1) inhibitory effect of lunathrombase/ibuprofen/aspirin (0.2 µM) was determined using the commercial kit (R&D systems, USA) following the instructions of the manufacturer.

Cytotoxicity assessment of lunathrombase. The cytotoxicity of lunathrombase was tested against human embryonic kidney cells (HEK 293 cell line), cultured and maintained in Dulbecco's modified eagle medium (DMEM) as described previously[75,76]. For the viability assay, 100 µl aliquots of 2×10^4 cells/ml were seeded into 96-well plates and treated with various concentrations (0.2 to 2.0 µM) of lunathrombase dissolved in 1x PBS, pH 7.4 and medium (control), and incubated at 37 °C for 24 h. Cell viability was then determined using the colorimetric MTT [3-(4,5-dimethylthiazol-2-yl)-2,5-diphenyltetrazolium bromide] assay following the manufacturer's instructions (ATCC)[73,74]. All assays were done in triplicate and repeated at least three times.

Calcein-AM cell viability staining. HEK 293 cells (2×10^4 cells/well), cultured in 96-well plates in DMEM media supplemented with 10% FBS, were treated with lunathrombase (2.0 µM) or medium (control) for 24 h. The cells were washed with 1x PBS, pH 7.4, stained with 5.0 µM calcein-AM (in 1x PBS, pH 7.4) and incubated for 5 min. The cells were washed with 1x PBS, pH 7.4, and visualized using an epi-fluorescence microscope at 40× magnification (Nikon ECLIPSE Ti-U, Tokyo, Japan)[77]. For the phase-contrast images, photomicrographs were captured using a Nikon ECLIPSE Ti-U (Tokyo, Japan) camera without filter.

Flow cytometric analysis to determine the cell cycle kinetics. The effect of lunathrombase on the cell cycle of HEK 293 cells was determined by flow cytometry analysis using propidium iodide (PI) DNA staining dye[77,78]. HEK 293 cells (1.5×10^5 cells per ml) were seeded in 96-well plates and allowed to adhere overnight at 37 °C. On the next day, the old medium was replaced with fresh media containing lunathrombase (2.0 µM) or only growth medium (control) and incubated for 24 h at 37 °C. Cells were collected by trypsinization and then fixed by adding chilled 70% ethanol before being stored at −20 °C until further analysis.

The fixed cells were centrifuged and washed with chilled 1x PBS, pH 7.4, following incubation with RNase at 37 °C for 1 h. Cells were then incubated with PI stain for 2 h before being analyzed by flow cytometry (FACscan, Becton Dickinson, Bedford, MA). The data was analyzed by ModFiT LT software.

Determination of *in vivo* anticoagulant activity, defibrinogenating activity, and toxicity in an animal model. Acute *in vivo* toxicity of lunathrombase was evaluated in Wistar strain rats, using the protocol of the OECD/OCED guidelines 425 (2001). Animal experiment protocols were approved by the Tezpur University Animal Ethical Committee (Approval no: DORDPro/TUAEC/10–56/14/Res-10) and the Institute of Advanced Study in Science and Technology, Guwahati (Approval no: IASST/IAEC/2016-17/04).

For *in vivo* toxicity assessment, lunathrombase was dissolved in 0.2 ml of 1x PBS, pH 7.4, and injected (10 mg/kg body weight, *i.p*) into the albino Wistar strain rats (n = 6) weighing between 120–150 g. The control group of rats received only 0.2 ml of PBS, pH 7.4 (placebo). The treated rats were observed at regular intervals up to 72 h post-injection for death or any physical or behavioral change[75]. After 72 h of treatment, the rats were sacrificed and blood was collected immediately by cardiac puncture. Hematological parameters of the blood were analyzed by a Hematology Auto Analyzer MS4-S (Melet Schloesing Laboratories, Osny, France). Plasma was obtained from control and the treated groups of rats and analyzed for total protein, glucose, serum glutamic oxaloacetic transaminase (SGOT), serum glutamic pyruvic transaminase (SGPT), alkaline phosphatase (ALP), cholesterol, triglyceride, urea, and uric acid, using commercial diagnostic kits following the manufacturers' instructions. All biochemical parameters were analyzed on an auto analyzer (Biochemical Systems International SRL Model 3000 evolution, Florence, Italy). Serum levels of immunoglobulins (IgA, IgE, IgG, and IgM) were determined by ELISA, using commercial kits and following the instructions of the manufacturer (Thermo Fisher Scientific, USA).

To examine possible lunathrombase-induced morphological alterations, the heart, liver, and kidney of the treated and control groups of rats were dissected. Tissues were cut into small pieces, washed with PBS, pH 7.2, to remove the adherent blood, and then placed in 10% buffered formaldehyde. The fixed tissues were dehydrated in a graded series of alcohol, embedded in paraffin, and processed routinely for light microscopic observation after hematoxylin-eosin staining[33].

To determine the *in vivo* defibrinogenating and anticoagulant activities, different doses of lunathrombase (0.125, 0.25, and 0.5 mg/kg body weight of rats)/heparin (0.5 mg/kg)/Nattokinase (0.5 mg/kg) were injected (*i.p*) in Wistar strain rats (n = 6) and blood was withdrawn 5 h after injection by retro orbital bleeding. The PT, APTT, tail bleeding time, and plasma Ca-clotting time of control and treated groups of rats were determined as described previously[35,58,79]. The fibrinogen content of plasma was measured using commercial kits following the manufacturer's protocol. At the end of the experiments, rats were euthanized with an overdose of Na-pentobarbital as per recommendations of the CPCSEA.

All experiments were carried out in accordance with the guidelines of the Tezpur University Ethical Committee, Institute of Advanced Study in Science and Technology, Guwahati and the bio-safety committee guidelines, Tezpur University.

Statistical analysis. The statistical analysis of the data was done by Student's t-test using the SigmaPlot 10.0 for Windows (version 7.0) software. A value of $p < 0.05$ was considered as a significant difference.

References

1. Choi, J. H., Sapkota, K., Park, S. E., Kim, S. & Kim, S. J. Thrombolytic, anticoagulant and antiplatelet activities of codiase, a bifunctional fibrinolytic enzyme from *Codium fragile*. *Biochimie* **95**, 1266–1277, https://doi.org/10.1016/j.biochi.2013.01.023 (2013).
2. Kang, S. R. *et al*. A bifunctional protease from green alga *Ulva pertusa* with anticoagulant properties: partial purification and characterization. *Journal of Applied Phycology* **28**, 599–607, https://doi.org/10.1007/s10811-015-0550-4 (2016).
3. Riddel, J. P. Jr., Aouizerat, B. E., Miaskowski, C. & Lillicrap, D. P. Theories of blood coagulation. *Journal of pediatric oncology nursing: official journal of the Association of Pediatric Oncology Nurses* **24**, 123–131, https://doi.org/10.1177/1043454206298693 (2007).
4. Fenton, J. W. 2nd, Ofosu, F. A., Brezniak, D. V. & Hassouna, H. I. Understanding thrombin and hemostasis. *Hematology/oncology clinics of North America* **7**, 1107–1119 (1993).
5. Turner, N. A. & Moake, J. Assembly and activation of alternative complement components on endothelial cell-anchored ultra-large von Willebrand factor links complement and hemostasis-thrombosis. *PloS one* **8**, e59372, https://doi.org/10.1371/journal.pone.0059372 (2013).
6. Monroe, D. M., Hoffman, M. & Roberts, H. R. Platelets and thrombin generation. *Arteriosclerosis, thrombosis, and vascular biology* **22**, 1381–1389 (2002).
7. Kerlin, B. *et al*. Cause-effect relation between hyperfibrinogenemia and vascular disease. *Blood* **103**, 1728–1734, https://doi.org/10.1182/blood-2003-08-2886 (2004).
8. Machlus, K. R., Cardenas, J. C., Church, F. C. & Wolberg, A. S. Causal relationship between hyperfibrinogenemia, thrombosis, and resistance to thrombolysis in mice. *Blood* **117**, 4953–4963, https://doi.org/10.1182/blood-2010-11-316885 (2011).
9. Pola, P., Tondi, P., Serricchio, M. & Pola, R. In *Textbook of Angiology* (ed. John, B. Chang) 419–426 (Springer New York, 2000).
10. Eriksson, B. I., Quinlan, D. J. & Eikelboom, J. W. Novel oral factor Xa and thrombin inhibitors in the management of thromboembolism. *Annual review of medicine* **62**, 41–57, https://doi.org/10.1146/annurev-med-062209-095159 (2011).
11. Esmon, C. T. Targeting factor Xa and thrombin: impact on coagulation and beyond. *Thrombosis and haemostasis* **111**, 625–633, https://doi.org/10.1160/TH13-09-0730 (2014).
12. Thakur, R. *et al*. A new peptide (Ruviprase) purified from the venom of *Daboia russelii russelii* shows potent anticoagulant activity via non-enzymatic inhibition of thrombin and factor Xa. *Biochimie* **105**, 149–158, https://doi.org/10.1016/j.biochi.2014.07.006 (2014).
13. Mukherjee, A. K., Dutta, S. & Mackessy, S. P. A new C-type lectin (RVsnaclec) purified from venom of *Daboia russelii russelii* shows anticoagulant activity via inhibition of FXa and concentration-dependent differential response to platelets in a $Ca^{(2)(+)}$-independent manner. *Thrombosis research* **134**, 1150–1156, https://doi.org/10.1016/j.thromres.2014.09.009 (2014).
14. Majumdar, S. *et al*. Characterization, mechanism of anticoagulant action, and assessment of therapeutic potential of a fibrinolytic serine protease (Brevithrombolase) purified from *Brevibacillus brevis* strain FF02B. *Biochimie* **103**, 50–60, https://doi.org/10.1016/j.biochi.2014.04.002 (2014).
15. Marder, V. J. & Novokhatny, V. Direct fibrinolytic agents: biochemical attributes, preclinical foundation and clinical potential. *Journal of Thrombosis and Haemostasis: JTH* **8**, 433–444, https://doi.org/10.1111/j.1538-7836.2009.03701.x (2010).
16. Menaldo, D. L. *et al*. Biochemical characterization and comparative analysis of two distinct serine proteases from *Bothrops pirajai* snake venom. *Biochimie* **94**, 2545–2558, https://doi.org/10.1016/j.biochi.2012.07.007 (2012).
17. Wang, T. J. *et al*. A risk score for predicting stroke or death in individuals with new-onset atrial fibrillation in the community: the Framingham Heart Study. *Jama* **290**, 1049–1056, https://doi.org/10.1001/jama.290.8.1049 (2003).
18. Ageno, W. *et al*. Oral anticoagulant therapy: Antithrombotic Therapy and Prevention of Thrombosis, 9th ed: American College of Chest Physicians Evidence-Based Clinical Practice Guidelines. *Chest* **141**, e44S–e88S, https://doi.org/10.1378/chest.11-2292 (2012).
19. Yamamoto, J., Yamada, K., Naemura, A., Yamashita, T. & Arai, R. Testing various herbs for antithrombotic effect. *Nutrition* **21**, 580–587, https://doi.org/10.1016/j.nut.2004.09.016.

20. Pawlaczyk, I., Czerchawski, L., Pilecki, W., Lamer-Zarawska, E. & Gancarz, R. Polyphenolic-polysaccharide compounds from selected medicinal plants of *Asteraceae* and *Rosaceae* families: Chemical characterization and blood anticoagulant activity. *Carbohydrate Polymers* **77**, 568–575, https://doi.org/10.1016/j.carbpol.2009.01.030 (2009).
21. Choi, J. H. *et al.* Novel thrombolytic protease from edible and medicinal plant *Aster yomena* (Kitam.) Honda with anticoagulant activity: purification and partial characterization. *Journal of bioscience and bioengineering* **118**, 372–377, https://doi.org/10.1016/j.jbiosc.2014.03.004 (2014).
22. Cai, W. *et al.* Purification, characterization and *in vitro* anticoagulant activity of polysaccharides from *Gentiana scabra* Bunge roots. *Carbohydrate Polymers* **140**, 308–313, https://doi.org/10.1016/j.carbpol.2015.12.054 (2016).
23. Luzak, B. *et al.* Extract from spent hop *(Humulus lupulus L.)* reduces blood platelet aggregation and improves anticoagulant activity of human endothelial cells *in vitro*. *Journal of functional Foods* **22**, 257–269, https://doi.org/10.1016/j.jff.2016.01.029 (2016).
24. Antao, C. M. & Malcata, F. X. Plant serine proteases: biochemical, physiological and molecular features. *Plant physiology and biochemistry: PPB* **43**, 637–650, https://doi.org/10.1016/j.plaphy.2005.05.001 (2005).
25. Asif-Ullah, M., Kim, K. S. & Yu, Y. G. Purification and characterization of a serine protease from *Cucumis trigonus* Roxburghi. *Phytochemistry* **67**, 870–875, https://doi.org/10.1016/j.phytochem.2006.02.020 (2006).
26. Gonzalez-Rabade, N., Badillo-Corona, J. A., Aranda-Barradas, J. S. & Oliver-Salvador Mdel, C. Production of plant proteases *in vivo* and *in vitro*–a review. *Biotechnology advances* **29**, 983–996, https://doi.org/10.1016/j.biotechadv.2011.08.017 (2011).
27. Singh, K. A., Kumar, R., Rao, G. R. K. & Jagannadham, M. V. Crinumin, a chymotrypsin-like but glycosylated serine protease from *Crinum asiaticum*: Purification and physicochemical characterisation. *Food Chemistry* **119**, 1352–1358, https://doi.org/10.1016/j.foodchem.2009.09.012 (2010).
28. Markland, F. S. Snake venoms and the hemostatic system. *Toxicon: official journal of the International Society on Toxinology* **36**, 1749–1800 (1998).
29. Kim, D.-W. *et al.* Direct acting anti-thrombotic serine protease from brown seaweed *Costaria costata*. *Process Biochemistry* **48**, 340–350, https://doi.org/10.1016/j.procbio.2012.12.012 (2013).
30. Kim, H. C. *et al.* Purification and characterization of a novel, highly potent fibrinolytic enzyme from *Paecilomyces tenuipes*. *Process Biochemistry* **46**, 1545–1553, https://doi.org/10.1016/j.procbio.2011.04.005 (2011).
31. Kim, J. S. *et al.* Purification and characterization of fibrinolytic metalloprotease from *Perenniporia fraxinea* mycelia. *Mycological research* **112**, 990–998, https://doi.org/10.1016/j.mycres.2008.01.029 (2008).
32. Mukherjee, A. K., Rai, S. K., Thakur, R., Chattopadhyay, P. & Kar, S. K. Bafibrinase: A non-toxic, non-hemorrhagic, direct-acting fibrinolytic serine protease from *Bacillus* sp. strain AS-S20-I exhibits *in vivo* anticoagulant activity and thrombolytic potency. *Biochimie* **94**, 1300–1308, https://doi.org/10.1016/j.biochi.2012.02.027 (2012).
33. Mukherjee, A. K. & Mackessy, S. P. Biochemical and pharmacological properties of a new thrombin-like serine protease (Russelobin) from the venom of Russell's Viper (*Daboia russelii russelii*) and assessment of its therapeutic potential. *Biochimica et biophysica acta* **1830**, 3476–3488, https://doi.org/10.1016/j.bbagen.2013.02.007 (2013).
34. Rai, S. K. & Mukherjee, A. K. Statistical optimization of production, purification and industrial application of a laundry detergent and organic solvent-stable subtilisin-like serine protease (Alzwiprase) from *Bacillus subtilis* DM-04. *Biochemical Engineering Journal* **48**, 173–180, https://doi.org/10.1016/j.bej.2009.09.007 (2010).
35. Majumdar, S., Chattopadhyay, P. & Mukherjee, A. K. *In vivo* anticoagulant and thrombolytic activities of a fibrinolytic serine protease (Brevithrombolase) with the k-carrageenan-induced rat tail thrombosis model. *Clinical and applied thrombosis/hemostasis: official journal of the International Academy of Clinical and Applied. Thrombosis/Hemostasis* **22**, 594–598, https://doi.org/10.1177/1076029615569567 (2016).
36. Mukherjee, A. K. *et al.* Structural and functional characterization of complex formation between two Kunitz-type serine protease inhibitors from Russell's Viper venom. *Biochimie* **128–129**, 138–147, https://doi.org/10.1016/j.biochi.2016.08.005 (2016).
37. Liu, J. *et al.* Spectrofluorimetric study of the binding of daphnetin to bovine serum albumin. *Journal of pharmaceutical and biomedical analysis* **35**, 671–677, https://doi.org/10.1016/j.jpba.2004.02.010 (2004).
38. Ward, W. H. & Holdgate, G. A. Isothermal titration calorimetry in drug discovery. *Progress in medicinal chemistry* **38**, 309–376 (2001).
39. Pozhidaeva, A. K. *et al.* Structural characterization of interaction between human ubiquitin-specific protease 7 and immediate-early protein ICP0 of herpes simplex virus-1. *The Journal of biological chemistry* **290**, 22907–22918, https://doi.org/10.1074/jbc.M115.664805 (2015).
40. Hirsh, J. *et al.* Oral anticoagulants: mechanism of action, clinical effectiveness, and optimal therapeutic range. *Chest* **119**, 8S–21S (2001).
41. Bhakuni, T. *et al.* Role of heparin and non heparin binding serpins in coagulation and angiogenesis: A complex interplay. *Archives of biochemistry and biophysics* **604**, 128–142, https://doi.org/10.1016/j.abb.2016.06.018 (2016).
42. Ruggeri, Z. M. & Mendolicchio, G. L. Adhesion mechanisms in platelet function. *Circulation research* **100**, 1673–1685, https://doi.org/10.1161/01.RES.0000267878.97021.ab (2007).
43. Ohlmann, P. *et al.* ADP induces partial platelet aggregation without shape change and potentiates collagen-induced aggregation in the absence of Gαq. *Blood* **96**, 2134–2139 (2000).
44. Hou, Y. *et al.* Platelets in hemostasis and thrombosis: Novel mechanisms of fibrinogen-independent platelet aggregation and fibronectin-mediated protein wave of hemostasis. *Journal of biomedical research* **29**, https://doi.org/10.7555/JBR.29.20150121 (2015)
45. Schafer, A. I. Antiplatelet therapy. *The American journal of medicine* **101**, 199–209 (1996).
46. Pulcinelli, F. M. *et al.* Inhibition of platelet aggregation by aspirin progressively decreases in long-term treated patients. *Journal of the American College of Cardiology* **43**, 979–984, https://doi.org/10.1016/j.jacc.2003.08.062 (2004).
47. Walter, U., Eigenthaler, M., Geiger, J. & Reinhard, M. Role of cyclic nucleotide-dependent protein kinases and their common substrate VASP in the regulation of human platelets. *Advances in experimental medicine and biology* **344**, 237–249 (1993).
48. Yang, D. *et al.* A new role for the A2b adenosine receptor in regulating platelet function. *Journal of Thrombosis and Haemostasis: JTH* **8**, 817–827, https://doi.org/10.1111/j.1538-7836.2010.03769.x (2010).
49. Loyau, S. *et al.* Platelet glycoprotein VI dimerization, an active process inducing receptor competence, is an indicator of platelet reactivity. *Arteriosclerosis, thrombosis, and vascular biology* **32**, 778–785, https://doi.org/10.1161/ATVBAHA.111.241067 (2012).
50. Fuentes, E., Caballero, J., Alarcon, M., Rojas, A. & Palomo, I. Chlorogenic acid inhibits human platelet activation and thrombus formation. *PloS one* **9**, e90699, https://doi.org/10.1371/journal.pone.0090699 (2014).
51. Enomoto, Y. *et al.* cAMP regulates ADP-induced HSP27 phosphorylation in human platelets. *International Journal of Molecular Medicine* **27**, 695–700, https://doi.org/10.3892/ijmm.2011.637 (2011).
52. Warner, T. D., Nylander, S. & Whatling, C. Anti-platelet therapy: cyclo-oxygenase inhibition and the use of aspirin with particular regard to dual anti-platelet therapy. *British Journal of Clinical Pharmacology* **72**, 619–633, https://doi.org/10.1111/j.1365-2125.2011.03943.x (2011).
53. Chang, C. C. *et al.* Potent antiplatelet activity of sesamol in an *in vitro* and *in vivo* model: pivotal roles of cyclic AMP and p38 mitogen-activated protein kinase. *Journal of Nutritional Biochemistry* **21**, 1214–1221, https://doi.org/10.1016/j.jnutbio.2009.10.009 (2010).
54. Niewiarowski, S., Budzynski, A. Z., Morinelli, T. A., Brudzynski, T. M. & Stewart, G. J. Exposure of fibrinogen receptor on human platelets by proteolytic enzymes. *The Journal of biological chemistry* **256**, 917–925 (1981).

55. Ruoslahti, E. RGD and other recognition sequences for integrins. *Annual Review of Cell and Developmental Biology* **12**, 697–715 (1996).
56. Sánchez-Cortés, J. & Mrksich, M. The platelet integrin αIIbβ3 binds to the RGD and AGD motifs in fibrinogen. *Chemistry & biology* **16**(9), 990–1000 (2009).
57. Ariens, R. A. Elevated fibrinogen causes thrombosis. *Blood* **117**, 4687–4688, https://doi.org/10.1182/blood-2011-03-340422 (2011).
58. Sahni, A., Simpson-Haidaris, P. J., Sahni, S. K., Vaday, G. G. & Francis, C. W. Fibrinogen synthesized by cancer cells augments the proliferative effect of fibroblast growth factor-2 (FGF-2). *Journal of Thrombosis and Haemostasis: JTH* **6**, 176–183, https://doi.org/10.1111/j.1538-7836.2007.02808.x (2008).
59. Lowry, O. H., Rosebrough, N. J., Farr, A. L. & Randall, R. J. Protein measurement with the Folin phenol reagent. *The Journal of biological chemistry* **193**, 265–275 (1951).
60. Laemmli, U. K. Cleavage of structural proteins during the assembly of the head of bacteriophage T4. *Nature* **227**, 680–685 (1970).
61. Mukherjee, A. K. The Pro-Coagulant fibrinogenolytic serine protease isoenzymes purified from *Daboia russelii russelii* venom coagulate the blood through factor V activation: role of glycosylation on enzymatic activity. *PloS one* **9**, e86823, https://doi.org/10.1371/journal.pone.0086823 (2014).
62. Dutta, S., Gogoi, D. & Mukherjee, A. K. Anticoagulant mechanism and platelet deaggregation property of a non-cytotoxic, acidic phospholipase A_2 purified from Indian cobra (*Naja naja*) venom: inhibition of anticoagulant activity by low molecular weight heparin. *Biochimie* **110**, 93–106, https://doi.org/10.1016/j.biochi.2014.12.020 (2015).
63. Gogoi, D. *et al*. Structural and physico-chemical characterization of a dirhamnolipid biosurfactant purified from *Pseudomonas aeruginosa*: application of crude biosurfactant in enhanced oil recovery. *RSC Advances* **6**(74), 70669–70681, https://doi.org/10.1039/C6RA11979D (2016).
64. Costa, F. L. *et al*. Biochemical and functional properties of a thrombin-like enzyme isolated from *Bothrops pauloensis* snake venom. *Toxicon: official journal of the International Society on Toxinology* **54**, 725–735, https://doi.org/10.1016/j.toxicon.2009.05.040 (2009).
65. Rutkowski, R. B. Human plasma and serum trypsin-like esterase activity. *Clinical chemistry* **12**, 350–359 (1966).
66. Masuko, T. *et al*. Carbohydrate analysis by a phenol-sulfuric acid method in microplate format. *Analytical biochemistry* **339**, 69–72, https://doi.org/10.1016/j.ab.2004.12.001 (2005).
67. Saikia, D., Thakur, R. & Mukherjee, A. K. An acidic phospholipase A_2 (RVVA-PLA_2-I) purified from *Daboia russelli* venom exerts its anticoagulant activity by enzymatic hydrolysis of plasma phospholipids and by non-enzymatic inhibition of factor Xa in a phospholipids/Ca^{2+} independent manner. *Toxicon* **57**, 841–850, https://doi.org/10.1016/j.toxicon.2011.02.018 (2011).
68. Doley, R. & Mukherjee, A. K. Purification and characterization of an anticoagulant phospholipase A_2 from Indian monocled cobra (*Naja kaouthia*) venom. *Toxicon* **41**, 81–91 (2003).
69. Doley, R., King, G. F. & Mukherjee, A. K. Differential hydrolysis of erythrocyte and mitochondrial membrane phospholipids by two phospholipase A_2 isoenzymes (NK-PLA_2-I and NK-PLA_2-II) from the venom of the Indian monocled cobra *Naja kaouthia*. *Archives of biochemistry and biophysics* **425**, 1–13, https://doi.org/10.1016/j.abb.2004.02.007 (2004).
70. Pretorius, E., Mbotwe, S., Bester, J., Robinson, C. J. & Kell, D. B. Acute induction of anomalous and amyloidogenic blood clotting by molecular amplification of highly substoichiometric levels of bacterial lipopolysaccharide. *Journal of the Royal Society, Interface* **13**, https://doi.org/10.1098/rsif.2016.0539 (2016).
71. Bednar, B., Condra, C., Gould, R. J. & Connolly, T. M. Platelet aggregation monitored in a 96 well microplate reader is useful for evaluation of platelet agonists and antagonists. *Thrombosis research* **77**, 453–463 (1995).
72. Barbouche, R. *et al*. Anti-platelet activity of the peptides composing the Lebetin 1 family, a new class of inhibitors of platelet aggregation. *Toxicon* **36**, 1939–1947 (1998).
73. Mukherjee, A. K., Kalita, B. & Mackessy, S. P. A proteomics analysis of Pakistan *Daboia russelii russelii* venom and assessment of potency of Indian polyvalent and monovalent antivenom. *Journal of Proteomics* **144**, 73–86 (2016).
74. Kalita, B., Patra, A. & Mukherjee, A. K. Unraveling the proteome composition and immuno-profiling of western India russell's viper venom for in-depth understanding of its pharmacological properties, clinical manifestations, and effective antivenom treatment. *Journal of proteome research* **16**(2), 583–598 (2017).
75. Mukherjee, A. K., Saviola, A. J., Burns, P. D. & Mackessy, S. P. Apoptosis induction in human breast cancer (MCF-7) cells by a novel venom L-amino acid oxidase (Rusvinoxidase) is independent of its enzymatic activity and is accompanied by caspase-7 activation and reactive oxygen species production. *Apoptosis: An international journal on programmed cell death* **20**, 1358–1372, https://doi.org/10.1007/s10495-015-1157-6 (2015).
76. Raza, A., Ghoshal, A., Chockalingam, S. & Ghosh, S. S. Connexin-43 enhances tumor suppressing activity of artesunate via gap junction-dependent as well as independent pathways in human breast cancer cells. *Scientific Reports* **7**(1), 7580 (2017).
77. Bratosin, D., Mitrofan, L., Palii, C., Estaquier, J. & Montreuil, J. Novel fluorescence assay using calcein-AM for the determination of human erythrocyte viability and aging. *Cytometry Part A* **66**(1), 78–84 (2005).
78. Arora, N. & Ghosh, S. S. Functional characterizations of interactive recombinant PTEN–silica nanoparticles for potential biomedical applications. *RSC Advances* **6**(115), 114944–114954 (2016).
79. Mukherjee, A. K. *et al*. Characterization of a pro-angiogenic, novel peptide from Russell's viper (*Daboia russelii russelii*) venom. *Toxicon: official journal of the International Society on Toxinology* **77**, 26–31, https://doi.org/10.1016/j.toxicon.2013.10.024 (2014).

Acknowledgements

The authors thank C-CAMP, NCBS, Bangalore and DBT-IPLS, Kolkata for LC-MS/MS analysis, de novo sequencing, and ITC study, respectively. The authors also thankful to Dr. M. Dey Dutta, Research Associate, IIT, Guwahati, for CD spectropolarimeter analysis and Dr. G. Wheeler for editing the manuscript. DG received SRF from DBT BIRAC project. This project received financial support from DBT- BIRAC-BIG Project [BT/TEMP2517/BIG-08/1] to AKM.

Author Contributions

A.K.M. conceived the idea and designed the experiments, D.G. performed the experiments, R.D. and R.S. helped in performing animal experiments. S.S.G. and N.A. performed MALDI analysis and cell cytotoxicity assay. B.K. performed the some of the antiplatelet studies. T.I. performed the glycosylation study. D.G. wrote the manuscript and A.K.M. edited and approved the final manuscript.

Additional Information

Supplementary information accompanies this paper at https://doi.org/10.1038/s41598-018-24422-y.

Competing Interests: The authors declare no competing interests.

Publisher's note: Springer Nature remains neutral with regard to jurisdictional claims in published maps and institutional affiliations.

JOURNAL OF NATURAL PRODUCTS

Cite This: J. Nat. Prod. XXXX, XXX, XXX−XXX

Article

pubs.acs.org/jnp

First Report of Plant-Derived β-Sitosterol with Antithrombotic, in Vivo Anticoagulant, and Thrombus-Preventing Activities in a Mouse Model

Debananda Gogoi,[†] Anirban Pal,[§] Pronobesh Chattopadhyay,[⊥] Subrata Paul,[‡] Ramesh C. Deka,[‡] and Ashis K. Mukherjee*[,†]

[†]Microbial Biotechnology and Protein Research Laboratory, Department of Molecular Biology and Biotechnology, School of Sciences and [‡]Department of Chemical Sciences, Tezpur University, Tezpur 784028, Assam, India

[§]*In-vivo* Testing Laboratory, Molecular Bioprospection Department, Central Institute of Medicinal and Aromatic Plants, Lucknow, India

[⊥]Division of Pharmaceutical Technology, Defense Research Laboratory, Tezpur, Assam, India

Supporting Information

ABSTRACT: Inhibitors of thrombin, a key enzyme in the blood coagulation cascade, are of great interest because of their selective specificity and effectiveness in anticoagulation therapy against cardiovascular disorders. The natural soybean phytosterol, β-sitosterol (BSS) demonstrated anticoagulant activity by dose-dependent inhibition of thrombin in an uncompetitive manner with a K_i value of 0.267 μM as well as by partial inhibition of thrombin-catalyzed platelet aggregation with a half-maximal inhibitory concentration (IC_{50}) value of 10.45 ± 2.88 μM against platelet-rich plasma and 9.2 ± 1.2 μM against washed platelets. An *in silico* study indicated binding of BSS to thrombin, which was experimentally verified by spectrofluorometric and isothermal calorimetric analyses. Under *in vitro* conditions, BSS demonstrated thrombolytic activity by activating plasminogen, albeit it is devoid of protease (fibrinogenolytic) activity. BSS was noncytotoxic to mammalian cells, nonhemolytic, demonstrated its *in vivo* anticoagulant activity when administered orally, and inhibited k-carrageen-induced thrombus formation in the tails of mice. Our results suggest that dietary supplementation of BSS may help to prevent thrombosis-associated cardiovascular disorders.

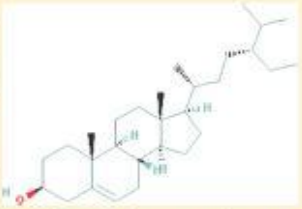

INTRODUCTION

Thrombotic events leading to stroke, heart attack, venous thrombosis, and other cardiovascular diseases (CVDs) are important causes of morbidity and mortality worldwide.[1] Thrombogenesis is a complicated biological process involving a number of enzymes that may be attractive targets for new therapies.[2] Several approved drugs, including warfarin (a vitamin K epoxide reductase inhibitor), dabigatran (a thrombin inhibitor), rivaroxaban, and apixaban (factor Xa inhibitors) are currently used prophylactically to reduce the risk of thrombotic events; however, these therapies carry associated adverse effects such as gastrointestinal bleeding that are significant concerns.[3] Therefore, the field of new oral antithrombotic drug development in the past two decades has been moving toward selectivity and specificity, such as the selective thrombin, factor Xa, or factor XIa inhibitors, with the hope of improving safety over the older, natural anticoagulants or their synthetic derivatives, like the heparins and coumarins with their broad and limited selectivity.[4]

Hemostasis is initiated when blood is exposed to tissue factors located in the adventitia of blood vessels, whereas thrombosis is initiated when blood is exposed to tissue factors in the necrotic core of the ruptured atherosclerotic plaques, in the subendothelium of injured vessels, or on the surface of activated leucocytes attracted to the damaged vessel.[5] The final common mediator of both the intrinsic and extrinsic coagulation pathways is a serine protease, thrombin (factor IIa), which plays a key role in inducing blood clotting. Thrombin also triggers platelet activation and the production of factors V, VIII, and IX and mediates the proteolytic cleavage of fibrinogen to fibrin, to which it binds and remains active.[6] Thrombin thus remains a major target for the development of novel anticoagulants. Three small-molecule thrombin inhibitors (ximelagatran, dabigatran, and argatroban) were recently introduced, though ximelagatran was subsequently withdrawn due to its liver toxicity.[7] Numerous other thrombin inhibitors are in various stages of development.[8]

The search for anticoagulant agents from natural sources that would be safe and easily absorbed is an area of renewed scientific interest with broad interdisciplinary research approaches.[9,10] Recent trends have clearly shown that plant-derived products and/or their synthetic counterparts will be among the most important sources of new drugs in the years to come. β-Sitosterol (BSS), a natural phytosterol (Figure 1), has shown various promising biological properties including

Received: July 13, 2018

DOI: 10.1021/acs.jnatprod.8b00574
J. Nat. Prod. XXXX, XXX, XXX−XXX

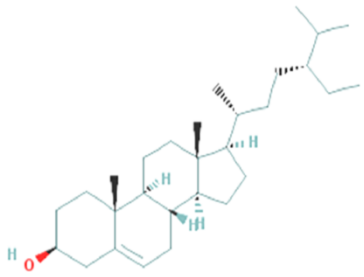

Figure 1. Chemical structure of β-sitosterol.

cholesterol-lowering, immunomodulatory, and anticancer activities,[11−13] and its safety has been assessed in preclinical studies.[14,15] Nevertheless, no direct evidence has been found for the anticoagulant or antithrombotic properties of BSS. In this study we present the mechanism of the antithrombotic action of a plant-derived BSS and a structural analysis of the binding of BSS to thrombin. Furthermore, we show that BSS can function as an oral anticoagulant, inhibiting *in vivo* thrombus formation in an experimental mouse model.

RESULTS AND DISCUSSION

BSS Demonstrated Dose-Dependent Anticoagulant Activity of PPP and Whole Blood. BSS dose-dependently prolonged the Ca^{2+} clotting time of platelet-poor plasma (PPP), and at a concentration of 2.5 μM of BSS saturated anticoagulant activity was observed (Figure 2a). The optimum anticoagulant activity of BSS was observed at 15 min of the preincubation with PPP (Figure 2b), indicating the rapid action of BSS to exert its anticoagulant activity. Several mechanisms could explain the anticoagulant action, such as the inhibition of thrombin, FXa; inhibition of platelet aggregation; vitamin K antagonism; and/or defibrinogenation of blood plasma.[16,17] BSS affected both intrinsic and extrinsic pathways of blood coagulation, which was demonstrated by the significant increase in the activated partial thromboplastin time (APTT) of PPP ($p < 0.05$); the APTT concentration−response curve was curvilinear and flattened at higher concentrations (10.0 μM) of BSS (Figure 2c). BSS has marginal effect on prothrombin time (PT) at lower doses; however, it affects the PT (INR) (INR = $\text{prothrombin}_{\text{test}}$/$\text{prothrombin}_{\text{control}}$) of PPP at higher doses (Figure 2d). Preincubation of mammalian blood with BSS resulted in prolongation of clotting time (Figure 2e) suggesting the anticoagulant nature of the BSS.

BSS Inhibited the Catalytic Activity of Thrombin but Did Not Influence FXa Activity and Devoid of Fibrinogenolytic Activity. The catalytic activity of thrombin is also regulated by two recognition domains: exosite-I and exosite-II that bind to fibrinogen and heparin/AT-III, respectively.[18,19] Both sites are distant from the catalytic pocket but are involved in the specific binding of thrombin to several macromolecular substrates, inhibitors, and modulators.[18,19] BSS dose-dependently inhibited the amidolytic activity of thrombin (Figure 3a). The Michaelis−Menten plot (Figure 3b) indicated a decrease in both the K_m as well as V_{max} values of thrombin for its substrate (T1637) in the presence of BSS indicating BSS inhibits thrombin in an uncompetitive manner (Figure 3b). The K_i value for the inhibition of thrombin by BSS was determined as 267.2 ± 34.3 nM (mean ± standard deviation (SD), $n = 3$). Therefore, the mode of BSS-mediated thrombin inhibition differed from that of dabigatran etexilate or argatroban (commercial direct thrombin inhibitors) that follow a competitive model of thrombin inhibition.[20−22]

BSS also prolonged the fibrinogen clotting time of thrombin in a dose-dependent manner, and at 7.5 μM concentration of BSS saturation in thrombin, inhibition was observed (Figure 3c). At the optimum concentration of BSS, optimum thrombin inhibition was observed at 20 min of preincubation of BSS with thrombin (Figure 3d) suggesting the slow binding kinetics of thrombin inhibition. Nevertheless, BSS failed to inhibit the amidolytic activity of FXa (Figure S1, Supporting Information) or the prothrombin activation by FXa (Figure S2, Supporting Information) suggesting that BSS does not inhibit FXa. BSS was also devoid of protease (fibrinogenolytic) activity indicating trace quantity of soybean protease was not copurified during the purification of BSS (Figure S3, Supporting Information), which nullifies the possible effect of copurified plant protease on thrombin inhibition and plasminogen activation property of BSS (see below).

Fibrinogen clotting and thrombin-induced aggregation of platelets are mediated by enzymatic cleavage of fibrinogen bound to exosite-I of thrombin and protease-activated receptors (PAR-1 and PAR-4, which are present on the surface of platelets) by thrombin, respectively.[18,23] Because BSS inhibited the amidolytic activity and fibrinogen clotting properties of thrombin to an equal extent, it would be reasonable to assume that the binding of BSS to the catalytic site of thrombin inhibited its enzymatic activity and subsequently diminished the fibrinogen clotting by thrombin. Further, preincubation of BSS/thrombin prior to the addition of heparin/AT-III did not jeopardize the catalytic activity of thrombin (Figure S4, Supporting Information), which suggests that BSS does not bind to exosite-II (the heparin/AT-III binding site) of thrombin. In any case, further structural analyses would be needed to pinpoint the thrombin binding region of BSS.

The *in Silico* Binding Study, Spectrofluorometric Analysis, and Isothermal Calorimetric Titration Suggest Interaction of BSS with Thrombin. The ligand−protein interaction study showed that the lowest binding energy and intermolecular energy for the binding of BSS with thrombin was −5.61 and −7.7 kcal mol^{-1}, respectively. Further, in the binding site of thrombin, the BSS ligand was shown to be in close proximity with protein residues PHE339, LEU346, ARG382, ARG388, THR389, ARG390, and TYR391. A prominent hydrogen-bond interaction at a distance of 2.088 Å was demonstrated with the protein residue ARG388 (Figure 4). The binding energy that results from BSS and thrombin that was obtained in the *in silico* study agrees with reports for thrombin inhibitors such as pachydictyol A and isopachydictyol A from marine sources.[24]

Because of their greater sensitivity and selectivity, fluorescence spectroscopy and isothermal calorimetry (ITC) were used to study the thrombin-BSS interaction[25−28] to verify the result of the *in silico* study. Both of these studies showed interactions between BSS and thrombin. A steady increase in the fluorescence intensity of thrombin in the presence of BSS was seen in comparison to the fluorescence intensity of individual protein/ligand (Figure 4b). No change in the fluorescence intensity of fibrinogen/FXa was observed in the presence of BSS, suggesting that it does not bind with fibrinogen or FXa (Figure S5a,b, Supporting Information).

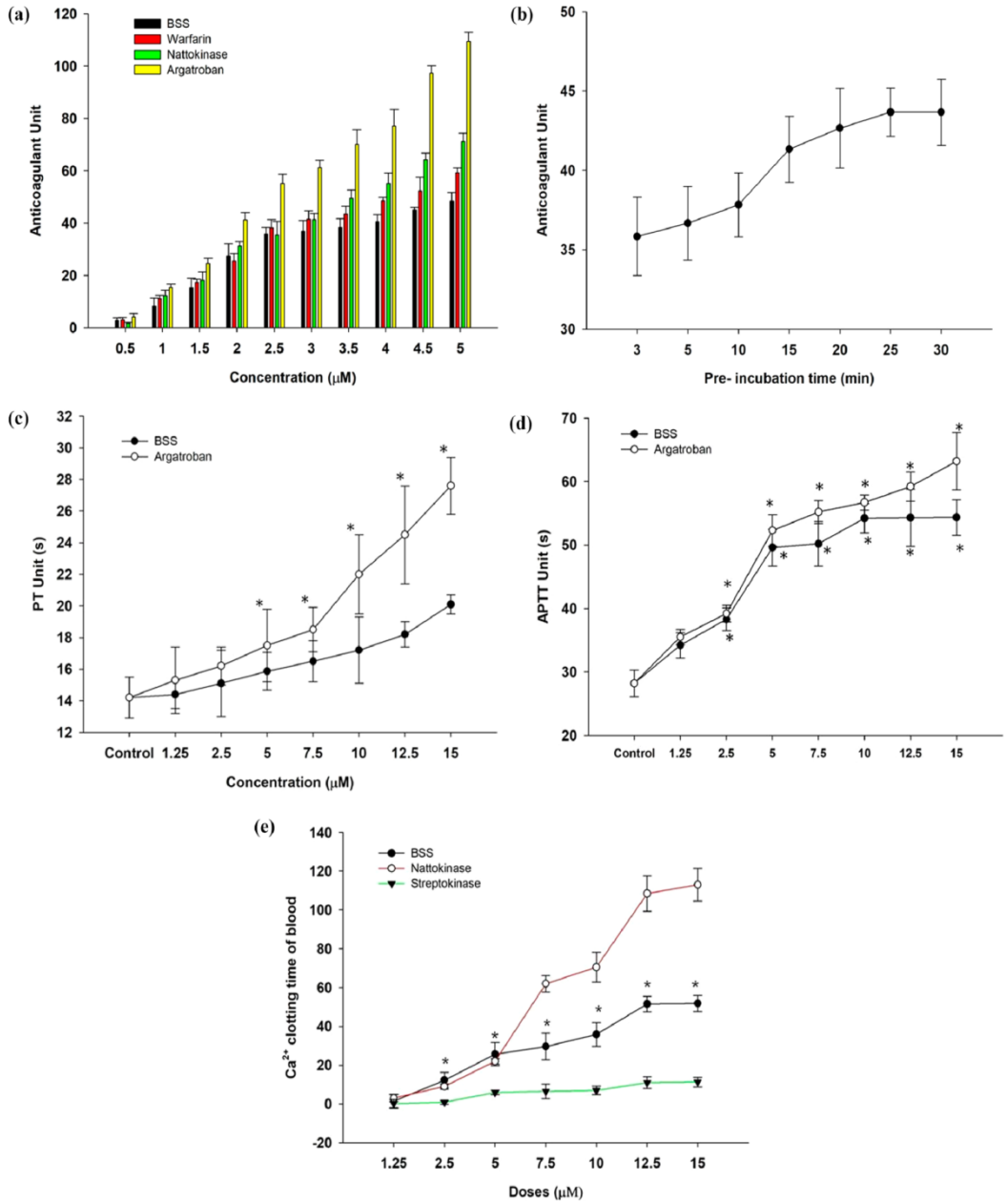

Figure 2. (a) Dose-dependent in vitro anticoagulant activity of BSS, warfarin, nattokinase, and argatroban against human PPP. One unit of anticoagulant activity is defined as 1 s increase in clotting time of the control PPP in the presence of samples. (b) Time-dependent in vitro anticoagulant activity of BSS (2.5 μM) against human PPP. (c) Effect of BSS/argatroban (1.25−15.0 μM) on PT of human PPP. (d) Effect of BSS/argatroban (1.25−15.0 μM) on APTT of human PPP. Control PT and APTT showing clotting times of 14.2 ± 1.3 and 28.2 ± 2.1 s, respectively (mean ± SD, n = 3). The values are means ± SD of three independent experiments. Significance of difference with respect to control (without BSS), * $p < 0.05$. (e) Dose-dependent *in vitro* whole blood clotting time of BSS, nattokinase, and streptokinase against mammalian (goat) blood. The plots are means of three independent experiments. Significance of difference with respect to streptokinase * $p < 0.05$.

The titration of thrombin with BSS was a strong exothermic reaction (generation of heat), and it showed a sigmoidal saturation curve indicating a direct binding interaction between BSS and thrombin (Figure 4c). The best fit for the titration curve was obtained with a one binding-site model with a binding constant (K_a) of 109 ± 20.5 M^{-1}, ΔH = −8371 ± 729.2 cal/mol, ΔS = −18.8 cal/mol/deg for the interaction between BSS and thrombin (Figure 4c).

BSS Demonstrated Antiplatelet Activity and Inhibited Thrombin-Induced Platelet Aggregation. A comparison of the dose-dependent platelet deaggregation (antiplatelet) property of BSS and aspirin (positive control)

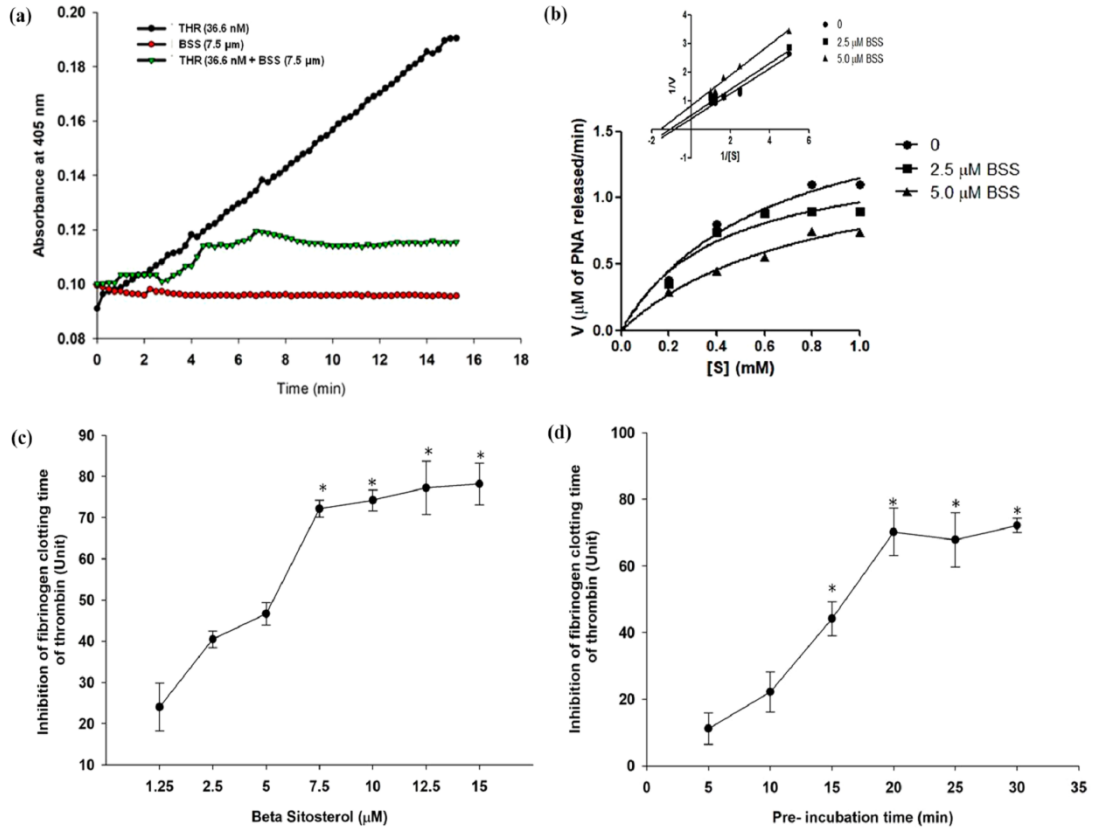

Figure 3. (a) Effect of BSS (7.5 μM) on amidolytic activity of thrombin (36.6 nM) against its chromogenic substrate T1637 (0.2 mM). Each data point is the mean of three independent measurements. (b) Michaelis−Menten plots and Lineweaver−Burk plots (inset) showing inhibition of thrombinactivity toward T1637 by BSS (0−5.0 μM). Each data point is the mean of three independent measurements. (c) Inhibition of fibrinogen clotting activity of thrombin (36.6 nM) by BSS (1.25−15 μM) at 37 °C, pH 7.4. (d) Time-dependent inhibition of fibrinogen clotting time of thrombin (36.6 nM) by BSS (7.5 μM) at 37 °C, pH 7.4. One unit of inhibition of fibrinogen clotting time of thrombin is defined as 1 s increase in clotting time of the control fibrinogen in the presence of BSS. The fibrinogen clotting time of thrombin under identical experimental conditions (control) was determined to be 39.17 ± 1.54 s. The values are means ± SD of three independent experiments. Significance of difference with respect to control (without BSS) *$p < 0.05$.

is shown in Figure 5a. Aspirin showed slightly higher antiplatelet activity compared to BSS (Figure 5a). Further, BSS in a concentration-dependent manner significantly ($p < 0.05$) inhibited the thrombin-induced aggregation of human platelet-rich plasma (PRP) and washed platelets. From the regression equation, the IC_{50} value of thrombin inhibition (concentration at which BSS demonstrated 50% inhibition of thrombin-induced platelet aggregation) was determined to be 10.5 ± 2.9 μM and 9.2 ± 1.2 μM (mean ± SD, $n = 3$) for PRP and washed platelets, respectively (Figure 5b). The *in vitro* antiplatelet effect of BSS against arachidonic acid- or adenosine diphosphate (ADP)-induced platelet aggregation was reported;[29] however, the IC_{50} values of these inhibitions (1.5 ± 0.4 and 1.5 ± 0.2 mM, respectively) were much higher compared to IC_{50} value of thrombin inhibition by BSS. Therefore, it is reasonable to anticipate that BSS functions as an inhibitor of platelet aggregation, by way of inhibiting thrombin activity suggesting that the antiplatelet activity of BSS contributes to its anticoagulant property.

BSS Demonstrated Antithrombotic Activity and Was Devoid of Hemolytic Activity or Cytotoxicity against Mammalian Cells. The thrombolytic potential of BSS was compared to commercial thrombolytic agents (streptokinase, nattokinase, and plasmin (Table 1). The in vitro thrombolytic activity of BSS was found to be lower than that of nattokinase and streptokinase. BSS and streptokinase demonstrated negligible activity in dissolving the heated blood clot (Table 1). Further, BSS did not possess plasmin-like activity (Figure S6, Supporting Information), though it activated the plasminogen to form plasmin that subsequently hydrolyzed the substrate for plasmin (Figure 6). Further, BSS did not display protease activity against fibrinogen (Figure S3, Supporting Information) and casein (data not shown). Moreover, incubation of BSS with 2 mM phenylmethylsulfonyl fluoride (PMSF) (serine protease inhibitor) did not affect its plasminogen activation property suggesting protease has no role to play in BSS-mediated plasminogen activation (Figure 6). However, further studies are necessary to pinpoint the mechanism of BSS-induced plasminogen activation.

Some reports have demonstrated the production of plasminogen activator in cultured endothelial cells from bovine carotid and in lung and kidney tissues.[30,31] In the present study, however, plasminogen is activated by BSS to form plasmin to dissolve the thrombus. Our results suggest that the

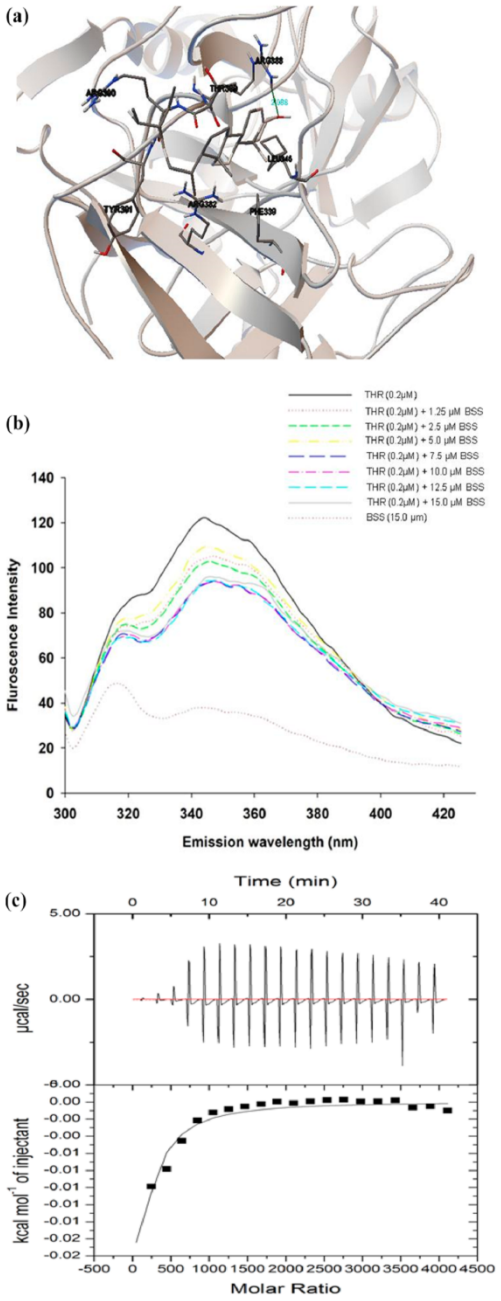

Figure 4. (a) Interaction site of the BSS around the thrombin residues, determined *in silico*. (b) Fluorescence spectra showing interaction of thrombin (0.2 μM) with different concentrations of BSS (1.25−15.0 μM). (c) ITC profile for BSS (10 μM) binding to thrombin (200 μM). (upper) Heat change upon ligand addition. (lower) An integrated ITC isotherm and its best fit to a one-site binding model.

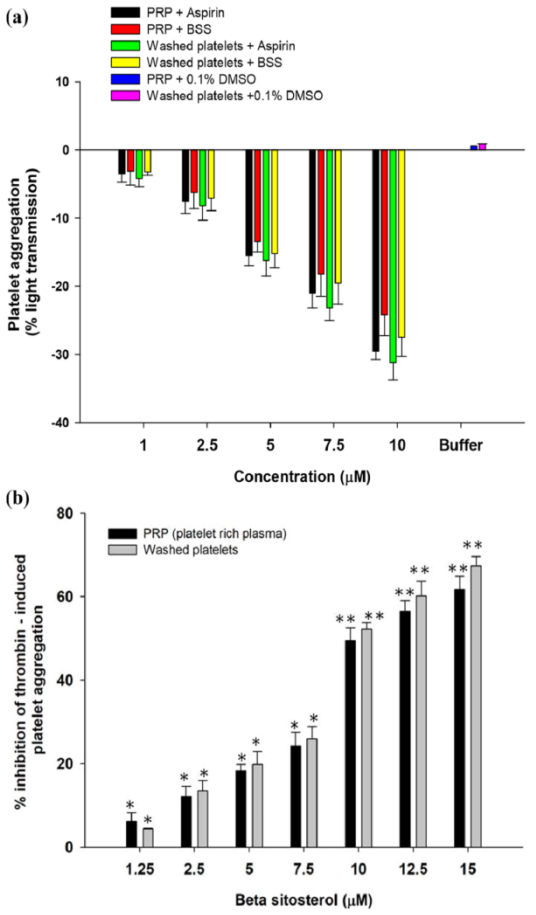

Figure 5. (a) Dose-dependent platelet deaggregation by BSS/aspirin. Different concentrations (1−10 μM) of BSS or aspirin or 1X PBS, pH 7.4 containing 0.1% DMSO (control) were incubated with PRP or washed platelets at 37 °C, and the absorbance was recorded at 540 nm. (b) Effect of BSS on thrombin-induced platelet aggregation. Thrombin (final concentration 0.03 U/ml) was incubated with BSS (1.25−15.0 μM)/1X PBS, pH 7.4 containing 0.1% DMSO (control) or 5 min at 37 °C. PRP/washed platelets were added to the mixture, and the decrease in absorbance was monitored at 540 nm for 5 min. The values are means ± SD of three independent experiments. Significance of difference with respect to control; * $p < 0.05$; ** $p < 0.01$.

thrombolytic potency of BSS depends on the activation of plasminogen to form plasmin, since endogenous plasminogen is inactivated by heating the blood,[32] which results in the loss of clot-bursting activity of BSS and streptokinase. Usually, patients who develop atrial fibrillation require anticoagulants to prevent the risk of clot formation, which could otherwise lead to cardiovascular diseases.[33] BSS delays the progressive coagulation of blood, and our results suggest that BSS plays a dual role in antithrombotic and thrombolytic activities.

BSS at a concentration of 50 μM (20 times greater than its in vitro minimum anticoagulant dose of 2.5 μM) did not show any adverse effects on the viability of HEK 293 cells (Figure S6, Supporting Information) indicating its lack of cytotoxicity against mammalian cells. BSS also did not cause *in vitro* hemolysis of mammalian erythrocytes (Figure S7, Supporting Information).

BSS Demonstrated *in Vivo* Anticoagulant Activity but Was Devoid of Defibrinogenation Activity. As shown in Table 2, tail bleeding time, plasma clotting time, and APTT were significantly prolonged in BSS-treated mice, in compar-

Table 1. Comparison of *in Vitro* Thrombolytic Activity Shown by BSS, Plasmin, Streptokinase, and Nattokinase under Identical Experimental Conditions[a]

	mg of clot lysed/μM of sample
Nonheated blood clot	
Negative control (1X PBS, pH 7.4)	2.1 ± 0.3
BSS	7.7 ± 0.3[b]
Streptokinase	15.5 ± 0.4[b]
Nattokinase	14.8 ± 1.2[b]
Plasmin	15.8 ± 1.6[b]
Heated blood clot	
Negative control (1X PBS, pH 7.4)	0.7 ± 0.2
BSS	1.0 ± 0.1[c]
Streptokinase	1.3 ± 0.1[c]
Nattokinase	9.9 ± 1.8[b]
Plasmin	9.2 ± 0.3[b]

[a]The values are mean ± SD of triplicate determinations. [b]$p < 0.05$ Significance of difference with respect to negative control. [c]$p < 0.05$ compared to positive controls.

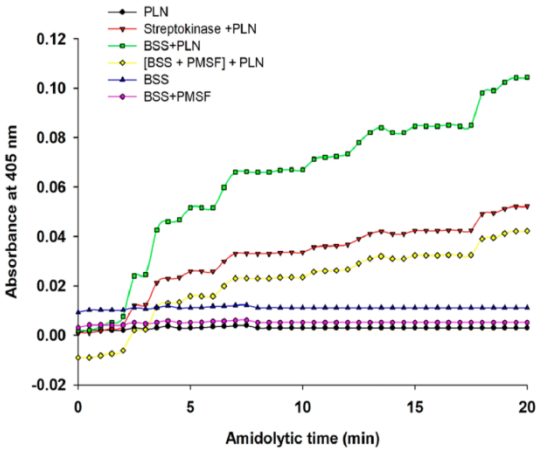

Figure 6. Effect of BSS (1.0 μM) and BSS (1.0 μM) preincubated with PMSF (2.0 mM) on amidolytic activity of plasminogen (20 μL, 10 U/ml) against the chromogenic substrate of plasmin, V0882, D-Val-Leu-Lys-*p*-nitroanilidedihydrochloride (0.2 mM). The values are means of three independent measurements.

ison to the control group ($p < 0.01$). Nevertheless, the *in vivo* anticoagulant potency of BSS was lower than the *in vivo* anticoagulant activity of heparin/nattokinase/argatroban (Table 2). BSS did not demonstrate *in vivo* defibrinogenation of mice plasma (Figure S8, Supporting Information).

Although the anticoagulant activity of BSS is lower than that of commercial drugs, potency may not be the sole reason for choosing an agent. Drug safety and the effectiveness of an anticoagulant when administered orally should also be considered. However, a recent study shows that supplementation of BSS to the anticoagulant active fraction of plant extract synergistically significantly enhanced anticoagulant activity as compared to the crude plant extract or the active fraction.[34]

Antithrombotic Effect of BSS in the Carrageenan-Induced Mouse Tail Thrombosis Model. BSS dose-dependently inhibited thrombus formation in the tail of carrageenan-treated mice (Figure 7, Table 3). The percent inhibition of thrombus formation induced by k-carrageenan in the mouse tail by BSS, nattokinase is shown in Table 3. Carrageenan-induced thrombosis in mice is a simple method for inducing thrombus in a small laboratory animal, and observations are easy without having to sacrifice the animals.[17,35] Our results suggest that BSS can prevent tail thrombosis induced by k-carrageenan and, therefore, could be a useful prophylactic antithrombotic drug.

Contradictory results have been presented to correlate the plasma levels of plant-sterol with CVDs.[36] Although the largest prospective trials and genome-wide association studies suggest that high plasma levels of plant sterols are associated with increased CVD risk, nevertheless, some other studies have reported no such association and even an inverse relationship.[36−38] Thus, the available data cannot confirm an increased CVD risk with level of plant sterols but cannot rule it out either. Only detailed interventional studies will provide deeper insight into the effects of plant-sterol-enriched food on the occurrence or prevention of CVDs.

The BSS is generally considered as an effective nutritional supplement, safer to administer, nontoxic,[39,40] inhibits mutagenecity,[41] and has no effect on reproductive systems.[42] BSS is well-tolerated in recommended doses for up to six months.[14,15,43] According to the Joint FAO/WHO Expert Committee on Food Additives (JECFA), the acceptable daily intake (ADI) of BSS is 40 mg/kg human body weight/day, and the No-Observed-Adverse-Effect-Level (NOAEL) is 4200 mg/kg_HBW/day. These doses are much higher than the *in vivo* anticoagulant dose of BSS suggesting its high therapeutic index. These results encourage clinical trials of BSS as an anticoagulant drug that may be used in combination with other drugs to prevent cardiovascular diseases.

EXPERIMENTAL SECTION

Chemicals. Natural β-sitosterol (≥95%) of soy bean origin, human thrombin, prothrombin, human fibrinogen, factor Xa, argatroban, warfarin, streptokinase, and plasmin were purchased from Sigma-Aldrich. Nattokinase was purchased from Healthy Origins. Coagulation proteins and chromogenic substrates were

Table 2. Comparison of *in Vivo* Anticoagulant Activity of BSS, Heparin, Nattokinase, and Argatroban-Treated Swiss Albino Mice

drugs (50 mg/kg)	PT (s)	PT (INR)	APTT (s)	APTT (INR)	tail bleeding time (s)	plasma clotting time (s)
1X PBS (control)	14.8 ± 0.7	1.0	28.3 ± 1.4	1.0	45.3 ± 2.5	175.5 ± 9.1
BSS	16.9 ± 0.6	1.1	46.8 ± 4.0[a]	1.6	61.0 ± 2.6[a]	193.5 ± 6.7[a]
Heparin	57.0 ± 4.3[a]	3.8	33.0 ± 2.0	1.1	153.3 ± 8.5[a]	215.6 ± 3.7[a]
Nattokinase	38.6 ± 2.8[a]	2.6	37.0 ± 3.6[a]	1.3	120.0 ± 4.1[a]	211.3 ± 12.8[a]
Argatroban	59.5 ± 2.5[a]	4.0	66.2 ± 4.2[a]	2.3	143.5 ± 5.6[a]	238.6 ± 9.2[a]

[a]Blood was drawn 5 h after iv injection of (50.0 mg/kg) BSS/heparin/nattokinase/argatroban. Values represent mean ± SD of six determinations. Significance of difference with respect to control, $p < 0.01$. INR = ($\text{prothrombin}_{test}/\text{prothrombin}_{control}$).

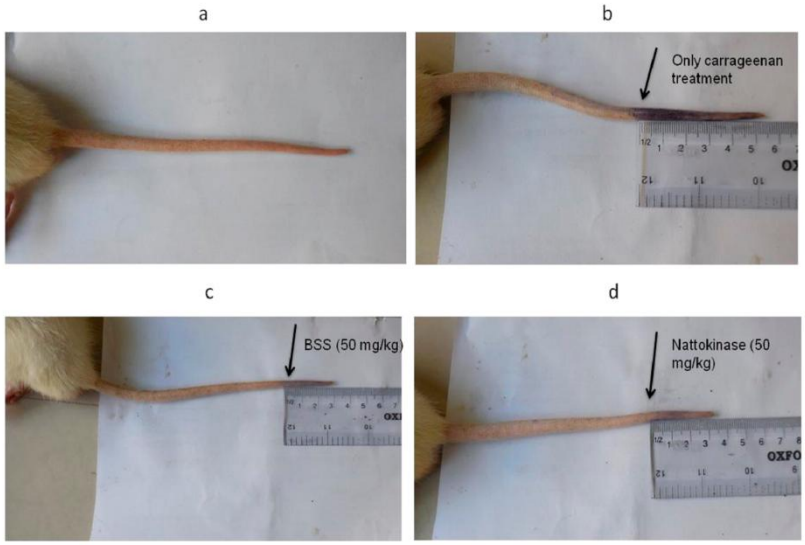

Figure 7. Effect of BSS and nattokinase on κ-carrageenan-induced mouse tail thrombus length (48 h after κ-carrageenan injection). (a) Tail without κ-carrageenan injection. (b) Control group of mice treated with 0.9 mg/kg κ-carrageenan only. (c) BSS (50 mg/kg) pretreated group of mice injected with 0.9 mg/kg κ-carrageenan. (d) Nattokinase (50 mg/kg) pretreated group of mice injected with 0.9 mg/kg κ-carrageenan. Arrows indicate thrombus formation region (wine and black colors) in tail of mice.

Table 3. Effect of BSS and Nattokinase on k-Carrageenan-Induced Mouse Tail Thrombus Model at 24, 48, and 72 h Post Treatment

drugs	dose	% inhibition of thrombus formation in mice tail after κ-carrageenan treatment		
		24 h	48 h	72 h
BSS	12.5 mg/kg	10.5 ± 3.1[b]	14.52 ± 3.5[b]	23.2 ± 1.8[b]
	25.0 mg/kg	15.2 ± 2.8[b]	31.26 ± 2.2[b]	36.5 ± 2.8[c]
	50.0 mg/kg	23.4 ± 2.1[b]	42.30 ± 2.8[c]	47.3 ± 3.1[c]
Nattokinase	50.0 mg/kg	26.5 ± 1.2[b]	46.18 ± 2.75[c]	52.3 ± 3.8[c]

[a]Values are mean ± SD of six mice. Significance of difference with respect to control group of mice. [b]$p < 0.05$. [c]$p < 0.01$.

procured from Sigma-Aldrich. PT and APTT kits were purchased from Tulip Diagnostics. κ-Carrageenan was purchased from Sigma-Aldrich.The fibrinogen assay kit was purchased from R^2 Diagnostics. All other reagents were of analytical grade and purchased from Sigma-Aldrich.

Assay of Anticoagulant Activity of BSS. The collection of blood from healthy volunteers (who were not under medication) was approved by the Tezpur University Ethical Committee, and informed consent was obtained from all participants. Platelet poor plasma (PPP) was prepared from citrated human blood according to our previously described protocol.[44,45] Stock solution of BSS was prepared by dissolving 1 mg of BSS in 100 μL of dimethyl sulfoxide (DMSO), and then volume was made to 1.0 mL with 1X phosphate-buffered saline (PBS; 20 mM potassium phosphate buffer and 150 mM NaCl, pH 7.4). Before the assay, stock solution was diluted appropriately with 1X PBS, pH 7.4. Different concentrations (1.25 to 15.0 μM) of BSS/1X PBS, pH 7.4 containing 0.1% DMSO (control) were preincubated with 300 μL of PPP for 3 min at 37 °C, and clotting was initiated by adding 40 μL of 250 mM $CaCl_2$.[44] As a positive control, warfarin, nattokinase, and argatroban were used. One unit of anticoagulant activity was defined as 1 s increase in clotting time of the control PPP.[44,45] The APTT and PT of BSS/argatroban-treated (positive control) and control (untreated) PPP were measured using commercial kits.[45]

Fibrinogenolytic Activity Assay. Human fibrinogen (2.6 μM, dissolved in 1X PBS, pH 7.4) was incubated with BSS (5.0 μM)/1X PBS, pH 7.4 containing 0.1% DMSO (control) for 30−120 min at 37 °C, and fibrinogenolytic activity assay was performed following a previously described protocol.[46]

Effect of BSS on Amidolytic Activity of Thrombin and FXa and Determination of the Inhibitory Constant (K_i). The inhibition of the amidolytic activity of thrombin (3.0 μL of 10 NIH/ml, 36.6 nM) or FXa (0.13 μM) by BSS (7.5 μM) /1X PBS, pH 7.4 containing 0.1% DMSO (control) against their chromogenic substrates T1637 [*N*-(*p*-tosyl)-Gly-Pro-Arg-*p*-nitroanilide acetate] and F3301 [*N*-benzoyl-Ile-Glu-Gly-Arg-*p*-nitroanilide acetate], respectively, was determined as described previously.[46,47] For the kinetics analysis, graded concentrations of BSS (0−5.0 μM) were incubated with a fixed concentration of thrombin (36.6 nM), and the reaction rate (V) was plotted against the different substrate concentration [S] (0.2−1.0 mM) at each inhibitor (BSS) concentration.[47] The data were fitted to a hyperbolic Michaelis−Menten model using GraphPad Prism 5.0 software.[47] The inhibitory constant (K_i) was determined using the uncompetitive models for enzyme inhibition for thrombin using the above software.[47]

Effect of BSS on the Physiological Substrate of Thrombin and FXa. To determine the effect of BSS on fibrinogen clotting activity of thrombin, different concentrations of BSS (1.25 to 12.5 μM) or 1X PBS, pH 7.4 containing 0.1% DMSO (control) were preincubated with thrombin (3 μL of 10 NIH U/mL in 20 mM potassium phosphate buffer, pH 7.4) for 30 min at 37 °C. The reaction was initiated by adding 2.6 μM human fibrinogen (dissolved in 20 mM potassium phosphate buffer, pH 7.4), and the time of the fibrin clot formation was monitored by visual inspection.[46,47]

To determine the kinetics of binding between BSS and thrombin, BSS (7.5 μM)/1X PBS, pH 7.4 containing 0.1% DMSO (control) was preincubated with thrombin (3 μL of 10 NIH U/ml in 20 mM potassium phosphate buffer, pH 7.4) for different time intervals (0 to 30 min) at room temperature. Thereafter, the fibrinogen clotting time of thrombin was assayed as described above.

For the FXa inhibition assay, BSS (7.5 μM)/1X PBS, pH 7.4 containing 0.1% DMSO (control) was preincubated with FXa (0.13 μM) in 20 mM sodium phosphate buffer, pH 7.4 at 37 °C for 30 min. Thereafter, 1.4 μM prothrombin (the physiological substrate for FXa) was added to the reaction mixture and incubated at 37 °C for 4 h. The prothrombin degradation products were analyzed by 12.5% sodium dodecyl sulfate poly(acrylamide) gel electrophoresis (SDS-PAGE) under reducing conditions.[47]

Determination of Interaction between BSS and Thrombin/Fibrinogen/FXa by Spectrofluorometric Analysis. Thrombin (0.2 μM)/fibrinogen (0.2 μM)/ FXa (0.2 μM) was incubated with different concentrations of BSS (1.25 μM to 15.0 μM) for 3 min at room temperature. The change in fluorescence intensity at an excitation of 280 nm was measured. The excitation and emission slits were set as 10 nm, and emission spectra were recorded from 300 to 425 nm at room temperature (~23 °C) using a fluorescence spectrometer (LS55, PerkinElmer) as we described previously.[46,47] All the binding experiments were done in triplicate to ensure the reproducibility. The fluorescence intensity of the coagulation protein or BSS alone recorded under identical experimental conditions served as control.

Isothermal Calorimetry Titration to Determine the Interaction of BSS with Thrombin. ITC experiments were performed at 37 °C on a MicroCal iTC-200 system (GE Healthcare) in a high gain mode at a reference power of 10 μcal^{-1}. Human thrombin (200 μM in 1X PBS buffer, pH 7.4) was titrated against 10 μM of BSS dissolved in the same buffer. A total of 20 injections were made with 300 s time intervals between.[48] By SDS-PAGE analysis we observed that thrombin was stable within this titration time (data not shown). For longer titrations, the syringe was refilled, and injections continued into the same cell sample. Control runs were performed where cell samples and syringe samples were titrated with buffer, and the data from these runs was subtracted from the experimental data. Data analysis was performed with Origin software, and the data fitting was done using a "one site binding" model.

***In Silico* Study to Determine Interaction between BSS and Thrombin.** A binding interaction between BSS and thrombin was determined by AutoDock 4.2 software.[49,50] The initial structure of the thrombin was taken from the protein data bank (PBDCode: 3u69). On the one hand, for the docking study, all water molecules from the protein crystal structure were removed, and polar hydrogen atoms were added to the thrombin. On the other hand, the initial structure of the ligand (BSS) was taken from the density functional theory (DFT) optimized structure at a B3LYP level of theory at 6-31+g(d,p) basis set using Gaussin09 software.[50] Prior to the docking calculation, a precalculated grid map was acquired by AutoDock to find the binding energy in the region of interest in the receptor molecule. Therefore, a grid box size of 60, 60, and 60 Å (coordinate at *X*, *Y*, and *Z* axes) with a grid spacing of 0.972 Å was used. During the BSS-thrombin interaction, 10 runs were conducted, and one docking pose was retained for the ligand.

Determination of Effect of BSS on Thrombin Inhibition by AT-III in the Presence or Absence of Heparin. The effect of BSS on thrombin inhibition produced by AT-III in the presence or absence of heparin was determined as per the protocol described by Arocas et al.[51] Briefly, thrombin (3 μL, 10 NIH/ml) was preincubated with BSS (7.5 μM, dissolved in 1X PBS, pH 7.4) for 30 min at 37 °C in a final reaction mixture of 100 μL adjusted with 1X PBS, pH 7.4. Heparin-free AT-III (100 nM) in the presence of 0.5 U/ml heparin was added to the samples, and the residual activity of thrombin was measured by hydrolysis of its chromogenic substrate T1637 at 10 min at 405 nm in a microplate reader.[52]

Determination of *in Vitro* Thrombolytic and Antithrombotic Activity of BSS. For the *in vitro* thrombolytic activity assay, 1.0 mL of mammalian (goat) blood collected in 3.8% sodium citrate (9:1 ratio) was allowed to clot in a preweighed microfuge tube at room temperature after the addition of 100 μL of 250 mM $CaCl_2$. The clot was weighed, and thereafter, BSS or commercial thrombolytic agents such as streptokinase (indirect thrombolytic agent)/plasmin (direct thrombolytic agent)/nattokinase (bacterial fibrinolytic enzyme) at a concentration ranging from 1.25 to 15 μM or 1X PBS, pH 7.4 containing 0.1% DMSO (control) were incubated with the blood clot for 3 h at 37 °C. The thrombolytic activity was determined as described by Majumdar et al.[46] The *in vitro* thrombolytic activity was expressed as milligrams of blood clot (thrombus) lysed per micromolar of BSS/commercial thrombolytic agent, compared to the control.[46]

In another set of experiments, the blood clot was heated at 80 °C for 30 min to denature the endogenous fibrin(ogen)olytic factors (plasmin, plasminogen, t-PA, etc.) prior to the thrombolytic activity assay.[46]

Plasminogen Activation Assay. For the determination of plasminogen activation property, 1 μM of BSS (in 20 mM phosphate buffer pH 7.4)/1X PBS, pH 7.4 containing 0.1% DMSO (control) was incubated with 20 μL of plasminogen (10 U/ml in 1X PBS buffer, pH 7.4) at 37 °C for 20 min. The formation of plasmin from plasminogen was determined by adding 0.2 mM of V0882 (D-Val-Leu-Lys-*p*-nitroanilidedihydrochloride), and the absorbance was monitored at 405 nm in a plate reader (Multiskan Go, Thermo Scientific) continuously for 15 min against the reagent blank. The activity of streptokinase (1 μM) under identical experimental conditions was used as a positive control.[53] To determine the plasmin-like activity of BSS, if any, BSS (1 μM) was directly added to the 0.2 mM of V0882 (D-Val-Leu-Lys-*p*-nitroanilidedihydrochloride), and the absorbance was monitored at 405 nm in a plate reader (Multiscan Go, Thermo Scientific) continuously for 15 min against the reagent blank.[46]

In an another set of experiments, to determine the role of soybean protease contamination, if any, in the BSS preparation, the BSS (1.0 μM) was preincubated with 2 mM PMSF (serine protease inhibitor) for 30 min at 37 °C, and then the plasminogen activation property was performed as described above.

Antiplatelet Effect of BSS against Thrombin-Induced Platelet Aggregation. The collection of blood from healthy volunteers (who were not under medication) was approved by the Tezpur University Ethical Committee, and informed consent was obtained from all participants. PRP and washed platelets were prepared from citrated human blood, following the procedure described by Bednar et al.[54] and Irfan et al.[55] and modified by Dutta et al.[45] Briefly, graded concentrations of BSS/aspirin (0−10 μM in final volume of 1 μL)/1X PBS, pH 7.4 containing 0.1% DMSO (control) were added to 100 μL of the PRP/washed platelets (1×10^4 platelets/ml), and the absorbance was measured continuously at 540 nm for 5 min in a microplate reader. The percent platelet deaggregation after 300 s of incubation of platelets with BSS/aspirin was calculated according to the method of Dutta et al.[45]

In another set of experiments, thrombin (3 μL of 10 NIH U/ml ~0.03 U/ml) was preincubated with different concentrations of BSS (0−15 μM) in 1X PBS, pH 7.4 containing 0.1% DMSO (control) for 5 min prior to the addition PRP/washed platelets. The aggregation induced by the identical concentration of thrombin (control) was considered as 100% activity, and the decrease in BSS-induced platelet aggregation (antiplatelet activity) was compared to that.[45]

Hemolytic Activity and Cytotoxicity of BSS. The hemolytic activity of graded concentrations of BSS (2.5 to 50 μM) was determined against mammalian (goat) washed erythrocytes as described previously.[53,56] The cytotoxicity of BSS was tested against human embryonic kidney cells (HEK 293 cell line), cultured, and maintained in Dulbecco's Modified Eagle Medium (DMEM) as described previously.[57,58] For the viability assay, 100 μL aliquots of 2×10^4 cells/ml were seeded into 96-well plates and treated with various concentrations (1 to 250 μM) of BSS and medium (control), and incubated at 37°C for 24 h. Cell viability was then determined using the colorimetric 3-(4,5-dimethylthiazol-2-yl)-2,5-diphenyltetrazolium bromide [MTT] assay following the manufacturer's instructions (ATCC).[57,58] All assays were done in triplicate and repeated at least three times to ensure reproducibility.

Determination of *in Vivo* Anticoagulant Activity in an Animal Model. Animal experimental protocols were approved by the Tezpur University Animal Ethical Committee (Approval No.

DORDPro/TUAEC/10-56/14/Res-10), Animal Ethical Committee of CSIR-CIMAP, Lucknow and Defense Research Laboratory, Tezpur (Approval No. DRL/02/Dec/2010-11/II).

To determine the dose-dependent *in vivo* anticoagulant and defibrinogenating activity, different doses of BSS (12.5, 25, and 50 mg/kg body weight of mice) or positive controls (heparin, nattokinase, or argatroban; 50 mg/kg) were injected intravenously (*i.v*) in Swiss albino mice ($n = 6$). Blood was drawn 5 h after injection (considering the half-life of BSS is 2.94 to 3 h and complete metabolism occurs within10−12 h) by retro orbital bleeding. The PT, APTT, tail bleeding time, and plasma Ca-clotting time of control and treated groups of mice were determined as described previously.[17] The fibrinogen content of plasma was measured using commercial kits following the manufacturer's protocol.

At the end of the experiments, mice were euthanized with an overdose of Na-pentobarbital as per recommendations of the CPCSEA.

Antithrombotic Effect of BSS in Carrageenan-Induced Mouse Tail Thrombosis Model. A total of 30 Swiss albino mice were randomly subdivided into five groups, each group containing six mice (three males and three females). The mice in group 1 were treated with 1X PBS, pH 7.4 (the control/placebo). The mice in groups 2, 3, and 4 were orally treated with graded concentrations (12.5, 25, and 50 mg/kg in 1X PBS, pH 7.4, respectively) of BSS in a total volume of 200 μL for one week. The mice in group 5 were orally treated with a 50 mg/kg dose of nattokinase for one week. Thirty minutes after the last treatment with BSS or nattokinase, the tails were ligated, and 0.9 mg/kg body weight of k-carrageenan was given by iv injection.[17] Ligatures were removed after 15 min of injection. The length of the infarcted region was measured, and the appearance of the wine-colored thrombus formation in the tail was measured and photographed at 24, 48, and 72 h.[17]

Statistical Analysis. The two sets of data were statistically analyzed by Student's *t* test and one way ANOVA using the SigmaPlot 10.0 for Windows (version 7.0) software and Graph Pad software, respectively. Values of $p < 0.05$ and 0.01 were considered to be statistically significant.

CONCLUSION

Our findings show that BSS exerts its anticoagulant activity by inhibiting thrombin via an uncompetitive mechanism. Further, BSS had *in vitro* antiplatelet and thrombolytic activities and demonstrated its *in vivo* antithrombotic effect in the k-carrageenan-induced thrombosis mouse model. Thus, these findings point to potential therapeutic applications of BSS in preventing and/or treating thrombosis-associated cardiovascular disorders. Moreover, dietary supplementation of BSS may help to reduce the risk of cardiovascular disorders.

ASSOCIATED CONTENT

Supporting Information

The Supporting Information is available free of charge on the ACS Publications website at DOI: 10.1021/acs.jnatprod.8b00574.

Effect of BSS (7.5 μM) on amidolytic activity of FXa (0.13 μM) against its chromogenic substrate F3301 (0.2 mM). The values are means of triplicate determinations. Inhibition of prothrombin activation property of FXa by BSS. After reduction with β-mercaptoethanol, degradation products were separated by 12.5% SDS-PAGE. Lane 1, protein molecular markers; lane 2, 1.4 μM PTH; lane 3, PTH (1.4 μM) incubated with FXa (0.13 μM) for 30 min at 37 °C, pH 7.4; lane 4, [FXa (0.13 μM) preincubated with BSS (7.5 μM) for 15 min] + PTH (1.4 μM). Kinetics of fibrinogenolytic activity of BSS. The degradation products were separated by 12.5% SDS-PAGE (reducing conditions). Lane 1, control human fibrinogen (0.25% w/v in 20 mM K-phosphate buffer, 150 mM NaCl, pH 7.4); lanes 2−4, human fibrinogen treated with BSS (5 μM) for 30, 60, and 120 min, respectively, at 37 °C, pH 7.4. Inhibition of amidolytic activity of thrombin against its substrate T1637 when 36.6 nM thrombin was preincubated with heparin/BSS (0.5 mIU/7.5 μM), AT III/BSS (2.5 μM/7.5 μM), and heparin/AT III/BSS (0.5 mIU/2.5 μM/7.5 μM). Fluorescence spectra showing interaction of fibrinogen (0.2 μM) with different concentrations of BSS (1.25−10.0 μM). Fluorescence spectra showing interaction of FXa (0.2 μM) with different concentrations of BSS (1.25−10.0 μM).*In vitro* cell viability assay using MTT assay. The HEK 293 cells were treated with BSS (2.5−50 μM) for 24 h at 37°C. All values are means ± SD of triplicate determinations. *In vitro* blood hemolysis assay. The human erythrocytes (5%, v/v) were treated with BSS (2.5−50 μM) for 90 min 37 °C. All values are mean ± SD of triplicate determinations. Dose-dependent *in vivo* defibrinogenating activity of BSS 5 h after *i.v* injection in mice. The values are means ± SD of triplicate determinations (PDF)

AUTHOR INFORMATION

Corresponding Author

*Phone: +917896003886. E-mail: akm@tezu.ernet.in.

ORCID

Ramesh C. Deka: 0000-0003-4352-2661

Ashis K. Mukherjee: 0000-0001-9869-858X

Funding

This project received financial support from a DBT-BIRAC-BIG Project [BT/TEMP2517/BIG-08/1] to A.K.M.

Notes

The authors declare no competing financial interest.

ACKNOWLEDGMENTS

The authors thank DBT-IPLS for support for the ITC study. D.G. received SRF from a DBT BIRAC project.

REFERENCES

(1) Nicola Dario Di Minno, M.; Momi, S.; Di Minno, A.; Russolillo, A. *Curr. Drug Targets* **2013**, *14* (1), 3−12.

(2) Versteeg, H. H.; Heemskerk, J. W.; Levi, M.; Reitsma, P. H. *Physiol. Rev.* **2013**, *93* (1), 327−58.

(3) Ageno, W.; Gallus, A. S.; Wittkowsky, A.; Crowther, M.; Hylek, E. M.; Palareti, G. *Chest* **2012**, *141* (2), e44S−e88S.

(4) Weitz, J. I. *Am. J. Hematol.* **2012**, *87* (S1), S133−S136.

(5) Davie, E. W.; Fujikawa, K.; Kisiel, W. *Biochemistry* **1991**, *30* (43), 10363−10370.

(6) Davie, E. W. *Thromb. Haemostasis* **1995**, *73* (1), 1.

(7) Eriksson, B. I.; Quinlan, D. J.; Eikelboom, J. W. *Annu. Rev. Med.* **2011**, *62*, 41−57.

(8) Winstanley, L.; Chen, R. *CNS Neurol. Disord.: Drug Targets* **2013**, *12* (2), 242−51.

(9) Atanasov, A. G.; Waltenberger, B.; Pferschy-Wenzig, E. M.; Linder, T.; Wawrosch, C.; Uhrin, P.; Temml, V.; Wang, L.; Schwaiger, S.; Heiss, E. H.; Rollinger, J. M.; Schuster, D.; Breuss, J. M.; Bochkov, V.; Mihovilovic, M. D.; Kopp, B.; Bauer, R.; Dirsch, V. M.; Stuppner, H. *Biotechnol. Adv.* **2015**, *33* (8), 1582−1614.

(10) Chen, C.; Yang, F.-Q.; Zhang, Q.; Wang, F.-Q.; Hu, Y.-J.; Xia, Z.-N. *Evidence-Based Complementary and Alternative Medicine* **2015**, *2015*, 1.

(11) Genser, B.; Silbernagel, G.; De Backer, G.; Bruckert, E.; Carmena, R.; Chapman, M. J.; Deanfield, J.; Descamps, O. S.; Rietzschel, E. R.; Dias, K. C.; Marz, W. *Eur. Heart J.* **2012**, *33* (4), 444−51.
(12) Zhao, H. L.; Houweling, A. H.; Vanstone, C. A.; Jew, S.; Trautwein, E. A.; Duchateau, G. S.; Jones, P. J. *J. Am. Coll. Nutr.* **2011**, *30* (2), 155−65.
(13) Bin Sayeed, M. S.; Ameen, S. S. *Nutr. Cancer* **2015**, *67* (8), 1216−20.
(14) Hendriks, H. F.; Brink, E. J.; Meijer, G. W.; Princen, H. M.; Ntanios, F. Y. *Eur. J. Clin. Nutr.* **2003**, *57* (5), 681−92.
(15) Tuomilehto, J.; Tikkanen, M. J.; Hogstrom, P.; Keinanen-Kiukaanniemi, S.; Piironen, V.; Toivo, J.; Salonen, J. T.; Nyyssonen, K.; Stenman, U. H.; Alfthan, H.; Karppanen, H. *Eur. J. Clin. Nutr.* **2009**, *63* (5), 684−91.
(16) Choi, J. H.; Sapkota, K.; Park, S. E.; Kim, S.; Kim, S. J. *Biochimie* **2013**, *95* (6), 1266−77.
(17) Majumdar, S.; Chattopadhyay, P.; Mukherjee, A. K. *Clin. Appl. Thromb./Hemostasis* **2016**, *22* (6), 594−8.
(18) Bode, W.; Turk, D.; Karshikov, A. *Protein Sci.* **1992**, *1* (4), 426−71.
(19) De Cristofaro, R.; De Candia, E. *J. Thromb. Thrombolysis* **2003**, *15* (3), 151−63.
(20) Cossy, J.; Belotti, D. *Bioorg. Med. Chem. Lett.* **2001**, *11* (15), 1989−92.
(21) Escolar, G.; Bozzo, J.; Maragall, S. *Drugs Today* **2006**, *42* (4), 223−36.
(22) Ryn, J. v.; Stangier, J.; Haertter, S.; Liesenfeld, K.-H.; Wienen, W.; Feuring, M.; Clemens, A. *Thromb. Haemostasis* **2010**, *103* (6), 1116.
(23) Stubbs, M. T.; Bode, W. *Thromb. Res.* **1993**, *69* (1), 1−58.
(24) Pereira, R. C.; Lourenco, A. L.; Terra, L.; Abreu, P. A.; Laneuville Teixeira, V.; Castro, H. C. *Mar. Drugs* **2017**, *15* (3), 79.
(25) Ward, W. H.; Holdgate, G. A. *Prog. Med. Chem.* **2001**, *38*, 309−76.
(26) Liu, J.; Tian, J.; He, W.; Xie, J.; Hu, Z.; Chen, X. *J. Pharm. Biomed. Anal.* **2004**, *35* (3), 671−7.
(27) Saikia, D.; Thakur, R.; Mukherjee, A. K. *Toxicon* **2011**, *57* (6), 841−850.
(28) Mukherjee, A. K.; Dutta, S.; Kalita, B.; Jha, D. K.; Deb, P.; Mackessy, S. P. *Biochimie* **2016**, *128*−*129*, 138−47.
(29) Saeed, S. A.; Farnaz, S.; Simjee, R. U.; Malik, A. *Biochem. Soc. Trans.* **1993**, *21* (4), 462S.
(30) Hagiwara, H.; Shimonaka, M.; Morisaki, M.; Ikekawa, N.; Inada, Y. *Thromb. Res.* **1984**, *33* (4), 363−70.
(31) Hoffmann, A.; Klocking, H.-P. *Fibrinolysis* **1988**, *115* (1−2), 189−96.
(32) Alkjaersig, N.; Fletcher, A. P.; Sherry, S. *J. Clin. Invest.* **1959**, *38* (7), 1086.
(33) Lopez-Sendon, J.; López, d. S. E.; Bobadilla, J.; Rubio, R.; Bermejo, J.; Delcan, J. *Revista espanola de cardiologia* **1995**, *48* (6), 407−439.
(34) Mukherjee, A. K.; Gogoi, D. Anticoagulant actives and synergistic anticoagulant composition and method for producing the same. *International patent* PCT/IN2016/050448 2017.
(35) Yuan, J.; Yang, J.; Zhuang, Z.; Yang, Y.; Lin, L.; Wang, S. *BMC Biotechnol.* **2012**, *12*, 36.
(36) Verges, B.; Fumeron, F. *Diabetes Metab.* **2015**, *41* (1), 76−81.
(37) Silbernagel, G.; Fauler, G.; Hoffmann, M. M.; Lutjohann, D.; Winkelmann, B. R.; Boehm, B. O.; Marz, W. *J. Lipid Res.* **2010**, *51* (8), 2384−93.
(38) Teupser, D.; Baber, R.; Ceglarek, U.; Scholz, M.; Illig, T.; Gieger, C.; Holdt, L. M.; Leichtle, A.; Greiser, K. H.; Huster, D.; Linsel-Nitschke, P.; Schafer, A.; Braund, P. S.; Tiret, L.; Stark, K.; Raaz-Schrauder, D.; Fiedler, G. M.; Wilfert, W.; Beutner, F.; Gielen, S.; Grosshennig, A.; Konig, I. R.; Lichtner, P.; Heid, I. M.; Kluttig, A.; El Mokhtari, N. E.; Rubin, D.; Ekici, A. B.; Reis, A.; Garlichs, C. D.; Hall, A. S.; Matthes, G.; Wittekind, C.; Hengstenberg, C.; Cambien, F.; Schreiber, S.; Werdan, K.; Meitinger, T.; Loeffler, M.; Samani, N. J.; Erdmann, J.; Wichmann, H. E.; Schunkert, H.; Thiery, J. *Circ.: Cardiovasc. Genet.* **2010**, *3* (4), 331−9.
(39) Malini, T.; Vanithakumari, G. *J. Ethnopharmacol.* **1990**, *28* (2), 221−34.
(40) Paniagua-Perez, R.; Madrigal-Bujaidar, E.; Reyes-Cadena, S.; Molina-Jasso, D.; Gallaga, J. P.; Silva-Miranda, A.; Velazco, O.; Hernandez, N.; Chamorro, G. *J. Biomed. Biotechnol.* **2005**, *2005* (3), 242−7.
(41) Villasenor, I. M.; Angelada, J.; Canlas, A. P.; Echegoyen, D. *Phytother. Res.* **2002**, *16* (5), 417−21.
(42) Nieminen, P.; Polonen, I.; Ikonen, K.; Maattanen, M.; Mustonen, A. M. *Chemosphere* **2008**, *71* (3), 493−9.
(43) Ulbricht, C. E. *J. Diet Suppl* **2016**, *13* (1), 35−92.
(44) Doley, R.; Mukherjee, A. K. *Toxicon* **2003**, *41* (1), 81−91.
(45) Dutta, S.; Gogoi, D.; Mukherjee, A. K. *Biochimie* **2015**, *110*, 93−106.
(46) Majumdar, S.; Sarmah, B.; Gogoi, D.; Banerjee, S.; Ghosh, S. S.; Banerjee, S.; Chattopadhyay, P.; Mukherjee, A. K. *Biochimie* **2014**, *103*, 50−60.
(47) Thakur, R.; Kumar, A.; Bose, B.; Panda, D.; Saikia, D.; Chattopadhyay, P.; Mukherjee, A. K. *Biochimie* **2014**, *105*, 149−58.
(48) Pretorius, E.; Mbotwe, S.; Bester, J.; Robinson, C. J.; Kell, D. B. *J. R. Soc., Interface* **2016**, *13* (122), 20160539.
(49) Bora, B.; Biswas, A. D.; Gurung, A. B.; Bhattacharjee, A.; Mattaparthi, V. S.; Mukherjee, A. K. *J. Biomol. Struct. Dyn.* **2017**, *35* (3), 622−644.
(50) Morris, G. M.; Huey, R.; Olson, A. J. Using AutoDock for Ligand-Receptor Docking. *Curr. Protoc. Bioinf.* **2008**. DOI: 10.1002/0471250953.bi0814s24
(51) Arocas, V.; Zingali, R. B.; Guillin, M. C.; Bon, C.; Jandrot-Perrus, M. *Biochemistry* **1996**, *35* (28), 9083−9.
(52) Mukherjee, A. K.; Mackessy, S. P. *Biochim. Biophys. Acta, Gen. Subj.* **2013**, *1830* (6), 3476−88.
(53) Saikia, D.; Bordoloi, N. K.; Chattopadhyay, P.; Choklingam, S.; Ghosh, S. S.; Mukherjee, A. K. *Biochim. Biophys. Acta, Biomembr.* **2012**, *1818* (12), 3149−57.
(54) Bednar, B.; Condra, C.; Gould, R. J.; Connolly, T. M. *Thromb. Res.* **1995**, *77* (5), 453−463.
(55) Irfan, M.; Jeong, D.; Saba, E.; Kwon, H. W.; Shin, J. H.; Jeon, B. R.; Kim, S.; Kim, S. D.; Lee, D. H.; Nah, S. Y.; Rhee, M. H. *Platelets* **2018**, 1−10.
(56) Doley, R.; King, G. F.; Mukherjee, A. K. *Arch. Biochem. Biophys.* **2004**, *425* (1), 1−13.
(57) Mukherjee, A. K.; Saviola, A. J.; Burns, P. D.; Mackessy, S. P. *Apoptosis* **2015**, *20* (10), 1358−72.
(58) Raza, A.; Ghoshal, A.; Chockalingam, S.; Ghosh, S. S. *Sci. Rep.* **2017**, *7* (1), 7580.

(12) INTERNATIONAL APPLICATION PUBLISHED UNDER THE PATENT COOPERATION TREATY (PCT)

(19) World Intellectual Property Organization
International Bureau

(43) International Publication Date
22 June 2017 (22.06.2017)

WIPO | PCT

(10) International Publication Number
WO 2017/103949 A1

(51) International Patent Classification:
A61K 36/53 (2006.01)

(21) International Application Number:
PCT/IN2016/050448

(22) International Filing Date:
17 December 2016 (17.12.2016)

(25) Filing Language: English

(26) Publication Language: English

(30) Priority Data:
1313/KOL/2015 18 December 2015 (18.12.2015) IN

(71) Applicant: **TEZPUR UNIVERSITY** [IN/IN]; (Central University), Napaam, Tezpur-784028, Assam, India., Tezpur 784028 (IN).

(72) Inventors: **MUKHERJEE, Ashis Kumar**; Flat B-29, Tezpur University, Napaam, Tezpur-784028, Assam, India, Tezpur 784028 (IN). **GOGOI, Debananda**; B-310, ONGC Colony, Nazira, P.O. Nazira – 785685, Sivasagar, Assam, India., Sivasagar 785685 (IN).

(74) Agent: **SEN, Anjan**; Anjan Sen & Associates., 17, Chakraberia Road South, Kolkata - 700 025 (IN).

(81) Designated States *(unless otherwise indicated, for every kind of national protection available)*: AE, AG, AL, AM, AO, AT, AU, AZ, BA, BB, BG, BH, BN, BR, BW, BY, BZ, CA, CH, CL, CN, CO, CR, CU, CZ, DE, DJ, DK, DM, DO, DZ, EC, EE, EG, ES, FI, GB, GD, GE, GH, GM, GT, HN, HR, HU, ID, IL, IN, IR, IS, JP, KE, KG, KH, KN, KP, KR, KW, KZ, LA, LC, LK, LR, LS, LU, LY, MA, MD, ME, MG, MK, MN, MW, MX, MY, MZ, NA, NG, NI, NO, NZ, OM, PA, PE, PG, PH, PL, PT, QA, RO, RS, RU, RW, SA, SC, SD, SE, SG, SK, SL, SM, ST, SV, SY, TH, TJ, TM, TN, TR, TT, TZ, UA, UG, US, UZ, VC, VN, ZA, ZM, ZW.

(84) Designated States *(unless otherwise indicated, for every kind of regional protection available)*: ARIPO (BW, GH, GM, KE, LR, LS, MW, MZ, NA, RW, SD, SL, ST, SZ, TZ, UG, ZM, ZW), Eurasian (AM, AZ, BY, KG, KZ, RU, TJ, TM), European (AL, AT, BE, BG, CH, CY, CZ, DE, DK, EE, ES, FI, FR, GB, GR, HR, HU, IE, IS, IT, LT, LU, LV, MC, MK, MT, NL, NO, PL, PT, RO, RS, SE, SI, SK, SM, TR), OAPI (BF, BJ, CF, CG, CI, CM, GA, GN, GQ, GW, KM, ML, MR, NE, SN, TD, TG).

Declarations under Rule 4.17:

— *of inventorship (Rule 4.17(iv))*

Published:

— *with international search report (Art. 21(3))*

(54) Title: ANTICOAGULANT ACTIVES AND SYNERGISTIC ANTICOAGULANT COMPOSITION AND METHOD FOR PRODUCING THE SAME

Addendum

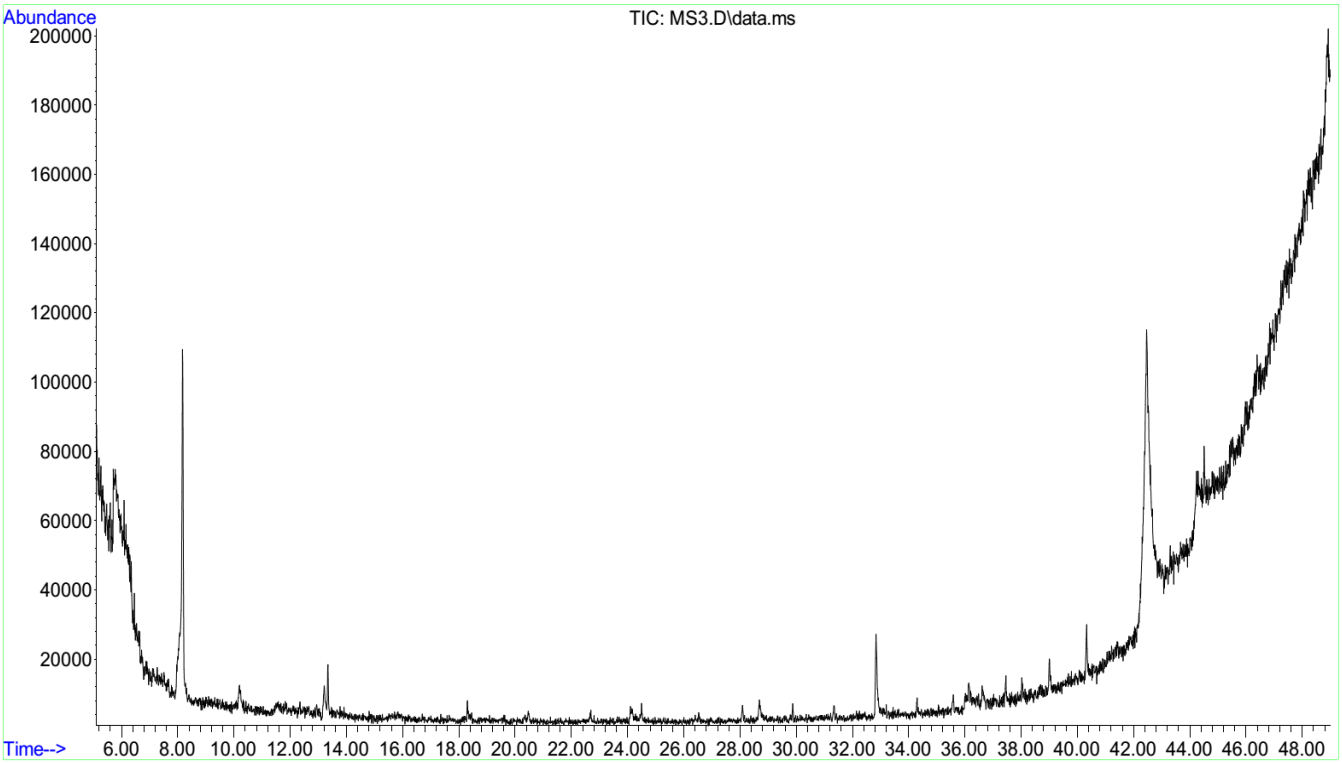

Figure A1. GC-MS chromatogram of active fraction of *Leucas indica* (AFLI)

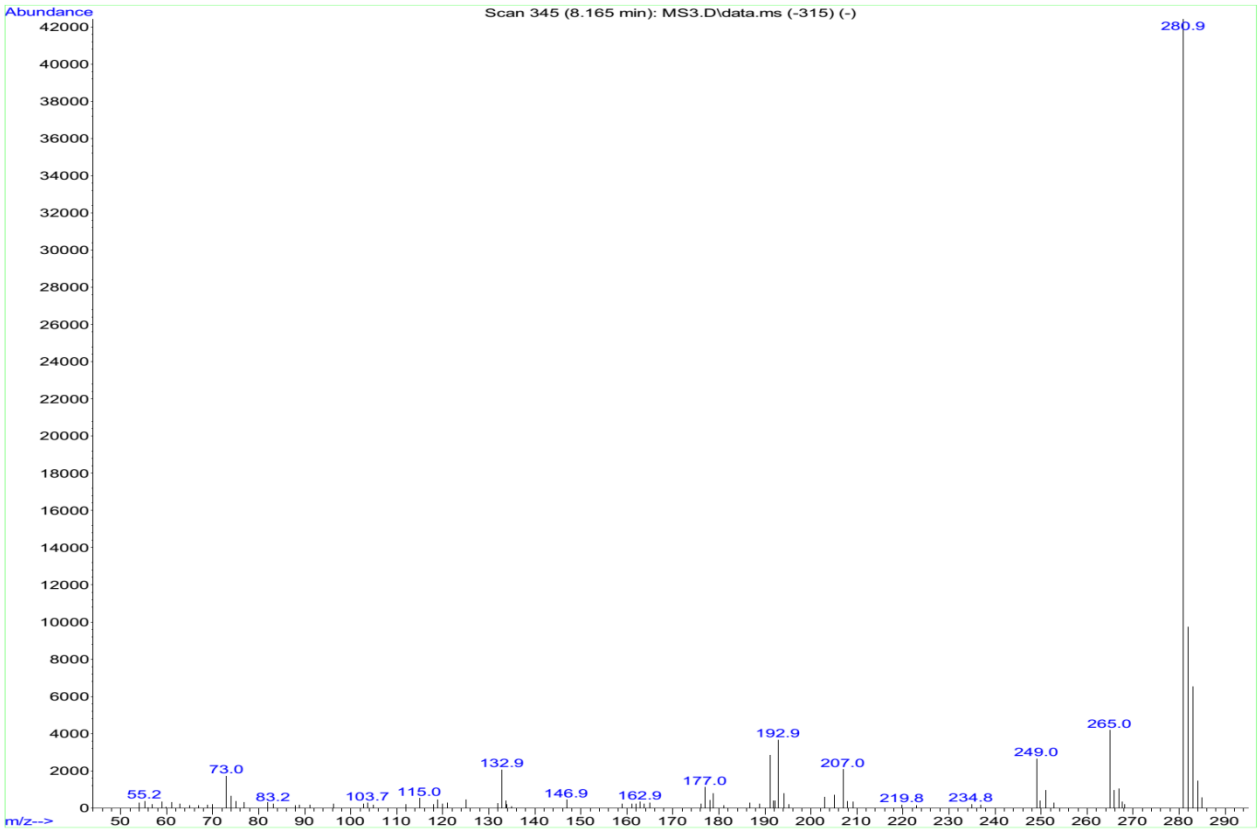

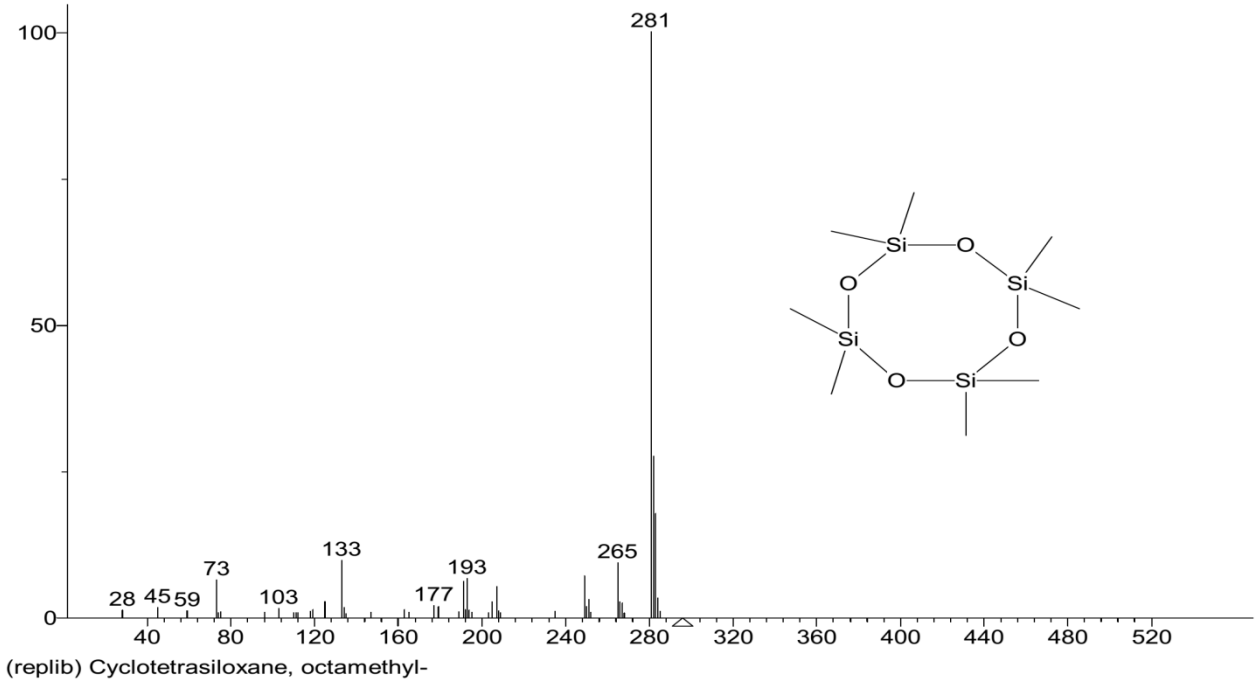

Figure A2. MS spectra of cyclotetrasiloxane, octamethyl

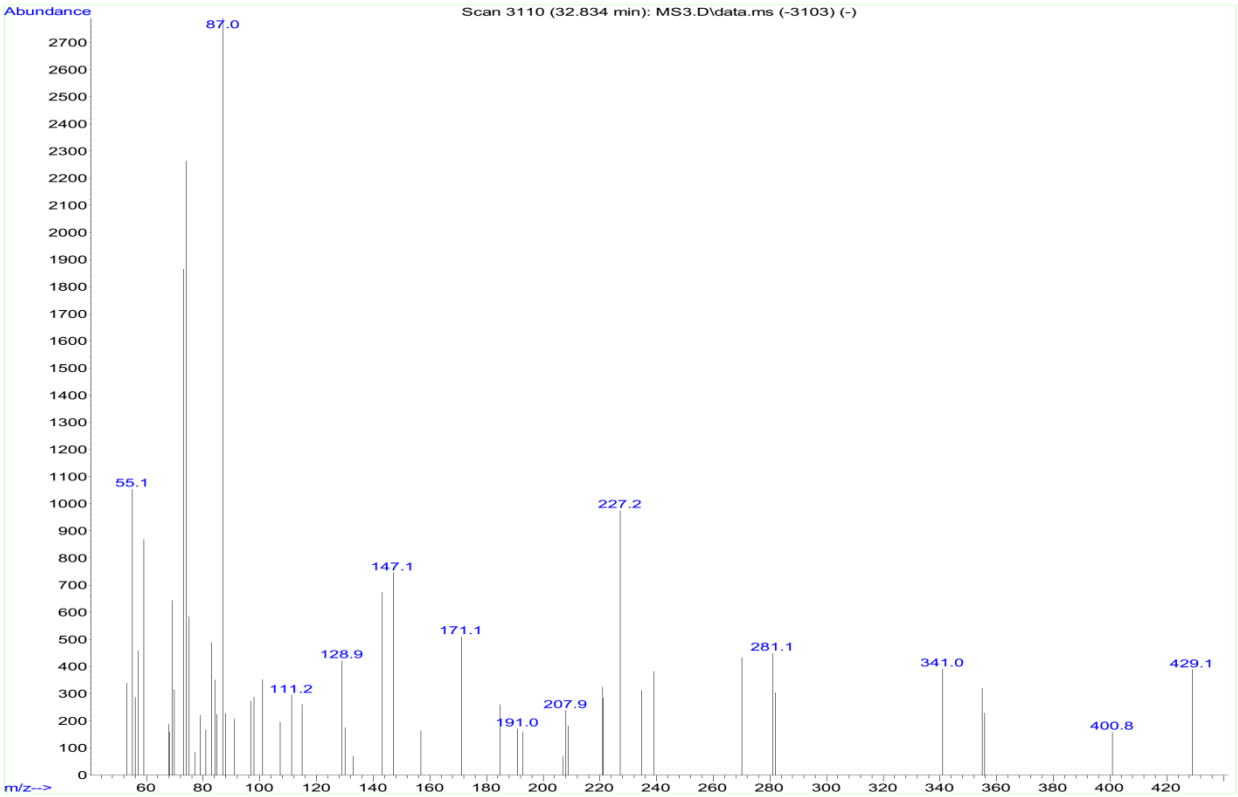

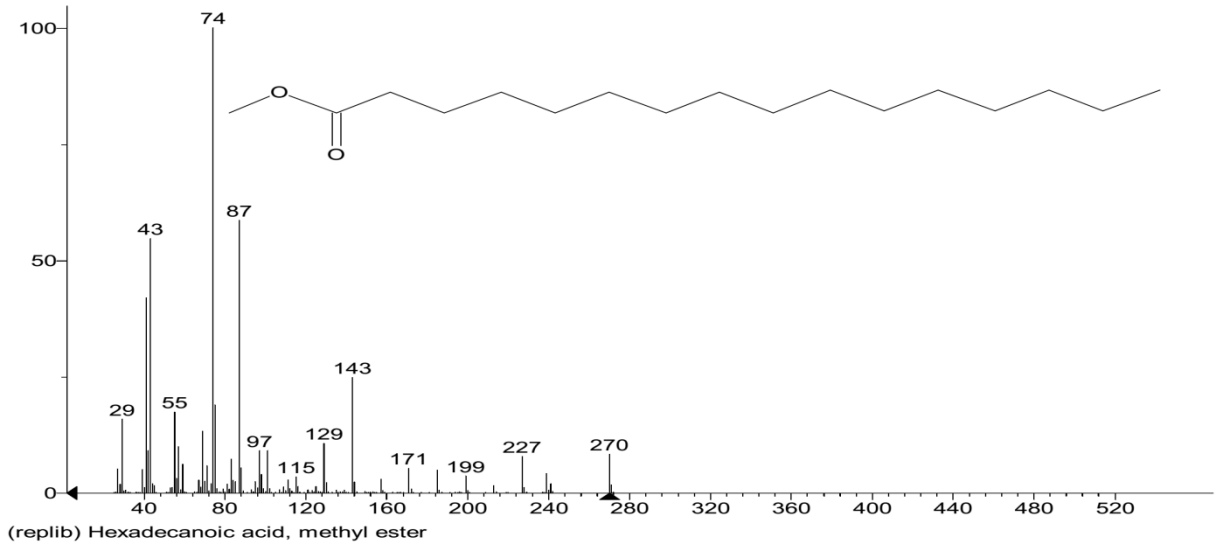

Figure A3. MS spectra of hexadecanoic acid, methyl ester

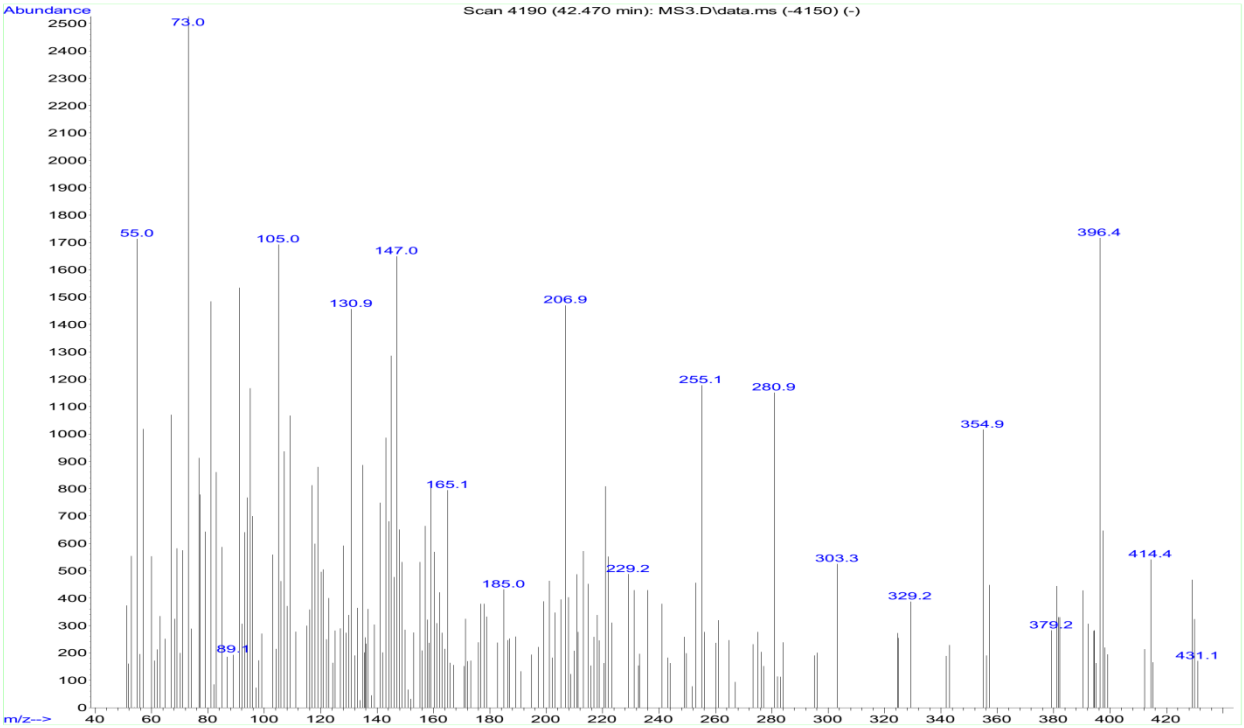

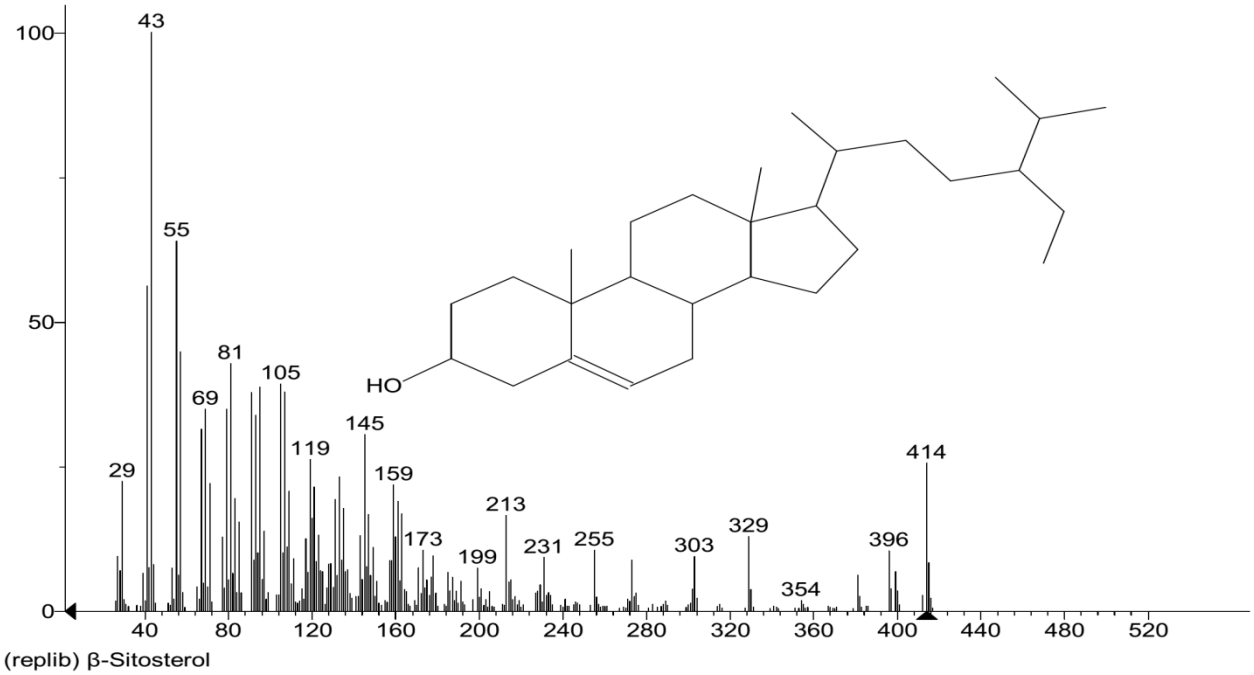

Figure A4. MS spectra of β-sitosterol

LC-MS/MS profile

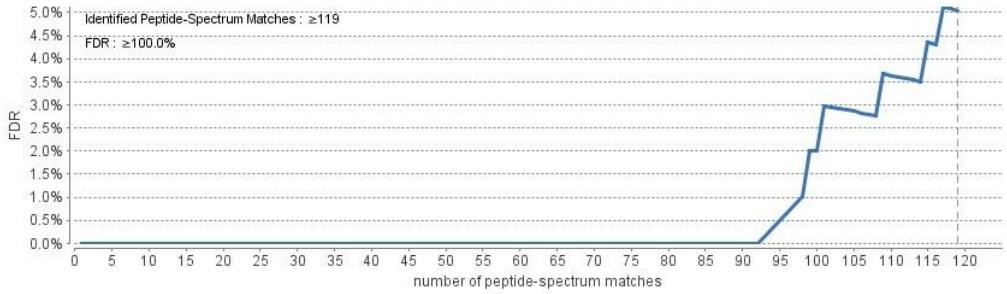

Figure A5.1. False discovery rate (FDR) curve. X axis is the number of peptide-spectrum matches (PSM) being kept. Y axis is the corresponding FDR.

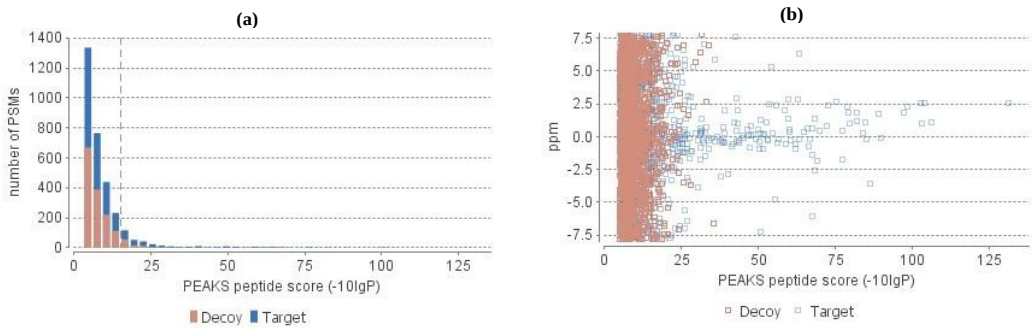

Figure A5.2. PSM score distribution. **(a)** Distribution of PEAKS peptide score; **(b)** Scatterplot of PEAKS peptide score versus precursor mass error.

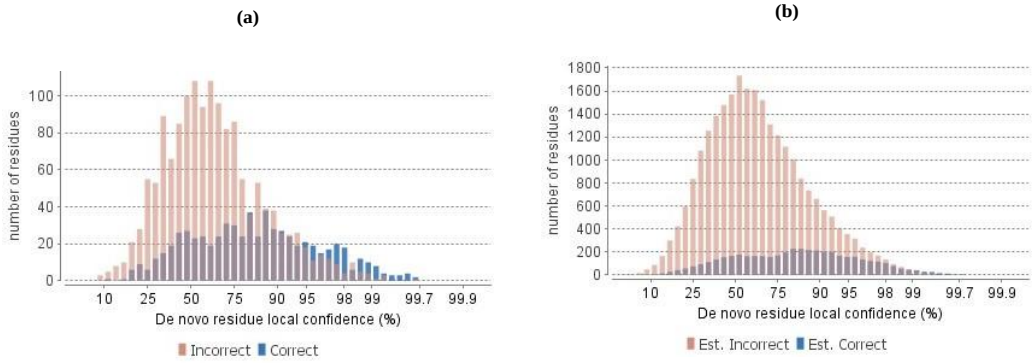

Figure A5.3. De novo result validation. Distribution of residue local confidence: (a) Residues in de novo sequences validated by confident database peptide assignment, (b)Residues in "de novo only" sequences

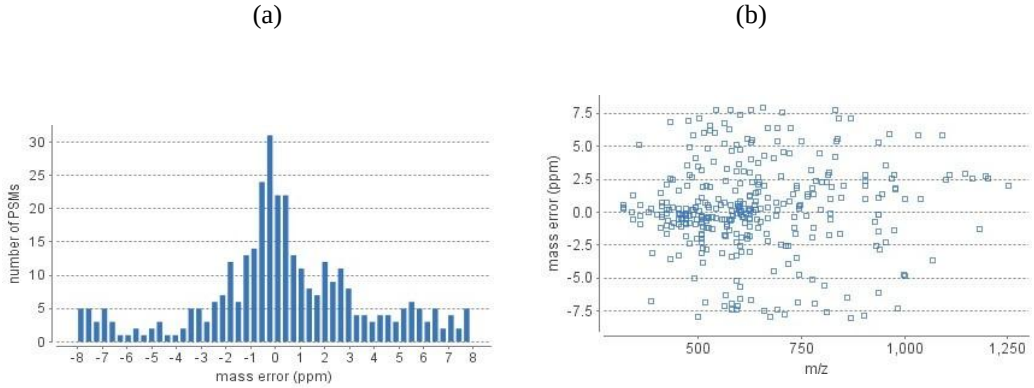

Figure A5.4. Precursor mass error of peptide-spectrum matches (PSM) in filtered result. **(a)** Distribution of precursor mass error in ppm; **(b)** Scatterplot of precursor m/z versus precursor mass error in ppm.

Protein List

Protein Group	Protein ID	Accession	-10lgP	Coverage (%)	#Peptides	#Unique	PTM	Avg. Mass	Description
1	11	gi|15599581	356.78	30	29	14	Y	57086	molecular chaperone GroEL [Pseudomonas aeruginosa PAO1]
2	79	gi|15599473	227.01	39	22	14	Y	43370	elongation factor Tu [Pseudomonas aeruginosa PAO1]
5	54	gi|15599955	222.98	35	21	15	Y	68403	molecular chaperone DnaK [Pseudomonas aeruginosa PAO1]
6	10950	gi|999193	196.34	58	13	12	Y	10267	GroES [Pseudomonas aeruginosa]
3	10944	gi|71557054	190.65	31	25	10	Y	57196	chaperonin, 60 kDa [Pseudomonas savastanoi pv. phaseolicola 1448A]

4	10945	gi|576715139	177.51	30	14	6	Y	43528	translation elongation factor Tu [Pseudomonas sp. GM30]
11	10952	gi|60549563	123.00	10	7	1	Y	68742	DnaK [Pseudomonas putida]
9	10946	gi|576714049	121.88	25	8	8	Y	29944	succinyl-CoA synthetase, alpha subunit [Pseudomonas sp. GM30]
18	10948	gi|320329264	108.84	9	5	5	Y	50101	dihydrolipoamide dehydrogenase [Pseudomonas savastanoi pv. glycinea str. race 4]
12	10953	gi|68347586	85.83	29	7	5	Y	27546	DNA-binding response regulator AlgR [Pseudomonas protegens Pf-5]
16	10955	gi|557557463	67.35	8	5	5	Y	66110	pyruvate carboxylase [Pseudomonas aeruginosa VRFPA05]
51	2499	gi|15599956	64.28	12	2	2	Y	20702	heat shock protein GrpE [Pseudomonas aeruginosa PAO1]
17	10956	gi|928212666	64.03	18	6	6	Y	43332	acetylornithine/succinylornithine aminotransferase [Pseudomonas fuscovaginae]
28	10954	gi|787858376	62.26	9	3	3	Y	49444	F0F1 ATP synthase subunit beta [Pseudomonas chlororaphis]
23	10961	gi|582004101	48.14	14	4	3	Y	48818	glutamate dehydrogenase [Pseudomonas pseudoalcaligenes CECT 5344]
15	10967	gi|15599529	44.46	4	3	3	N	54763	fumarase [Pseudomonas aeruginosa PAO1]
total 55 proteins									

Protein Group	Protein ID	Accession	-10lgP	Coverage (%)	#Peptides	#Unique	PTM	Avg. Mass	Description
153	11042	gi|15599917	42.02	7	1	1	Y	17344	suppressor protein DksA [Pseudomonas aeruginosa PAO1]
26	10974	gi|333113900	40.70	12	4	4	Y	51863	glutamate synthase, small subunit [Pseudomonas fulva 12-X]
53	10963	gi|213928538	38.16	3	2	2	Y	82656	catalase/peroxidase HPI [Pseudomonas syringae pv. tomato T1]
33	10968	gi|404302499	32.92	15	2	2	N	20893	GrpE [Pseudomonas fluorescens R124]
54	10972	gi|1256708	32.40	12	2	2	Y	29144	dihydrodiol dehydrogenase [Pseudomonas fluorescens]
24	10991	gi|310696647	31.59	6	3	3	Y	47089	RhlB [Pseudomonas aeruginosa]
25	10999	gi|619865635	30.27	4	2	2	Y	61022	COG0488 ATPase components of ABC transporters with duplicated ATPase domains [Pseudomonas aeruginosa RB]
52	10985	gi|15600131	29.54	6	2	2	Y	46814	adenylosuccinate synthetase [Pseudomonas aeruginosa PAO1]
81	10969	gi|928214863	28.98	2	1	1	N	65577	acyl-CoA dehydrogenase [Pseudomonas fuscovaginae]
30	10984	gi|928214574	27.54	3	2	2	Y	79783	isocitrate dehydrogenase, NADP-dependent, monomeric type [Pseudomonas fuscovaginae]
144	11179	gi|320330409	27.26	8	1	1	Y	31995	thioredoxin [Pseudomonas savastanoi pv. glycinea str. race 4]
57	11013	gi|761895334	27.07	7	2	2	Y	43425	dioxygenase [Pseudomonas sp. 10-1B]
34	10981	gi|768690557	26.99	1	2	2	Y	161593	putative glutamate synthase [NADPH], large subunit [Pseudomonas sp. HMSC05H02]
59	11069	gi|6002915	26.75	5	2	2	N	39765	chloromuconate cycloisomerase [Pseudomonas aeruginosa]
35	7839	gi|15596597	26.74	2	2	2	Y	116878	pyruvate carboxylase [Pseudomonas aeruginosa PAO1]
80	10966	gi|974971520	26.72	4	1	1	Y	32627	dTDP-4-dehydrorhamnose reductase [Pseudomonas syringae pv. tomato]
80	10975	gi|992142104	26.72	4	1	1	Y	32940	dTDP-4-dehydrorhamnose reductase [Pseudomonas aeruginosa]
62	11012	gi|937421302	26.61	8	2	2	Y	27549	putative catechol-o-methyltransferase [Mycobacterium fortuitum]
64	11148	gi|32967107	26.59	4	2	2	N	58910	LapN [Pseudomonas alkylphenolia]
40	11024	gi|10764670	25.95	5	2	1	Y	69402	GidA [Pseudomonas syringae pv. syringae]
88	10970	gi|666690932	25.92	2	1	1	Y	72721	acetyl-CoA hydrolase [Pseudomonas amygdali pv. tabaci str. 6605]
98	10977	gi|108769013	25.76	3	1	1	N	37213	phthalate 3,4-dihydrodiol dehydrogenase [Mycobacterium sp. MCS]
55	11006	gi|15599784	25.46	7	2	1	Y	48857	glutamate dehydrogenase [Pseudomonas aeruginosa PAO1]
50	11018	gi|553897368	25.00	4	2	1	N	69638	tRNA uridine 5-carboxymethylaminomethyl modification enzyme GidA [Pseudomonas aeruginosa PAO1-VE13]
45	11017	gi|787858374	24.68	4	2	2	N	55366	F0F1 ATP synthase subunit alpha [Pseudomonas chlororaphis]
27	10965	gi|913661954	24.63	2	1	1	Y	63674	succinate dehydrogenase [Pseudomonas fluorescens NCIMB 11764]
60	11057	gi|145692874	24.63	6	2	2	N	36331	HCH-reductase LinF [Pseudomonas aeruginosa]
102	10976	gi|940307717	23.54	5	1	1	Y	32437	Dihydrodipicolinate synthase/N-acetylneuraminate lyase [Pseudomonas amygdali pv. ulmi]
56	11014	gi|359763600	23.47	8	2	1	Y	27615	AlgR [Pseudomonas fluorescens F113]
56	11021	gi|426270388	23.47	8	2	1	Y	27656	two-component response regulator AlgR [Pseudomonas sp. UW4]
141	11169	gi|928211953	21.86	4	1	1	Y	30652	aldo/keto reductase, diketogulonate reductase [Pseudomonas fuscovaginae]
110	11002	gi|331024675	21.55	3	1	1	N	53948	acetyl-CoA hydrolase [Pseudomonas coronafaciens pv. oryzae str. 1_6]
116	11071	gi|15598209	21.55	3	1	1	Y	41643	3-ketoacyl-CoA thiolase [Pseudomonas aeruginosa PAO1]
99	11031	gi|499793935	21.41	2	1	1	Y	48478	cytochrome P450 [Rhodopseudomonas palustris]
126	11086	gi|15600356	20.97	4	1	1	N	32457	glucose-1-phosphate thymidylyltransferase [Pseudomonas aeruginosa PAO1]
126	11199	gi|543436230	20.97	4	1	1	N	32086	glucose-1-phosphate thymidylyltransferase [Pseudomonas alcaligenes NBRC 14159]
126	11226	gi|514084306	20.97	4	1	1	N	32375	Glucose-1-phosphate thymidylyltransferase [Pseudomonas syringae pv. syringae SM]
87	11094	gi|957651990	20.79	5	1	1	N	35984	TDP-rhamnosyltransferase 2 RhlC [Pseudomonas aeruginosa]
89	10996	gi|489230774	20.60	3	1	1	N	40132	muconate cycloisomerase [Pseudomonas aeruginosa]
total 55 proteins									

gi|15599581

| Protein Coverage |

Supporting Peptides | Protein

Coverage:

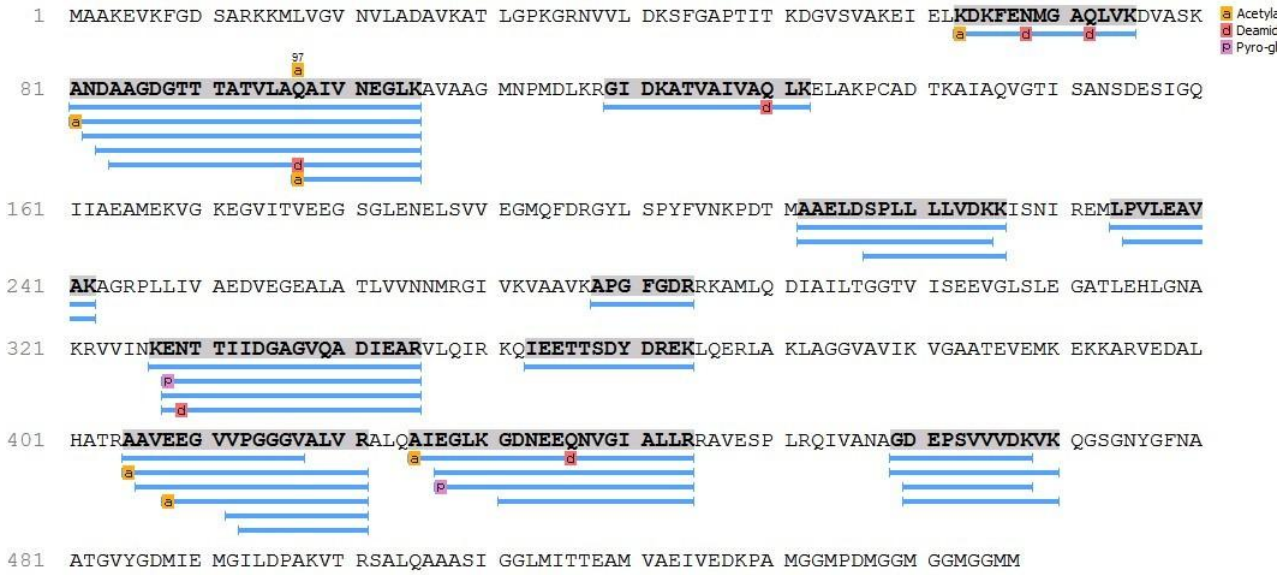

Supporting Peptides:

Peptide	Uniq	-10lgP	Mass	ppm	m/z	z	RT	Scan	#Spec	Start	End	PTM
K.ANDAAGDGTTTATVLAQAIVNEGLK.A	Y	131.43	2400.2131	2.6	1201.1169	2	104.68	9240	2	81	105	
total 33 peptides												

Peptide	Uniq	-10lgP	Mass	ppm	m/z	z	RT	Scan	#Spec	Start	End	PTM
K.ENTTIIDGAGVQADIEAR.V	Y	106.32	1871.9225	1.1	936.9695	2	63.37	5819	5	328	345	
A.NDAAGDGTTTATVLAQAIVNEGLK.A	Y	103.73	2329.1760	2.6	1165.5983	2	104.65	9236	2	82	105	
N.KENTTIIDGAGVQADIEAR.V	Y	103.24	2000.0173	1.0	1001.0170	2	56.78	5207	2	327	345	
I.E(-18.01)GLKGDNEEQNVGIALLR.R	Y	102.75	1936.0013	2.6	969.0104	2	79.54	7228	2	427	444	Pyro-glu from E
I.EGLKGDNEEQNVGIALLR.R	Y	89.18	1954.0120	1.7	978.0150	2	68.67	6267	3	427	444	
Q.IEETTSDYDREK.L	Y	83.96	1484.6631	0.2	743.3390	2	13.97	823	2	353	364	
K.GDNEEQNVGIALLR.R	Y	82.16	1526.7688	1.2	764.3926	2	67.64	6173	4	431	444	
M.AAELDSPLLLLVDKK.I	Y	78.74	1623.9447	2.3	812.9815	2	102.83	9095	2	212	226	
V.VPGGGVALVR.A	N	66.74	923.5552	-0.2	462.7848	2	28.31	2431	3	412	421	
N.DAAGDGTTTATVLAQAIVNEGLK.A	Y	62.80	2215.1331	2.8	1108.5769	2	105.53	9316	2	83	105	
G.DEPSVVVDKVK.Q	N	60.66	1213.6554	-0.3	607.8348	2	23.33	1890	1	460	470	
M.AAELDSPLLLLVDK.K	Y	60.12	1495.8497	0.6	748.9326	2	109.59	9647	1	212	225	
D.SPLLLLVDKK.I	N	59.11	1124.7168	-0.6	563.3654	2	64.41	5906	1	217	226	
V.PGGGVALVR.A	N	56.76	824.4868	-0.2	413.2506	2	51.12	4662	3	413	421	
M.LPVLEAVAK.A	N	56.24	938.5800	-0.5	470.2971	2	48.60	4430	9	234	242	
K.APGFGDR.R	N	50.19	718.3398	-0.9	360.1768	2	14.37	868	1	278	284	
A.GDEPSVVVDKVK.Q	N	50.07	1270.6769	0.6	636.3461	2	25.14	2094	3	459	470	
K.E(-18.01)NTTIIDGAGVQADIEAR.V	Y	41.37	1853.9119	-0.7	927.9625	2	61.86	5683	1	328	345	Pyro-glu from E
Q.A(+42.01)IEGLKGDNEEQ(+.98)NVGIALLR.R	Y	35.84	2181.1277	5.9	1091.5775	2	77.26	7026	1	425	444	Acetylation (N-term), Deamidation (NQ)
G.DEPSVVVDK.V	N	33.80	986.4920	-0.9	494.2528	2	17.29	1220	1	460	468	
L.PVLEAVAK.A	N	33.21	825.4960	0.7	413.7556	2	49.18	4482	2	235	242	
K.EN(+.98)TTIIDGAGVQADIEAR.V	Y	32.65	1872.9065	-1.4	937.4592	2	87.35	7853	1	328	345	Deamidation (NQ)
A.AVEEGVVPGGGVALVR.A	N	26.27	1507.8358	0.1	503.6193	3	14.55	889	3	406	421	
A.GDEPSVVVDK.V	N	26.05	1043.5134	0.6	522.7643	2	16.64	1151	2	459	468	
R.A(+42.01)AVEEGVVPGGGVALVR.A	N	23.52	1620.8834	6.0	541.3050	3	24.35	2007	1	405	421	Acetylation (N-term)
D.AAGDGTTTATVLAQ(+.98)AIVNEGLK.A	Y	22.40	2101.0903	-2.4	701.3690	3	103.43	9140	1	84	105	Deamidation (NQ)
K.A(+42.01)NDAAGDGTTTATVLAQAIVNEGLK.A	Y	21.03	2442.2239	2.9	815.0842	3	105.04	9275	1	81	105	Acetylation (N-term)
A.Q(+42.01)AIVNEGLK.A	N	20.78	1012.5553	-0.8	507.2845	2	21.30	1668	1	97	105	Acetylation (N-term)
L.K(+42.01)DKFEN(+.98)MGAQ(+.98)LVK.D	Y	18.06	1550.7650	-5.1	776.3858	2	49.73	4538	1	63	75	Acetylation (N-term), Deamidation (NQ)
R.AAVEEGVVPGGGV.A	N	15.76	1139.5822	3.3	570.8002	2	44.76	4065	2	405	417	
R.GIDKATVAIVAQ(+.98)LK.E	Y	15.73	1426.8395	7.0	476.6237	3	42.88	3898	1	119	132	Deamidation (NQ)
V.E(+42.01)EGVVPGGGVALVR.A	N	15.00	1379.7408	0.2	690.8778	2	16.39	1121	2	408	421	Acetylation (N-term)
total 33 peptides												

gi|15599473

| Protein Coverage |

Supporting Peptides | Protein

Coverage:

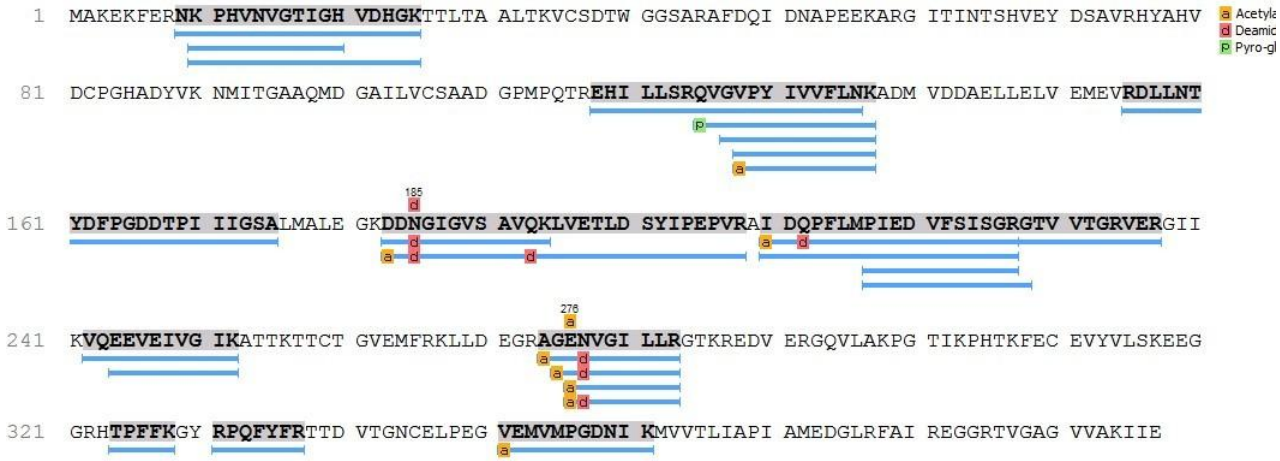

Supporting Peptides:

Peptide	Uniq	-10lgP	Mass	ppm	m/z	z	RT	Scan	#Spec	Start	End	PTM
N.KPHVNVGTIGHVDHGK.T	Y	84.58	1693.9012	1.1	847.9588	2	16.49	1134	5	10	25	
G.VPYIVVFLNK.A	N	77.22	1190.7063	0.5	596.3607	2	101.53	8989	4	128	137	
K.DDN(+.98)GIGVSAVQK.L	Y	72.13	1202.5779	0.8	602.2967	2	19.40	1452	4	183	194	Deamidation (NQ)
R.NKPHVNVGTIGHVDHGK.T	Y	69.10	1807.9441	-1.9	603.6542	3	21.16	1651	10	9	25	
M.PIEDVFSISGRG.T	N	59.76	1275.6459	1.4	638.8311	2	70.40	6414	2	217	228	
Y.RPQFYFR.T	N	52.54	1012.5242	1.1	507.2699	2	35.88	3205	4	331	337	
V.GVPYIVVFLNK.A	N	50.69	1247.7278	0.3	624.8713	2	101.35	8972	10	127	137	
H.TPFFK.G	N	46.30	638.3428	0.5	320.1788	2	30.14	2624	4	324	328	
Q.EEVEIVGIK.A	Y	43.72	1014.5597	-0.5	508.2869	2	41.95	3807	2	244	252	
V.RDLLNTYDFPGDDTPIIIGSA.L	Y	42.75	2292.1274	2.9	1147.0743	2	102.74	9087	1	155	175	
A.I(+42.01)DQ(+.98)PFLMPIEDVFSISGR.G	Y	42.41	2106.0342	7.6	703.0240	3	118.01	10174	1	210	227	Acetylation (N-term), Deamidation (NQ)
M.PIEDVFSISGR.G	N	33.76	1218.6244	-0.3	610.3193	2	82.53	7478	3	217	227	
K.VQEEVEIVGIK.A	Y	26.75	1241.6866	0.2	621.8507	2	92.19	8266	2	242	252	
R.Q(-17.03)VGVPYIVVFLNK.A	N	26.57	1457.8282	1.4	729.9224	2	118.87	10215	1	125	137	Pyro-glu from Q
A.IDQPFLMPIEDVFSISGR.G	Y	26.25	2063.0398	5.8	1032.5332	2	120.84	10328	1	210	227	
G.E(+42.01)N(+.98)VGILLR.G	Y	26.13	955.5338	2.8	478.7755	2	47.32	4309	2	276	283	Acetylation (N-term), Deamidation (NQ)
R.GTVVTGRVER.G	Y	22.20	1072.5989	3.8	537.3088	2	53.93	4929	1	228	237	
R.A(+42.01)GEN(+.98)VGILLR.G	Y	22.19	1083.5924	7.7	542.8077	2	63.21	5806	1	274	283	Acetylation (N-term), Deamidation (NQ)
total 25 peptides												

Peptide	Uniq	-10lgP	Mass	ppm	m/z	z	RT	Scan	#Spec	Start	End	PTM
R.EHILLSRQVGVPYIVVFLN.K	N	21.18	2195.2466	-1.2	732.7552	3	71.90	6557	1	118	136	
K.D(+42.01)DN(+.98)GIGVSAVQ(+.98)KLVETLDSYIPEPVR.A	Y	19.28	2857.4233	-2.3	953.4796	3	76.28	6941	1	183	208	Acetylation (N-term), Deamidation (NQ)
N.KPHVNVGTIGH.V	Y	18.82	1157.6305	0.3	386.8842	3	15.90	1055	2	10	20	
G.E(+42.01)NVGILLR.G	Y	17.55	954.5498	-0.8	478.2818	2	40.98	3710	1	276	283	Acetylation (N-term)
A.G(+42.01)EN(+.98)VGILLR.G	Y	15.44	1012.5553	3.2	507.2865	2	46.72	4254	3	275	283	Acetylation (N-term), Deamidation (NQ)
G.V(+42.01)PYIVVFLNK.A	N	15.13	1232.7168	-0.1	617.3656	2	127.96	10708	2	128	137	Acetylation (N-term)
G.V(+42.01)EMVMPGDNIK.M	Y	15.10	1273.6046	2.1	425.5430	3	56.53	5183	1	351	361	Acetylation (N-term)
total 25 peptides												

gi|15599955

| Protein Coverage |

Supporting Peptides | Protein

Coverage:

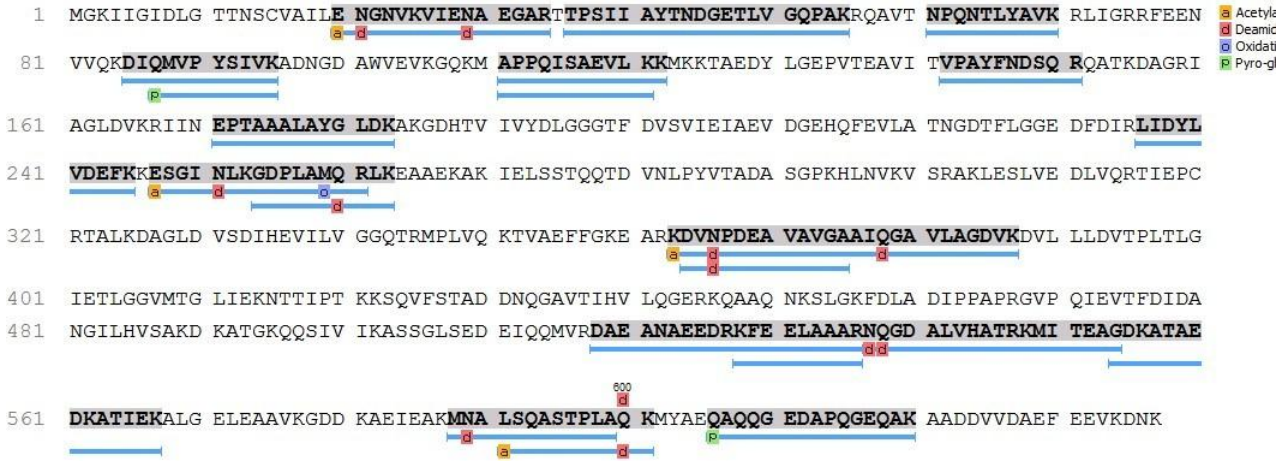

Supporting Peptides:

Peptide	Uniq	-10lgP	Mass	ppm	m/z	z	RT	Scan	#Spec	Start	End	PTM
R.DAEANAEEDRKFEELAAAR.N	N	86.44	2133.9927	-3.6	1067.9998	2	52.07	4751	3	518	536	
A.GDKATAEDKATIEK.A	Y	82.01	1475.7467	1.8	738.8820	2	12.06	604	2	554	567	
T.TPSIIAYTNDGETLVGQPAK.R	Y	79.47	2074.0581	1.0	1038.0374	2	76.38	6951	1	36	55	
E.Q(-17.03)AQQGEDAPQGEQAK.A	Y	72.79	1566.6910	2.4	784.3547	2	12.53	658	1	606	620	Pyro-glu from Q
T.NPQNTLYAVK.R	Y	67.35	1146.6033	-1.4	574.3081	2	23.76	1936	1	61	70	
T.VPAYFNDSQR.Q	Y	64.84	1195.5621	0.4	598.7886	2	26.27	2216	1	142	151	
M.APPQISAEVLKK.M	N	31.21	1279.7499	0.2	640.8823	2	34.99	3120	2	111	122	
R.LIDYLVDEFK.K	Y	28.78	1253.6543	5.3	627.8378	2	54.97	5027	1	236	245	
M.APPQISAEVLK.K	N	25.41	1151.6550	-0.6	576.8345	2	43.47	3956	1	111	121	
R.K(+42.01)DVN(+.98)PDEAVAVGAAIQ(+.98)GAVLAGDVK.D	Y	23.80	2450.2539	-1.8	817.7571	3	44.02	3997	1	363	387	Acetylation (N-term), Deamidation (NQ)
K.DIQMVPYSIVK.A	Y	23.21	1291.6846	3.8	646.8520	2	36.39	3249	5	85	95	
N.EPTAAALAYGLDK.A	Y	21.74	1318.6769	-7.5	660.3408	2	25.23	2106	2	171	183	
A.L(+42.01)SQASTPLAQ(+.98)K.M	Y	19.10	1185.6241	-1.7	593.8184	2	36.70	3278	1	591	601	Acetylation (N-term), Deamidation (NQ)
R.N(+.98)Q(+.98)GDALVHATRKMITEAG.D	Y	18.48	1912.9313	0.1	638.6511	3	75.01	6830	1	537	554	Deamidation (NQ)
K.E(+42.01)SGIN(+.98)LKGDPLAM(+15.99)QR.L	Y	18.36	1686.8247	-1.6	844.4183	2	96.52	8592	1	247	261	Acetylation (N-term), Deamidation (NQ), Oxidation (M)
R.KFEELAAAR.N	N	17.90	1033.5555	-6.9	517.7815	2	42.91	3902	1	528	536	
I.Q(-17.03)MVPYSIVK.A	Y	17.06	1046.5470	4.9	524.2833	2	26.62	2257	1	87	95	Pyro-glu from Q
K.DVN(+.98)PDEAVAVGA.A	Y	16.72	1156.5248	7.8	579.2742	2	32.43	2858	1	364	375	Deamidation (NQ)
L.E(+42.01)N(+.98)GNVKVIEN(+.98)AEGAR.T	N	15.93	1642.7798	1.9	822.3987	2	31.68	2784	1	20	34	Acetylation (N-term), Deamidation (NQ)
K.GDPLAMQ(+.98)RLK.E	N	15.23	1128.5961	5.2	565.3082	2	43.03	3913	1	254	263	Deamidation (NQ)
K.MN(+.98)ALSQASTPLA.Q	Y	15.06	1203.5806	7.4	602.8020	2	28.48	2448	1	588	599	Deamidation (NQ)
total 21 peptides												

gi|999193

| Protein Coverage |

Supporting Peptides | Protein

Coverage:

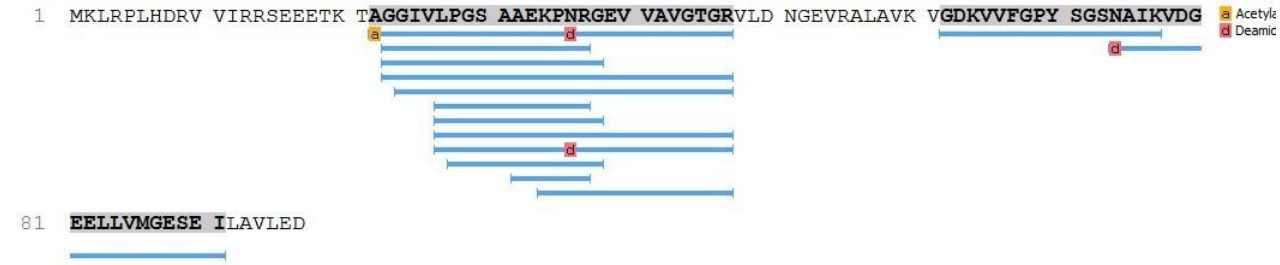

Supporting Peptides:

Peptide	Uniq	-10lgP	Mass	ppm	m/z	z	RT	Scan	#Spec	Start	End	PTM
V.GDKVVFGPYSGSNAIK.V	Y	89.88	1637.8413	-0.1	819.9279	2	47.41	4318	2	62	77	
total 14 peptides												

Peptide	Uniq	-10lgP	Mass	ppm	m/z	z	RT	Scan	#Spec	Start	End	PTM
A.GGIVLPGSAAEKPNRGEVVAVGTGR.V	Y	75.22	2390.3030	2.7	1196.1620	2	52.76	4820	4	23	47	
V.LPGSAAEKPNR.G	Y	61.94	1138.6094	-0.9	570.3115	2	12.32	632	2	27	37	
E.KPNRGEVVAVGTGR.V	Y	47.44	1438.8004	0.8	720.4081	2	14.78	917	3	34	47	
A.GGIVLPGSAAEKPNR.G	Y	42.89	1464.8048	-0.4	733.4094	2	29.83	2590	1	23	37	
L.PGSAAEKPNRG.E	Y	38.80	1082.5469	-0.5	542.2805	2	12.83	695	1	28	38	
V.LPGSAAEKPN(+.98)RGEVVAVGTGR.V	Y	38.56	2065.0916	0.8	689.3716	3	27.94	2395	1	27	47	Deamidation (NQ)
A.GGIVLPGSAAEKPNRG.E	Y	37.79	1521.8263	-0.3	761.9202	2	30.10	2620	2	23	38	
G.GIVLPGSAAEKPNRGEVVAVGTGR.V	Y	31.37	2333.2815	1.4	778.7689	3	52.04	4748	1	24	47	
V.LPGSAAEKPNRGEVVAVGTGR.V	Y	30.37	2064.1074	-0.3	689.0429	3	27.16	2312	2	27	47	
T.A(+42.01)GGIVLPGSAAEKPN(+.98)RGEVVAVGTGR.V	Y	26.00	2504.3347	5.4	835.7900	3	54.12	4947	3	22	47	Acetylation (N-term), Deamidation(NQ)
V.LPGSAAEKPNRG.E	Y	25.11	1195.6309	-0.2	399.5508	3	12.57	662	2	27	38	
S.N(+.98)AIKVDGEELLVMGESEI.L	Y	16.90	1945.9553	2.9	973.9877	2	27.65	2365	1	74	91	Deamidation (NQ)
A.AEKPNR.G	N	16.57	713.3820	5.1	357.7001	2	24.76	2056	1	32	37	
total 14 peptides												

gi|71557054

| Protein Coverage |

Supporting Peptides | Protein

Coverage:

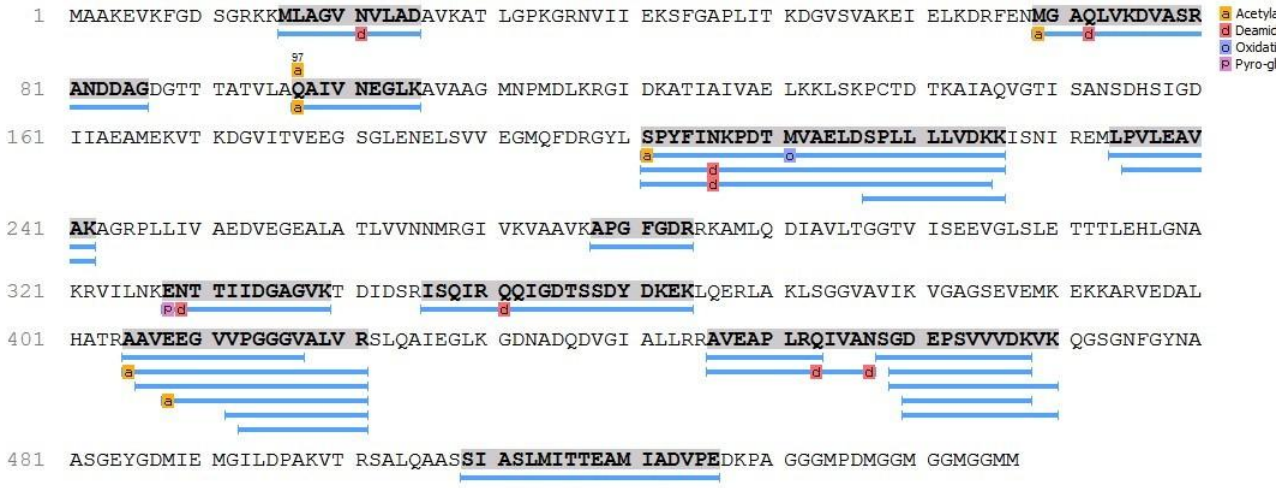

Supporting Peptides:

Peptide	Uniq	-10lgP	Mass	ppm	m/z	z	RT	Scan	#Spec	Start	End	PTM
V.VPGGGVALVR.S	N	66.74	923.5552	-0.2	462.7848	2	28.31	2431	3	412	421	
G.DEPSVVVDKVK.Q	N	60.66	1213.6554	-0.3	607.8348	2	23.33	1890	1	460	470	
D.SPLLLLVDKK.I	N	59.11	1124.7168	-0.6	563.3654	2	64.41	5906	1	217	226	
V.PGGGVALVR.S	N	56.76	824.4868	-0.2	413.2506	2	51.12	4662	3	413	421	
M.LPVLEAVAK.A	N	56.24	938.5800	-0.5	470.2971	2	48.60	4430	9	234	242	
L.S(+42.01)PYFINKPDTM(+15.99)VAELDSPLLLLVDKK.I	Y	55.37	3003.5879	-4.8	1002.1984	3	107.18	9453	1	201	226	Acetylation (N-term), Oxidation (M)
L.SPYFIN(+.98)KPDTMVAELDSPLLLLVDKK.I	Y	50.75	2946.5664	-7.3	983.1889	3	107.69	9495	1	201	226	Deamidation (NQ)
K.APGFGDR.R	N	50.19	718.3398	-0.9	360.1768	2	14.37	868	1	278	284	
S.GDEPSVVVDKVK.Q	N	50.07	1270.6769	0.6	636.3461	2	25.14	2094	3	459	470	
G.DEPSVVVDK.V	N	33.80	986.4920	-0.9	494.2528	2	17.29	1220	1	460	468	
L.PVLEAVAK.A	N	33.21	825.4960	0.7	413.7556	2	49.18	4482	2	235	242	
R.ISQIRQ(+.98)QIGDTSSDYDKEK.L	Y	27.42	2211.0654	-3.4	738.0266	3	69.94	6374	1	346	364	Deamidation (NQ)
A.AVEEGVVPGGGVALVR.S	N	26.27	1507.8358	0.1	503.6193	3	14.55	889	3	406	421	
K.E(-18.01)N(+.98)TTIIDGAGVK.T	Y	26.22	1199.6034	-5.6	600.8056	2	15.06	954	1	328	339	Pyro-glu from E, Deamidation (NQ)
S.GDEPSVVVDK.V	N	26.05	1043.5134	0.6	522.7643	2	16.64	1151	2	459	468	
R.A(+42.01)AVEEGVVPGGGVALVR.S	N	23.52	1620.8834	6.0	541.3050	3	24.35	2007	1	405	421	Acetylation (N-term)
A.Q(+42.01)AIVNEGLK.A	N	20.78	1012.5553	-0.8	507.2845	2	21.30	1668	1	97	105	Acetylation (N-term)
L.SPYFIN(+.98)KPDTMVAELDSPLLLLVDK.K	Y	19.81	2818.4714	-2.8	940.4951	3	113.14	9881	1	201	225	Deamidation (NQ)
R.AVEAPLRQ(+.98)IVAN(+.98).S	Y	18.05	1281.6929	-0.6	641.8533	2	38.31	3434	1	446	457	Deamidation (NQ)
N.SGDEPSVVVDK.V	Y	17.97	1130.5455	-6.3	566.2765	2	80.54	7314	1	458	468	
S.SIASLMITTEAMIADVPE.D	Y	16.33	1890.9319	1.3	946.4745	2	53.76	4912	2	509	526	
R.AAVEEGVVPGGGV.A	N	15.76	1139.5822	3.3	570.8002	2	44.76	4065	2	405	417	
R.AVEAPLRQ.I	Y	15.29	882.4923	-0.8	442.2531	2	26.59	2254	2	446	453	
K.MLAGVN(+.98)VLAD.A	Y	15.13	1002.5056	7.1	502.2636	2	18.41	1346	1	16	25	Deamidation (NQ)
V.E(+42.01)EGVVPGGGVALVR.S	N	15.00	1379.7408	0.2	690.8778	2	16.39	1121	2	408	421	Acetylation (N-term)
N.M(+42.01)GAQ(+.98)LVKDVASRANDDAG.D	Y	15.00	1859.8683	-2.6	930.9390	2	31.56	2772	1	69	86	Acetylation (N-term), Deamidation (NQ)
total 26 peptides												

gi|576715139

| Protein Coverage |

Supporting Peptides | Protein Coverage:

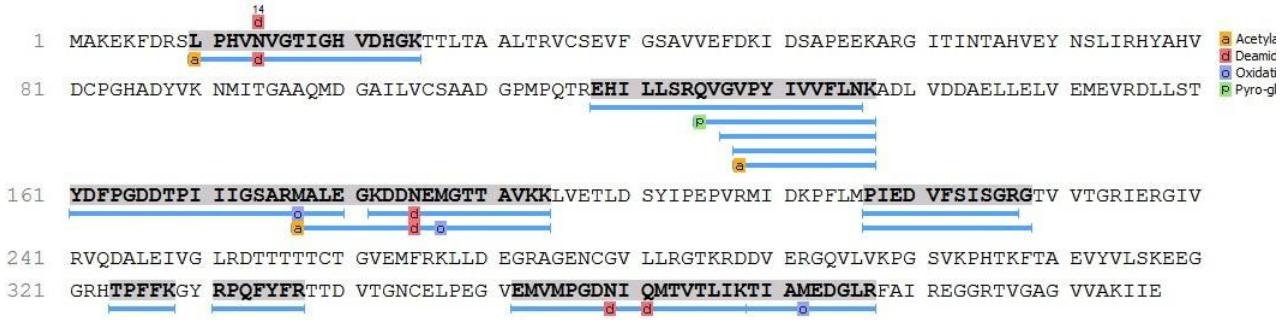

Supporting Peptides:

Peptide	Uniq	-10lgP	Mass	ppm	m/z	z	RT	Scan	#Spec	Start	End	PTM
G.VPYIVVFLNK.A	N	77.22	1190.7063	0.5	596.3607	2	101.53	8989	4	128	137	
S.L(+42.01)PHVN(+.98)VGTIGHVDHGK.T	Y	63.31	1721.8849	6.3	574.9725	3	22.62	1813	2	10	25	Acetylation (N-term), Deamidation (NQ)
M.PIEDVFSISGRG.T	N	59.76	1275.6459	1.4	638.8311	2	70.40	6414	2	217	228	
Y.RPQFYFR.T	N	52.54	1012.5242	1.1	507.2699	2	35.88	3205	4	331	337	
V.GVPYIVVFLNK.A	N	50.69	1247.7278	0.3	624.8713	2	101.35	8972	10	127	137	
H.TPFFK.G	N	46.30	638.3428	0.5	320.1788	2	30.14	2624	4	324	328	
M.PIEDVFSISGR.G	N	33.76	1218.6244	-0.3	610.3193	2	82.53	7478	3	217	227	
R.Q(-17.03)VGVPYIVVFLNK.A	N	26.57	1457.8282	1.4	729.9224	2	118.87	10215	1	125	137	Pyro-glu from Q

R.EHILLSRQVGVPYIVVFLN.K	N	21.18	2195.2466	-1.2	732.7552	3	71.90	6557	1	118	136	
G.KDDN(+.98)EMGTTAVKK.L	Y	18.49	1436.6816	-2.6	719.3463	2	41.35	3749	1	182	194	Deamidation (NQ)
K.TIAM(+15.99)EDGLR.F	Y	17.83	1020.4910	-2.8	511.2513	2	20.12	1528	2	369	377	Oxidation (M)
R.M(+42.01)ALEGKDDN(+.98)EM(+15.99)GTTAVKK.L	Y	16.44	1995.9128	-1.6	666.3105	3	102.76	9090	1	177	194	Acetylation (N-term), Deamidation (NQ), Oxidation (M)
V.EMVMPGDN(+.98)IQ(+.98)MTVTLIK.T	Y	16.41	1920.9247	5.9	961.4753	2	73.54	6700	1	352	368	Deamidation (NQ)
T.YDFPGDDTPIIIGSARM(+15.99)ALE.G	Y	15.59	2196.0408	2.5	1099.0304	2	82.43	7469	1	161	180	Oxidation (M)
G.V(+42.01)PYIVVFLNK.A	N	15.13	1232.7168	-0.1	617.3656	2	127.96	10708	2	128	137	Acetylation (N-term)
total 15 peptides												

gi|60549563

| Protein Coverage |

Supporting Peptides | Protein

Coverage:

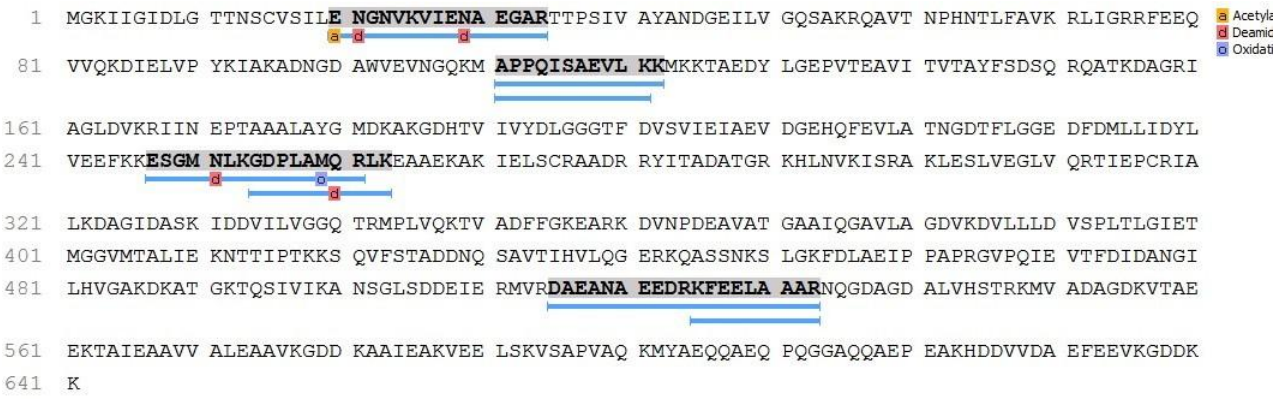

Supporting Peptides:

Peptide	Uniq	-10lgP	Mass	ppm	m/z	z	RT	Scan	#Spec	Start	End	PTM
R.DAEANAEEDRKFEELAAAR.N	N	86.44	2133.9927	-3.6	1067.9998	2	52.07	4751	3	515	533	
M.APPQISAEVLKK.M	N	31.21	1279.7499	0.2	640.8823	2	34.99	3120	2	111	122	
M.APPQISAEVLK.K	N	25.41	1151.6550	-0.6	576.8345	2	43.47	3956	1	111	121	
R.KFEELAAAR.N	N	17.90	1033.5555	-6.9	517.7815	2	42.91	3902	1	525	533	
L.E(+42.01)N(+.98)GNVKVIEN(+.98)AEGAR.T	N	15.93	1642.7798	1.9	822.3987	2	31.68	2784	1	20	34	Acetylation (N-term), Deamidation (NQ)
K.ESGMN(+.98)LKGDPLAM(+15.99)QR.L	Y	15.86	1662.7705	7.8	832.3990	2	94.44	8433	1	247	261	Deamidation (NQ), Oxidation (M)
K.GDPLAMQ(+.98)RLK.E	N	15.23	1128.5961	5.2	565.3082	2	43.03	3913	1	254	263	Deamidation (NQ)
total 7 peptides												

gi|576714049

| Protein Coverage |

Supporting Peptides | Protein

Coverage:

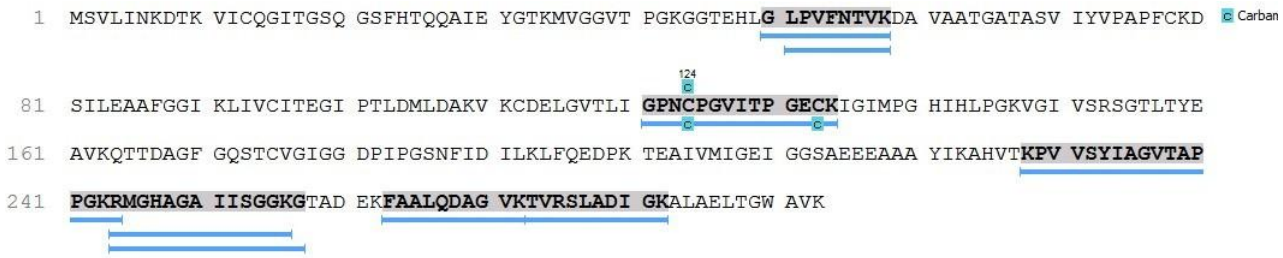

Supporting Peptides:

Peptide	Uniq	-10lgP	Mass	ppm	m/z	z	RT	Scan	#Spec	Start	End	PTM
I.GPNC(+57.02)PGVITPGEC(+57.02)K.I	Y	69.71	1484.6752	0.5	743.3452	2	21.20	1657	1	121	134	Carbamidomethylation
T.KPVVSYIAGVTAPPGKR.M	Y	44.92	1739.0093	0.0	580.6771	3	49.33	4497	3	228	244	
K.FAALQDAGVK.T	Y	30.51	1018.5447	-3.9	510.2776	2	25.04	2084	3	263	272	
G.LPVFNTVK.D	Y	24.44	916.5382	-1.1	459.2759	2	43.75	3977	2	51	58	
K.RMGHAGAIISGGK.G	Y	23.88	1253.6663	7.8	627.8453	2	40.22	3630	2	244	256	
K.RMGHAGAIISGGKG.T	Y	22.59	1310.6877	7.9	656.3563	2	40.36	3644	1	244	257	
L.GLPVFNTVK.D	Y	20.88	973.5596	-0.2	487.7870	2	40.99	3711	4	50	58	
K.TVRSLADIGK.A	Y	15.12	1058.6084	1.9	530.3125	2	66.35	6067	1	273	282	
total 8 peptides												

gi|320329264

| Protein Coverage |

Supporting Peptides | Protein

Coverage:

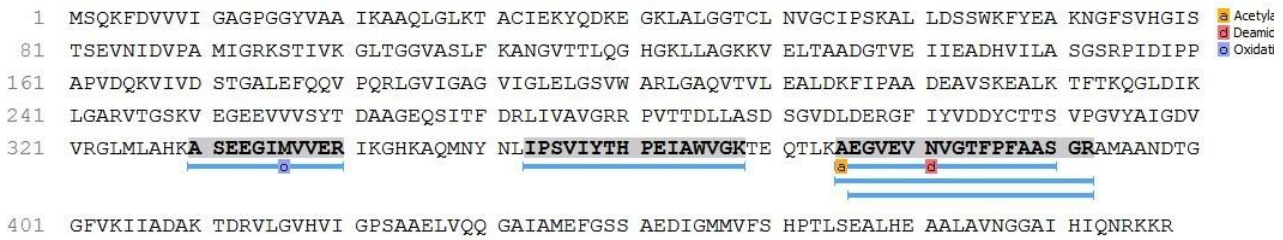

Supporting Peptides:

Peptide	Uniq	-10lgP	Mass	ppm	m/z	z	RT	Scan	#Spec	Start	End	PTM
K.AEGVEVNVGTFPFAASGR.A	Y	59.89	1806.8900	2.8	904.4548	2	87.38	7856	1	375	392	
L.IPSVIYTHPEIAWVGK.T	Y	55.99	1808.9824	2.3	905.5006	2	89.93	8070	2	353	368	
A.EGVEVNVGTFPFAASGR.A	Y	32.25	1735.8529	7.1	868.9399	2	88.03	7906	1	376	392	
K.ASEEGIM(+15.99)VVER.I	Y	23.22	1234.5863	-1.7	618.2994	2	29.38	2539	1	330	340	Oxidation (M)
K.A(+42.01)EGVEVN(+.98)VGTFPFAAS.G	Y	21.96	1636.7620	-0.5	819.3878	2	49.70	4535	1	375	390	Acetylation (N-term), Deamidation (NQ)
total 5 peptides												

gi|68347586

| Protein Coverage |

Supporting Peptides | Protein

Coverage:

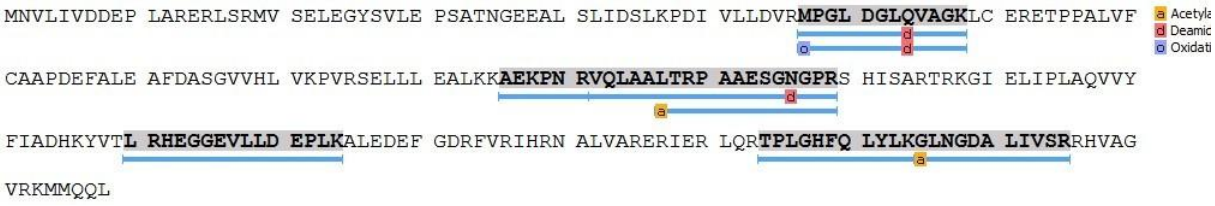

Supporting Peptides:

Peptide	Uniq	-10lgP	Mass	ppm	m/z	z	RT	Scan	#Spec	Start	End	PTM
R.TPLGHFQLYLK.G	Y	53.40	1315.7288	2.4	439.5846	3	80.64	7324	2	214	224	
A.L(+42.01)TRPAAESGNGPR.S	Y	25.49	1366.6953	4.1	684.3577	2	56.34	5162	1	127	139	Acetylation (N-term)
R.M(+15.99)PGLDGLQ(+.98)VAGK.L	Y	22.16	1201.6012	-2.6	601.8063	2	36.51	3261	2	57	68	Oxidation (M), Deamidation (NQ)
R.MPGLDGLQ(+.98)VAGK.L	Y	21.77	1185.6063	-3.3	593.8085	2	49.43	4508	3	57	68	Deamidation (NQ)
K.AEKPNR.V	N	16.57	713.3820	5.1	357.7001	2	24.76	2056	1	116	121	
R.VQLAALTRPAAESGN(+.98)GPR.S	Y	16.43	1807.9540	-3.0	603.6568	3	109.42	9632	1	122	139	Deamidation (NQ)
T.LRHEGGEVLLDEPLK.A	Y	15.91	1703.9205	-1.1	568.9802	3	36.66	3274	1	170	184	
K.G(+42.01)LNGDALIVSR.R	N	15.40	1155.6248	0.5	578.8199	2	71.40	6512	1	225	235	Acetylation (N-term)
total 8 peptides												

gi|557557463

| Protein Coverage |

Supporting Peptides | Protein

Coverage:

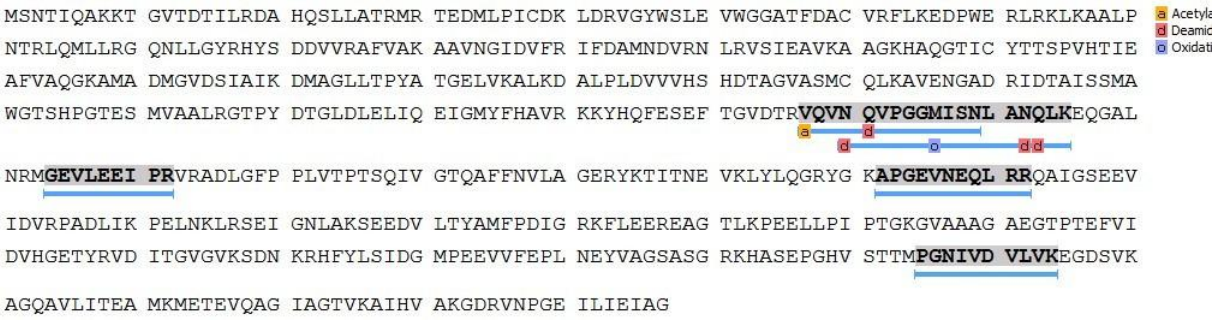

Supporting Peptides:

Peptide	Uniq	-10lgP	Mass	ppm	m/z	z	RT	Scan	#Spec	Start	End	PTM
M.GEVLEEIPR.V	Y	40.26	1040.5502	-2.8	521.2809	2	42.95	3905	1	324	332	
M.PGNIVDVLVK.E	Y	24.57	1052.6229	-0.5	527.3185	2	66.07	6044	2	545	554	
K.APGEVNEQLRR.Q	Y	22.02	1267.6632	-0.1	423.5616	3	15.91	1057	1	382	392	
R.V(+42.01)QVNQ(+.98)VPGGMISN.L	Y	17.31	1384.6656	-7.4	693.3350	2	37.46	3349	1	297	309	Acetylation (N-term), Deamidation (NQ)
V.N(+.98)QVPGGM(+15.99)ISNLAN(+.98)Q(+.98)LK.E	Y	15.68	1701.8243	2.0	851.9211	2	51.84	4728	2	300	315	Deamidation (NQ), Oxidation (M)
total 5 peptides												

gi|15599956

| Protein Coverage |

Supporting Peptides | Protein

Coverage:

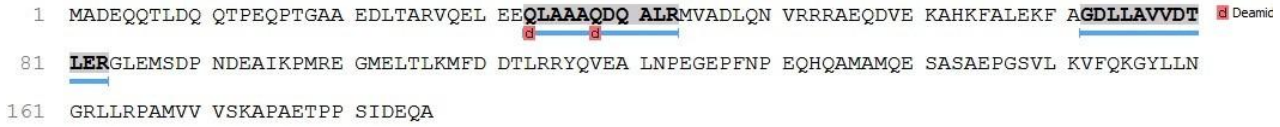

Supporting Peptides:

Peptide	Uniq	-10lgP	Mass	ppm	m/z	z	RT	Scan	#Spec	Start	End	PTM
A.GDLLAVVDTLER.G	Y	54.50	1299.7034	0.3	650.8591	2	100.50	8911	1	72	83	
E.Q(+.98)LAAAQ(+.98)DQALR.M	Y	19.54	1185.5989	5.1	593.8098	2	35.19	3140	1	33	43	Deamidation (NQ)
total 2 peptides												

gi|928212666

| Protein Coverage |

Supporting Peptides | Protein

Coverage:

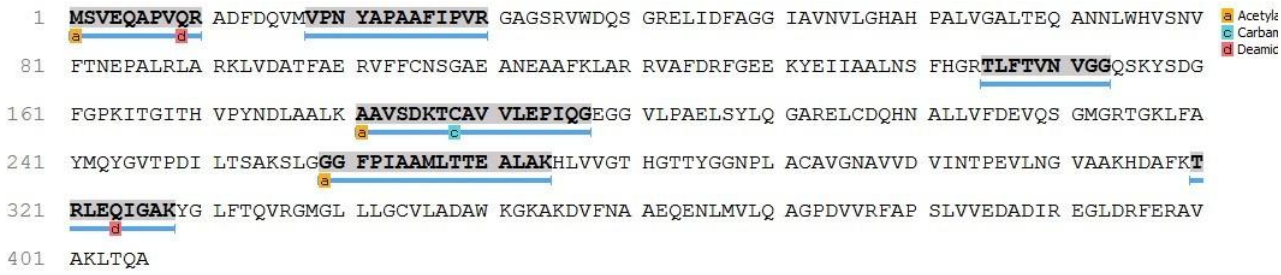

Supporting Peptides:

Peptide	Uniq	-10lgP	Mass	ppm	m/z	z	RT	Scan	#Spec	Start	End	PTM
K.TRLEQ(+.98)IGAK.Y	Y	31.14	1015.5662	-0.8	508.7899	2	16.53	1139	1	320	328	Deamidation (NQ)
M.VPNYAPAAFIPVR.G	Y	31.03	1413.7769	0.7	707.8962	2	80.89	7346	1	18	30	
M(+42.01)SVEQAPVQ(+.98)R.A	Y	21.02	1186.5652	-5.2	594.2868	2	19.89	1500	1	1	10	Acetylation (N-term), Deamidation (NQ)
K.A(+42.01)AVSDKTC(+57.02)AVVLEPIQG.E	Y	18.20	1798.9135	-6.5	600.6412	3	45.03	4095	1	181	197	Acetylation (N-term),Carbamidomethylation
G.G(+42.01)GFPIAAMLTTEALAK.H	Y	16.57	1631.8593	3.0	816.9393	2	33.71	2987	1	259	274	Acetylation (N-term)
R.TLFTVNVGG.Q	Y	15.01	906.4811	-3.3	454.2463	2	10.47	510	1	145	153	
total 6 peptides												

gi|787858376

| Protein Coverage |

Supporting Peptides | Protein

Coverage:

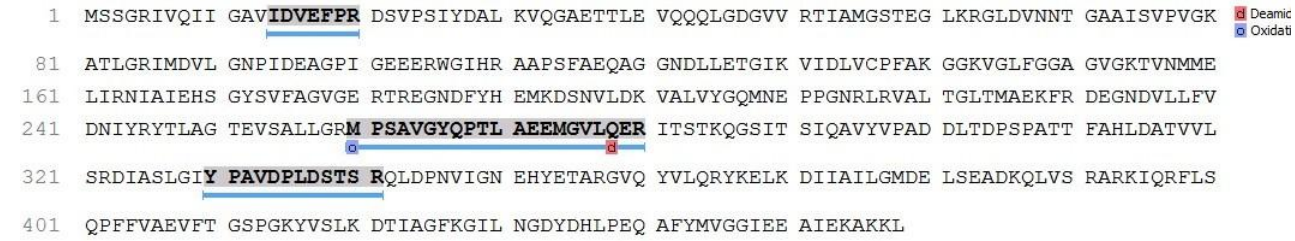

Supporting Peptides:

Peptide	Uniq	-10lgP	Mass	ppm	m/z	z	RT	Scan	#Spec	Start	End	PTM
I.YPAVDPLDSTSR.Q	Y	39.06	1319.6357	2.0	660.8265	2	40.79	3688	1	330	341	
V.IDVEFPR.D	Y	31.56	874.4548	0.4	438.2349	2	46.25	4207	1	14	20	
R.M(+15.99)PSAVGYQPTLAEEMGVLQ(+.98)ER.I	Y	22.25	2322.0872	3.2	775.0388	3	93.28	8349	1	260	280	Oxidation (M), Deamidation (NQ)
total 3 peptides												

gi|582004101

| Protein Coverage |

Supporting Peptides | Protein

Coverage:

Supporting Peptides:

Peptide	Uniq	-10lgP	Mass	ppm	m/z	z	RT	Scan	#Spec	Start	End	PTM
K.RVAISGSGNVAQ(+.98)YAAQ(+.98)K.V	Y	26.93	1720.8744	-6.5	861.4389	2	71.68	6538	1	232	248	Deamidation (NQ)
Y.A(+42.01)PGKASNAGGVATSGLEM(+15.99)SQNAMR.L	Y	22.28	2362.1006	-1.3	1182.0560	2	93.06	8331	1	365	388	Acetylation (N-term), Oxidation (M)
R.F(+42.01)HPSVN(+.98)LGVLK.F	N	17.43	1252.6815	-6.6	627.3439	2	56.52	5182	1	95	105	Acetylation (N-term), Deamidation (NQ)
D.VPAGDIGVGGR.E	Y	17.00	996.5352	0.8	499.2753	2	22.95	1849	2	162	172	
total 4 peptides												

gi|15599529

| Protein Coverage |

Supporting Peptides | Protein

Coverage:

```
  1  MAVIKQDDLI QSVADALQFI SYYHPVDFIQ AMHEAYLREE SPAARDSMAQ ILINSRMCAT GHRPICQDTG IVTVFVRVGM
 81  DVRWDGATMS VDDMINEGVR RAYNLPENVL RASILADPAG ARKNTKDNTP AVIHYSIVPG DKVEVDVAAK GGGSENKSKM
161  AMLNPSDSIV DWVLKTVPTM GAGWCPPGML GIGIGGTAEK AAVMAKEVLM DPIDIHELKA RGPQNRIEEL RLELFEKVNQ
241  LGIGAQGLGG LTTVLDVKIM DYPTHAASLP VCMIPNCAAT RHAHFVLDGS GPAELEAPSL DAYPEIVWEA GPSARRVDLD
321  KITPEEVQSW KPGETLLLNG KMLTGRDAAH KRMVDMLNKG ETLPVDLKGR FIYYVGPVDP VGDEVVGPAG PTTATRMDKF
401  TRQILEQTGL LGMIGKSERG PIAIEAIKDN KAVYLMAVGG AAYLVAQAIK KSKVLAFAEL GMEAIYEFEV KDMPVTVAVD
481  TNGESVHITG PAVWQKKIAE SLAVEVK
```

Supporting Peptides:

Peptide	Uniq	-10lgP	Mass	ppm	m/z	z	RT	Scan	#Spec	Start	End	PTM
R.ASILADPAGAR.K	Y	25.99	1040.5614	-1.2	521.2874	2	61.05	5611	4	112	122	
T.LPVDLK.G	Y	24.19	683.4218	-0.6	342.7180	2	25.75	2158	2	363	368	
K.GETLPVDLK.G	Y	19.11	970.5334	0.2	486.2741	2	38.87	3495	1	360	368	
total 3 peptides												

gi|15599917

| Protein Coverage |

Supporting Peptides | Protein Coverage:

```
  1  MSTKAKQQSS QQMTRGFEPY QETKGEEYMS ERMRAHFTAI LNKWKQELME EVDRTVHHMQ DEAANFPDPA DRASQEEEFS  C Carban
                                                                    132 135
 81  LELRARDRER KLIKKIDETL QLIEDEEYGW CDSCGVEIGI RRLEARPTAT LCIDCKTLAE IREKQLGS
                                                      C   C
```

Supporting Peptides:

Peptide	Uniq	-10lgP	Mass	ppm	m/z	z	RT	Scan	#Spec	Start	End	PTM
A.RPTATLC(+57.02)IDC(+57.02)K.T	Y	42.02	1333.6482	1.1	667.8321	2	23.56	1914	1	126	136	Carbamidomethylation
total 1 peptides												

gi|333113900

Protein Coverage:

```
  1  MAERLNNDFQ FIDVGRKDPK KKLLRQRKKE FVEIYDTFKP AQASDQAHRC LGCGNPYCEW KCPVHNFIPN WLKLVSEGNI  a Acetyla
                                                                                              C Carban
 81  LAAAELSHQT NTLPEVCGRV CPQDRLCEGA CTLNDGFGAV TIGSVEKYIT DTAFAMGWRP DMSKVKPTGK RVAVIGAGPA  d Deamic
161  GLGCADVLVR NGVTPVVFDK NPEIGGLLTF GIPEFKLEKS VLSNRREVFT GMGIEFRLNT EIGKDVTMQQ LLDEYDAVFM
241  GMGTYTYMKG GFPGEDLPGV HDALDFLIAN VNRNLGFEKS PEDFVDMKGK RVVVLGGGDT AMDCNRTSIR QGAKAVTCAY
                                                                a                 d     C
321  RRDEANMPGS RKEVKNAKEE GVKFLFNRQP IAIVGEDKVE GVKVVETRLG EPDARGRRSP EPIPGSEEII PAEAVLIAFG
                                    a
401  FRPSPAPWFE EFDIRIDTQG RVVAPEKATF KHQTSNPKVF AGGDMVRGSD LVVTAIYEGR NAAEGILDYL GV
```

Supporting Peptides:

Peptide	Uniq	-10lgP	Mass	ppm	m/z	z	RT	Scan	#Spec	Start	End	PTM
R.V(+42.01)VVLGGGDTAMDCNRTSIR.Q	Y	22.96	2004.9720	0.4	669.3315	3	52.18	4763	1	292	310	Acetylation (N-term)
R.VAVIGAGPAGLGCADVLVR.N	Y	17.28	1736.9607	-8.0	869.4807	2	80.94	7350	1	152	170	
R.Q(+.98)GAKAVTC(+57.02)AYR.R	Y	15.78	1224.5920	-0.8	613.3028	2	17.64	1256	1	311	321	Deamidation (NQ),Carbamidomethylation
R.Q(+42.01)PIAIVGEDK.V	Y	15.35	1110.5920	0.5	556.3036	2	53.65	4904	1	349	358	Acetylation (N-term)
total 4 peptides												

gi|213928538

| Protein Coverage |

Supporting Peptides | Protein

Coverage:

```
   1  MSTESKCPFN HAAGGGTTNR DWWPKQLNLK ILHQHSSLSD PMGEDFDYAK EFKSLDFEAV KQDLRDVMTR SQDWWPADFG
  81  HYGPLFIRMA WHSAGTYRTG DGRGGAGAGQ QRFAPLNSWP DNVSLDKARR LIWPVKQKYG RKISWADLIV LTGNVALESM
 161  GFKTFGFSGG RPDVWEPEED VYWGSETTWL GGEERYGAQK KMQQPGDGTL VAEPENHANE ESRTASGERN LENPLAAVQM
 241  GLIYVNPEGP EGVPDPVASA RDIRETFGRM AMNDEETVAL IAGGHAFGKT HGAGPADNVG PEPEAAGLEQ QGFGWSNKFG
 321  TGKGGDTITS GLEVTWTSTP TQWSNEYLEN LFAFDWELTK SPAGAHQWTP KNGAGAGKIP DAHDPSKRHA PSMLTSDLAL
 401  RFDPAYEQIS RRFLANPEQL ADAFARAWFK LTHRDMGPLA RYLGPETPTE ELLWQDPIPD VTHPLVDDQD VAALKGKILA
 481  SGLSVSQLVS TAWAAASTFR GSDKRGGANG GRLRLAPQKD WAVNQPAQLA NVLSTLESIQ SEFNAAQSNG KKVSIADLIV
 561  LAGSAGVEQA AKNAGQQVTV PFTAGRADAS QEQTDVESFS FLEPIADGFR NYQKGRYKVS AESLLVDKAQ LLTLTAPEMA
 641  VLLGGLRVLN INVGQSKHGV FTDKSETLTN DFFKNLLDMA VEWKATSGAN DTFEARDRKT GEVKWTGSRV DLVFGSHAQL
 721  RAISEVYGSA DAQERFVKDF VAVWTKVMNL DRFDLA
```

Supporting Peptides:

Peptide	Uniq	-10lgP	Mass	ppm	m/z	z	RT	Scan	#Spec	Start	End	PTM
R.FLAN(+.98)PEQLADAFAR.A	Y	25.89	1562.7728	-7.0	782.3882	2	40.60	3668	1	413	426	Deamidation (NQ)
R.GSDKRGGANGGR.L	Y	24.53	1130.5541	2.4	566.2856	2	26.48	2242	1	501	512	
total 2 peptides												

gi|404302499

| Protein Coverage |

Supporting Peptides | Protein

Coverage:

```
   1  MADEQTVDTQ NPEANQAPET SGDDLATRVQ VLEEQLAAAQ DQSLRVAADL QNVRRRAEQD VEKAHKFALE KFASDLLPIV
  81  DSLERGLELS SPDDESIRPM REGIELTLKM FHDTLKRYQL EAIDPHGEPF NAVHHQAMAM QESADVEPNS VLKVFQKGYQ
 161  LNGRLLRPAM VVVSKAPAPI SPSIDEKA
```

Supporting Peptides:

Peptide	Uniq	-10lgP	Mass	ppm	m/z	z	RT	Scan	#Spec	Start	End	PTM
K.APAPISPSIDEK.A	Y	25.16	1223.6396	-1.2	408.8867	3	36.96	3302	2	176	187	
R.GLELSSPDDESIRPMR.E	Y	15.51	1800.8676	-7.9	901.4340	2	40.57	3666	1	86	101	
total 2 peptides												

gi|1256708

| Protein Coverage |

Supporting Peptides | Protein

Coverage:

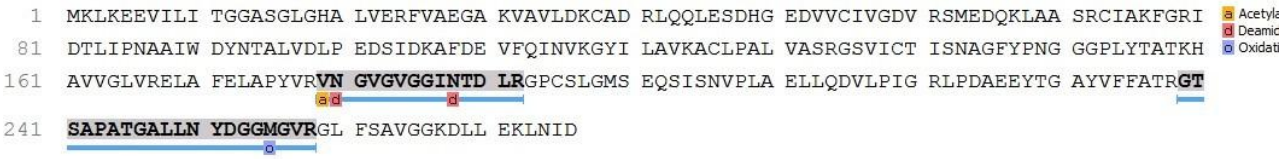

Supporting Peptides:

Peptide	Uniq	-10lgP	Mass	ppm	m/z	z	RT	Scan	#Spec	Start	End	PTM
R.V(+42.01)N(+.98)GVGVGGIN(+.98)TDLR.G	Y	23.60	1413.7100	4.6	707.8655	2	39.71	3584	1	179	192	Acetylation (N-term), Deamidation(NQ)
R.GTSAPATGALLNYDGGM(+15.99)GVR.G	Y	17.60	1922.9156	5.9	962.4708	2	13.02	717	1	239	258	Oxidation (M)
total 2 peptides												

gi|310696647

| Protein Coverage | Supporting Peptides | Protein Coverage

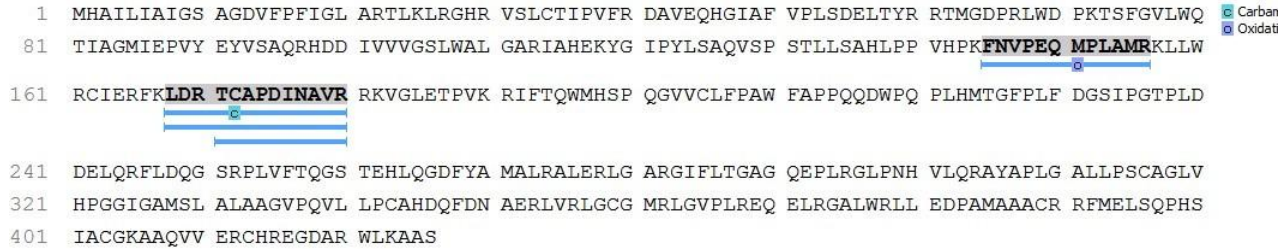

Supporting Peptides:

Peptide	Uniq	-10lgP	Mass	ppm	m/z	z	RT	Scan	#Spec	Start	End	PTM
K.LDRTCAPDINAVR.R	Y	17.61	1442.7300	4.5	722.3755	2	84.56	7631	1	168	180	
K.FNVPEQM(+15.99)PLAMR.K	Y	17.28	1447.6952	6.4	724.8595	2	70.74	6446	1	145	156	Oxidation (M)
R.TCAPDINAVR.R	Y	16.03	1058.5178	6.2	530.2695	2	30.29	2643	1	171	180	
K.LDRTC(+57.02)APDINAVR.R	Y	15.17	1499.7515	5.4	750.8870	2	72.67	6622	3	168	180	Carbamidomethylation
total 4 peptides												

Prepared with PEAKS ™ (bioinfor.com)

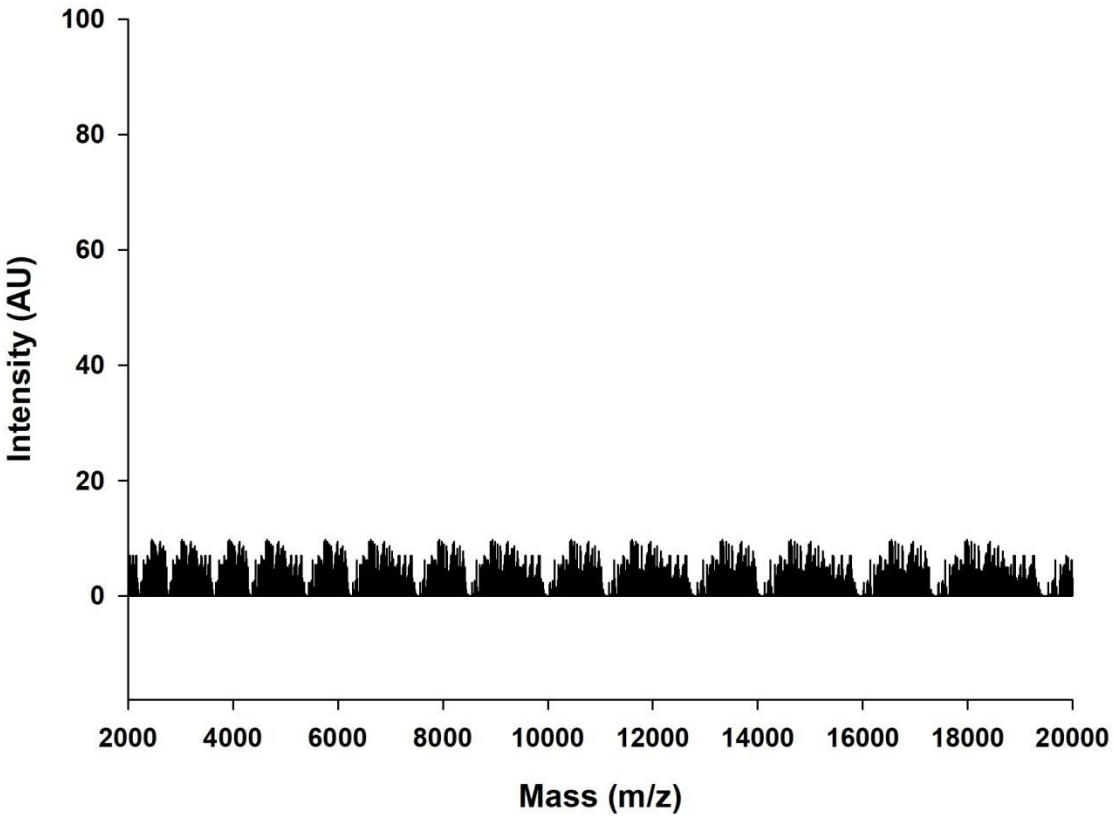

Figure A6. MALDI-ToF mass spectra of lunathrombase (5.0 µg). 1.0 µg of the lunathrombase was mixed with 1 µg of a-cyano-4 hydroxycinnamic acid matrix dissolved in 50% (v/v) acetonitrile containing 0.1 % (v/v) TFA. The mixture was then spotted onto an Opti-TOF-384 plate (ABSciex), dried, and analyzed in positive linear mode using an acceleration voltage of 25 kV and laser intensity of 3000. For experimental details see section 3.2.6.1.2.

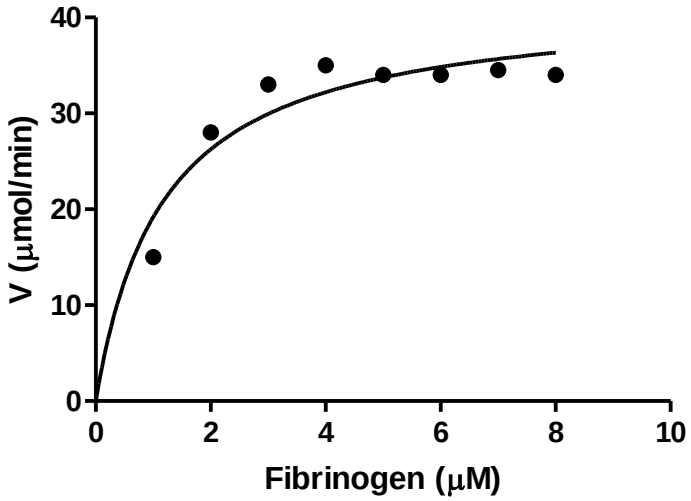

Figure A7. Determination of *Km* and *Vmax* values of lunathrombase against fibrinogen by Michaelis-Menton plot